

Project Labnotes

Kylie Tailin Zhu

March 30, 2020

Catch up the work done from the Teaching Block 1:

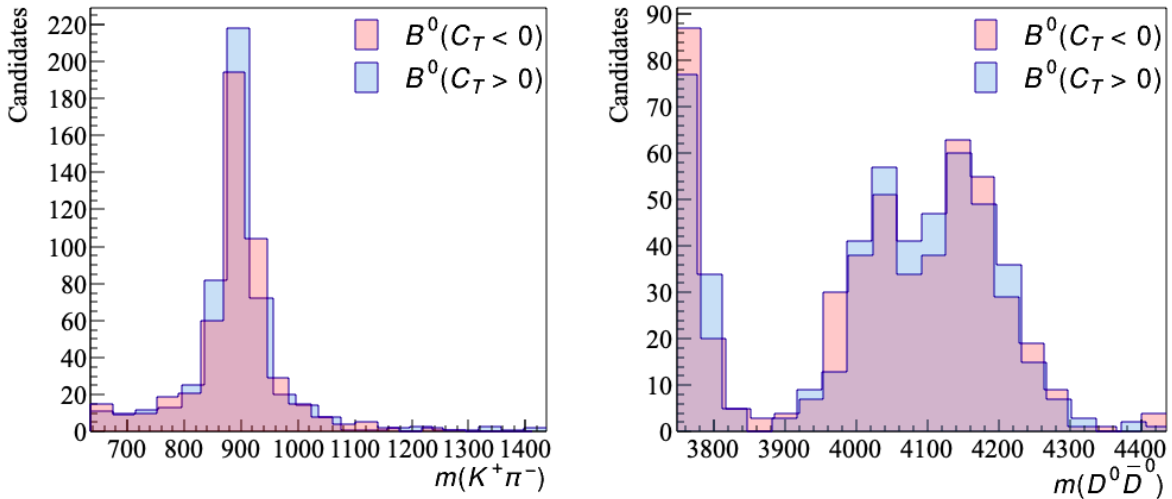


Figure 1: The binned distributions of simulated B^0 events in the variables of $m(K^+\pi^-)$ (left) and $m(D^0\bar{D}^0)$ (right) for different values of C_T .

A summary of previous work:

- Looked at the MC data file of the decay contains the four-momentum of the particles generated from MINT, and counted the number of events with $C_T > 0$ and $C_T < 0$, using $C_T = \vec{p}_{K^+} \cdot (\vec{p}_{D^0} \times \vec{p}_{\bar{D}^0})$.
- Find the triple product asymmetry of MC data: $A_T = (501 - 499)/(501 + 499) = 0.002$ (using Eq. 1).
- Plotted the resonance for the $K\pi$ and $D\bar{D}$ final states with the 1000 events for the $C_T > 0$ and $C_T < 0$ cases. The data given has already been in the rest frame of B^0 , so no further Lorentz boost is required.
- Calculated the invariant mass of $m(D^0\bar{D}^0K^+\pi^-)$ and finding that all the values equal to 5279.4 MeV/ c^2 , which is the mass of B^0 , which verifies the invariant masses are calculated correctly.

Next Steps:

- Find the uncertainties in the triple product asymmetry.
- Fit the binned distributions using the Breit-Wigner distributions
- Find the distribution of other CM variables (ϕ , helicity angles)

Triple Product asymmetry:

Denote the triple product asymmetry as:

$$A_T = \frac{N(C_T > 0) - N(C_T < 0)}{N(C_T > 0) + N(C_T < 0)}, \quad (1)$$

The error in $N(C_T > 0)$ is $\sqrt{N(C_T > 0)}$ and in $N(C_T < 0)$ is $\sqrt{N(C_T < 0)}$ for a large number of samples, given a Poisson distribution. The error in A_T is then:

$$\begin{aligned} \Delta A_T &= \sqrt{\left(\frac{\partial A_T}{\partial N(C_T > 0)} \Delta N(C_T > 0) \right)^2 + \left(\frac{\partial A_T}{\partial N(C_T < 0)} \Delta N(C_T < 0) \right)^2} \\ &= \sqrt{\left(\frac{2N(C_T < 0)}{(N(C_T > 0) + N(C_T < 0))^2} \right)^2 N(C_T > 0) + \left(\frac{-2N(C_T > 0)}{(N(C_T > 0) + N(C_T < 0))^2} \right)^2 N(C_T < 0)}. \end{aligned} \quad (2)$$

The result is $A_T = 0.002 \pm 0.0316$. This error is much larger than the result which indicates that no CP violation is in this sample.

Aiming to find the distribution of the five CM variables:

- the invariant masses of daughter pairs in the rest frame of B^0 : $m(D^0\bar{D}^0)$, $m(K^+\pi^-)$. This has been found in Fig.1 using $\sqrt{\mathbf{P} \cdot \mathbf{P}}$, where \mathbf{P} is the sum of the 4-momentum of the daughter pairs.
- the cosine of the helicity angles between the daughter particle and the mother-particle B^0 , in the rest frame of its daughter pairs
 - $\cos(\theta_{D^0})$, θ_{D^0} is the angle between the momentum of D^0 and B^0 in the rest frame of $D^0\bar{D}^0$
 - $\cos(\theta_{K^+})$, θ_{K^+} is the angle between the momentum of K^+ and B^0 in the rest frame of $K^+\pi^-$
 - to boost the momenta to the daughter pair's rest frame:
daughter pair's rest frame has four-momentum

$$\mathbf{P} = (p_{1x} + p_{2x}, p_{1y} + p_{2y}, p_{1z} + p_{2z}, M_1 + M_2) = \mathbf{p}_1 + \mathbf{p}_2, \quad (3)$$

the boost vector is then

$$\vec{v} = (p_{1x} + p_{2x}, p_{1y} + p_{2y}, p_{1z} + p_{2z})/(M_1 + M_2) = (\vec{p}_1 + \vec{p}_2)/M. \quad (4)$$

- M is not the invariant mass of the daughter pair, but the sum of the masses of the pair.
- The boost is performed using the built-in function in ROOT, which has the analytical form:¹

$$\mathbf{p}' = \begin{pmatrix} \gamma & -\gamma\boldsymbol{\beta}^T \\ -\gamma\boldsymbol{\beta} & \mathbf{I} + (\gamma - 1)\boldsymbol{\beta}\boldsymbol{\beta}^T/\beta^2 \end{pmatrix} \mathbf{p}, \quad \text{where } \gamma = \frac{1}{\sqrt{1 - \beta^2}}, \boldsymbol{\beta} = \vec{v}/c. \quad (5)$$

Hence, e.g., $\cos(\theta_{D^0}) = \frac{\vec{p}'_{D^0} \cdot \vec{p}'_{B^0}}{|\vec{p}'_{D^0}| |\vec{p}'_{B^0}|}$.

- particularly check the direction of the boost, sometimes need to add a minus sign before the boost vector. To check if the boost is correct:
 - boost the daughter pair's Lorentz vector to its rest frame gives zero in the three-momentum.
 - the distribution of the $\cos(\text{angle})$ should look uniform and not peak at one side of the graph.
- the angle ϕ between the planes of the daughter pairs in the rest frame of mother particle B^0 . In this case, the angle between the plane $D^0\bar{D}^0$ and the plane $K^+\pi^-$: $\phi = \cos^{-1} \left(\frac{(\vec{p}_{D^0} \times \vec{p}_{\bar{D}^0}) \cdot (\vec{p}_{K^+} \times \vec{p}_{\pi^-})}{|\vec{p}_{D^0} \times \vec{p}_{\bar{D}^0}| |\vec{p}_{K^+} \times \vec{p}_{\pi^-}|} \right)$.

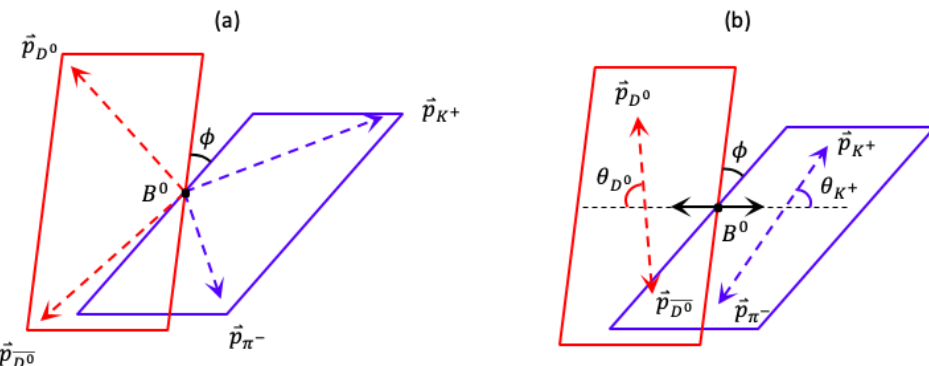


Figure 2: (a) The four-body B^0 decay geometry in the rest frame of B^0 . (b) Definition of the helicity angles θ_{D^0} and θ_{K^+} , and the decay-plane angle ϕ .

¹Wikipedia contributors. *Lorentz transformation — Wikipedia, The Free Encyclopedia*. [Online; accessed 23-March-2020]. 2014. URL: https://en.wikipedia.org/w/index.php?title=Lorentz_transformation&oldid=600359480.

The distributions were found with 100 bins, where the error bars come from the default option when drawing the histogram in ROOT. The data has been separated for different values of C_T as shown in blue and red data points. The helicity angles distributed uniformly and the 3-momenta of the daughter pairs in their own frame is zero, which indicates the boost is performed correctly.

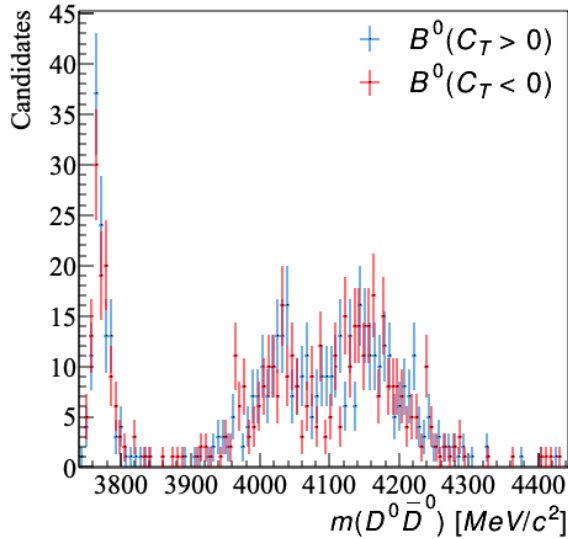


Figure 3: The binned distributions of invariant mass $m(D^0 \bar{D}^0)$ for different values of C_T .

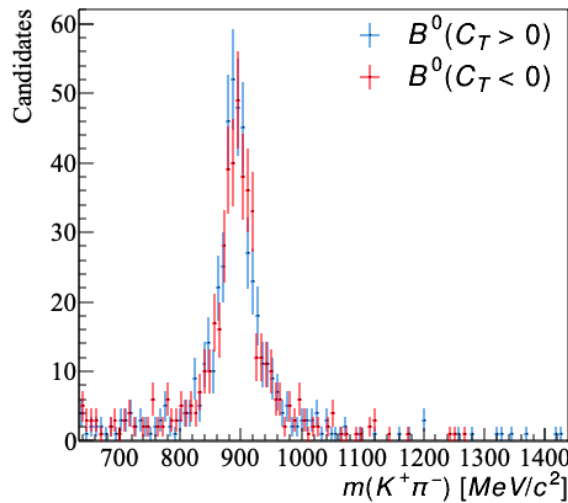


Figure 4: The binned distributions of invariant mass $m(K^+ \pi^-)$ for different values of C_T .

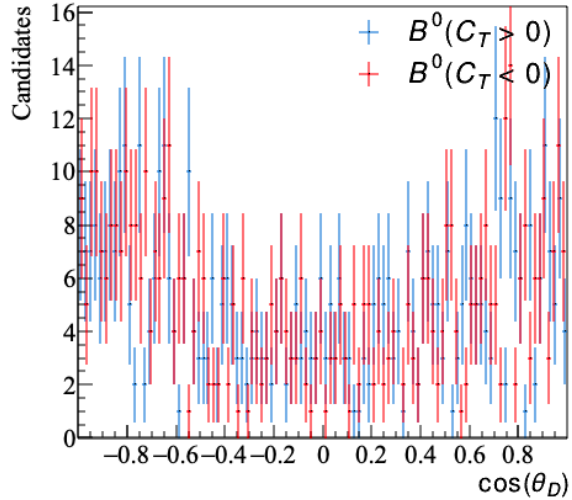


Figure 5: The binned distributions of helicity angle $\cos(\theta_{D^0})$ for different values of C_T .

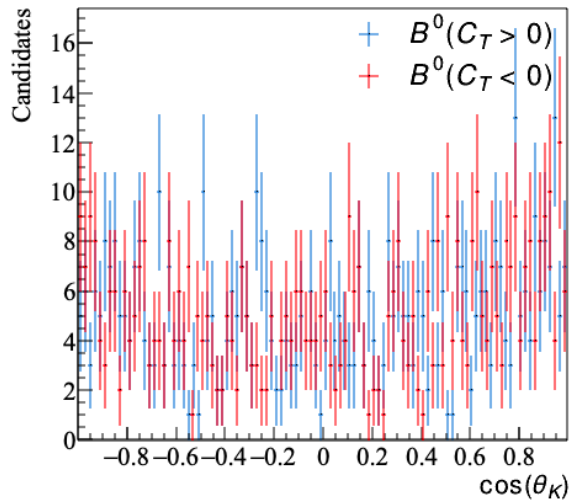


Figure 6: The binned distributions of helicity angle $\cos(\theta_{K^+})$ for different values of C_T .

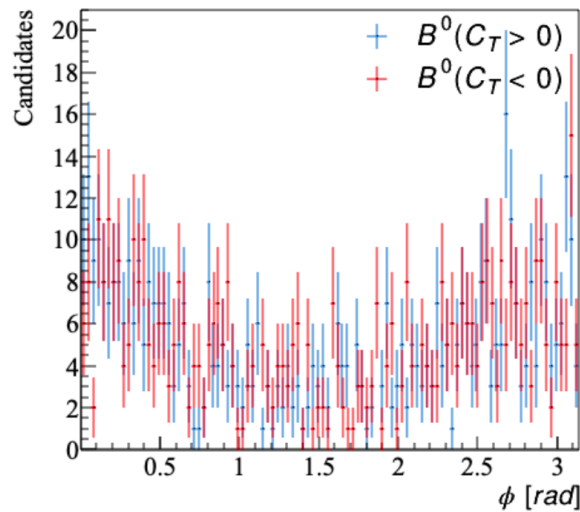


Figure 7: The binned distributions of the angle ϕ between the plane $D^0\bar{D}^0$ and the plane $K^+\pi^-$ for different values of C_T .

Fitting the invariant mass distributions using the relativistic Breit-Wigner distribution:²

$$f(E) = \frac{k}{(E^2 - M^2)^2 + M^2\Gamma^2}, \quad (6)$$

$$k = \frac{2\sqrt{2}M\Gamma\gamma}{\pi\sqrt{M^2+\gamma}},$$

$$\gamma = \sqrt{M^2(M^2 + \Gamma^2)},$$

E - center of mass energy that produce the resonance,

M - mass of the resonance,

Γ - resonance width.

The fitting was performed using ROOT framework by defining a class for the fitting function. The left and right limit of the fit was roughly approximated from the left and right ends of the peaks in the histogram. This gives individual fitting for each peak. The initial values for the mass and the width were obtained from PDG.

The fitted results are given by:

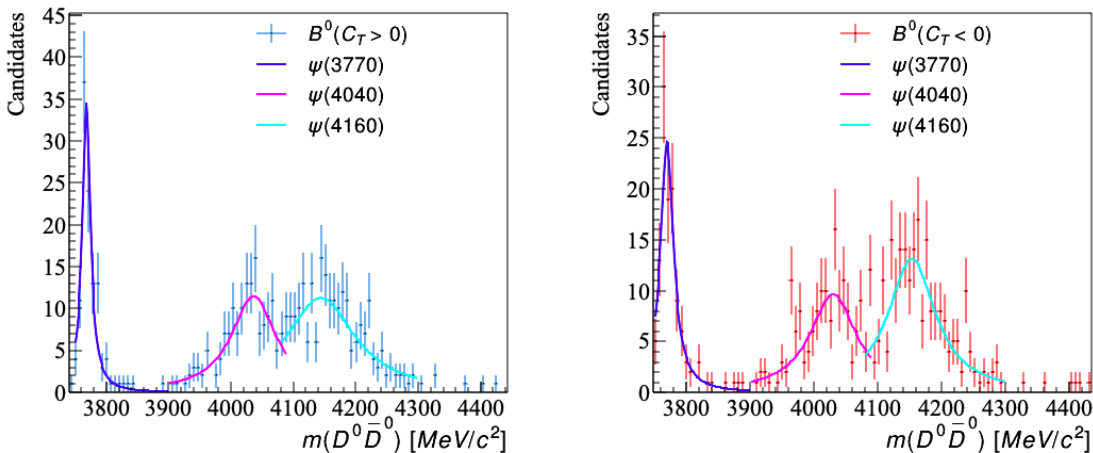


Figure 8: The binned distributions of invariant mass $m(D^0 \bar{D}^0)$ for different values of C_T fitted using Eq.6

resonance	mass(M)	err_mass	width(Gamma)	err_width	Chi2	type
psi(3770)	3770	0.33	27.2	1		PDG
psi(3770)	3768.30	1.11	15.98	3.17	10.52	$C_T > 0$
psi(3770)	3769.36	1.62	24.52	3.96	8.95	$C_T < 0$
psi(4040)	4039	1	80	10		PDG
psi(4040)	4036.19	5.57	86.47	15.25	13.92	$C_T > 0$
psi(4040)	4030.10	5.21	88.63	17.02	29.27	$C_T < 0$
psi(4160)	4191	5	70	10		PDG
psi(4160)	4144.08	8.52	134.07	20.90	22.05	$C_T > 0$
psi(4160)	4153.57	4.17	90.23	11.73	30.86	$C_T < 0$

Figure 9: The fitted values from the curves in MeV

²Wikipedia contributors. *Relativistic Breit–Wigner distribution — Wikipedia, The Free Encyclopedia*. [Online; accessed 23-March-2020]. 2019. URL: https://en.wikipedia.org/w/index.php?title=Relativistic_Breit%20%93Wigner_distribution&oldid=912044809.

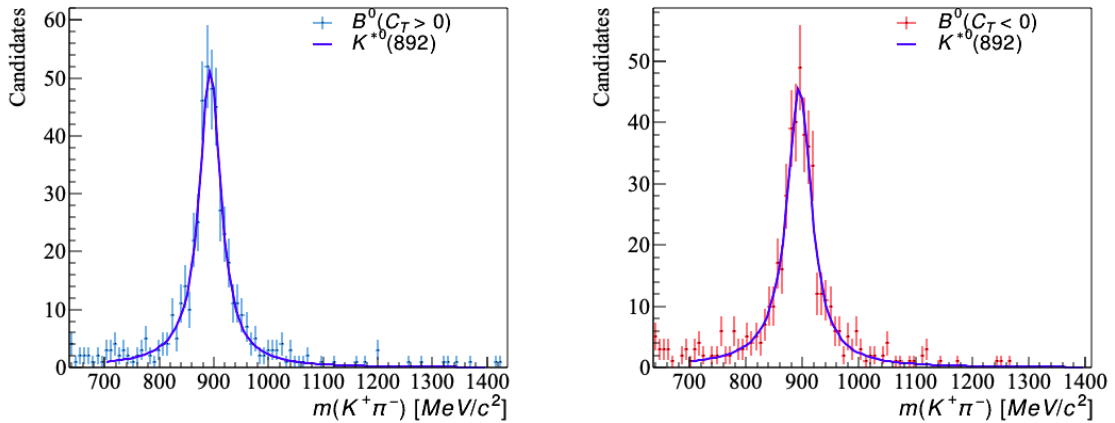


Figure 10: The binned distributions of invariant mass $m(K^+\pi^-)$ for different values of C_T fitted using Eq.6

resonance	mass(M)	err_mass	width(Gamma)	err_width	Chi2	type
K*0(892)	895.55	0.2	47.3	0.5		PDG
K*0(892)	893.52	1.53	48.07	3.55	37.29	$C_T > 0$
K*0(892)	894.35	1.65	52.39	3.90	34.30	$C_T < 0$

Figure 11: The fitted values from the curves in MeV

30 Jan 2020, Thursday

To generate more events, an amplitude generator is required - use AmpGen

Start trying to install AmpGen:

AmpGen is downloaded but not be able to compile it. At the stage of make, there exist the error:

```
ignoringfile/Library/Developer/CommandLineTools/SDKs/MacOSX10.14.sdk/usr/lib/libSystem.tbd, filewasbuiltforunsupportedfileformat(0x2D0x2D0x200x210x740x610x700x690x2D0x740x620x640x2D0x760x33) which  
isnotthearchitecturebeinglinked(x86_64):/Library/Developer/CommandLineTools/SDKs/MacOSX10.14.sdk/usr/lib/libSystem.tbd  
Undefined symbols for architecture x86_64:
```

One method tried:

Download a different version of the sdk: MacOSX10.10.sdk.tzr.xz, which is suggested from [here](#) and [here](#).

Uncompress it to the /opt directory in the laptop:

```
sudo tar xf /Downloads/MacOSX10.10.sdk.tar.xz -C /opt
```

Add the lines into the file \$HOME/.condarc:

```
conda_build:  
  config_file:~/.conda/conda_build_config.yaml
```

Here is more details of using [conda_build](#).

Then create the file \$HOME/.conda/conda_build_config.yaml and add:

```
CONDA_BUILD_SYSROOT:  
  - /opt/MacOSX10.10.sdk # [osx]
```

- But this doesn't work.

AmpGen: now find a way to work from Paras - Remove everything that has been done before and follow the instructions written in the "Installation Notes.ipynb".

AmpGen has been successfully installed - now try to generate and analyse the events for the $D \rightarrow K^+K^-\pi^+\pi^-$ decay and check if AmpGen is working correctly. The results can be compared with the literature.³

The file contains the amplitude model for the $D \rightarrow K^+K^-\pi^+\pi^-$ decay is: DtoKKpipi_v2.opt.

Inside the file, the structure is:

```
EventType D0 K+ K- pi+ pi-
```

- to specify the particles involved in the decay. This can also be specified as an argument in the command line.

```
#                                         Real / Amplitude | Imaginary / Phase
#                                         Fix? Value Step | Fix? Value Step
D0 [D] {K*(1680)0{K+,pi-},K*(892)bar0{K-,pi+}} 0 1.20197 0.0898679 0 -2.44153 0.0844467
```

- This is one of the intermediate resonances that contribute to the decay:
 $D^0 \rightarrow K^{*0}(1680)(\rightarrow K^+\pi^-)K^{*0}(892)(\rightarrow K^-\pi^+)$.
- For each resonance, it has an vertex gives the probability of the decay to happen.
- For the six numbers, the left three are the parameters for the real part while the right three are the parameters for the imaginary part of the vertex.
- Each parameter is specified in terms of three numbers: the fix flag, the initial value, and the step size.
- The fix term is to specify whether the initial value is fixed (fix=2) or free (fix=0) ...
- step?
- the [D] specify the spin in the orbital angular momentum in the final states, one can also use [P], [S] ..for different spins.

³The LHCb collaboration. "Search for CP Violation using T-odd Correlations in $D^0 \rightarrow K^+K^-\pi^+\pi^-$ Decays". In: *J. HEP* 2014.10 (2014). ISSN: 1029-8479.

6 Feb 2020, Thursday

Outputs from AmpGen generated events:

1. $D^0 \rightarrow K^+ K^- \pi^+ \pi^-$

run the DtoKKpipi_v2.opt file with 171300 events.

$$C_T = \vec{p}_{\pi^-} \cdot (\vec{p}_{K^+} \times \vec{p}_{K^-})$$

TP Asymmetry $A_T = -0.0740 \pm 0.0024$

The distributions of CM variables with 100 bins:

The distributions match the results in the literature, which means the code is correct and AmgGen can work properly.

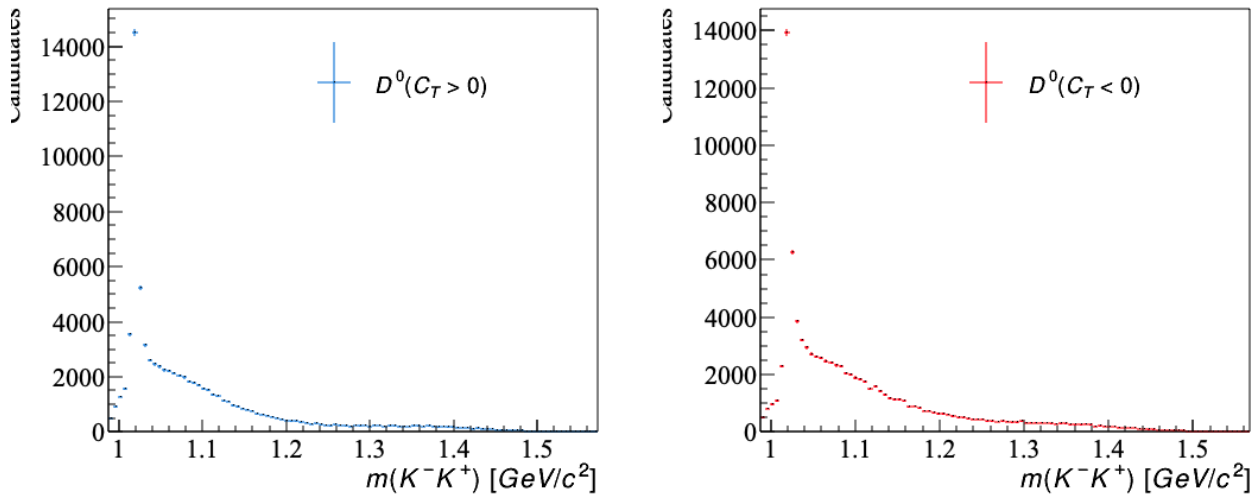


Figure 12: The binned distributions of invariant mass $m(K^-K^+)$ for different values of C_T .

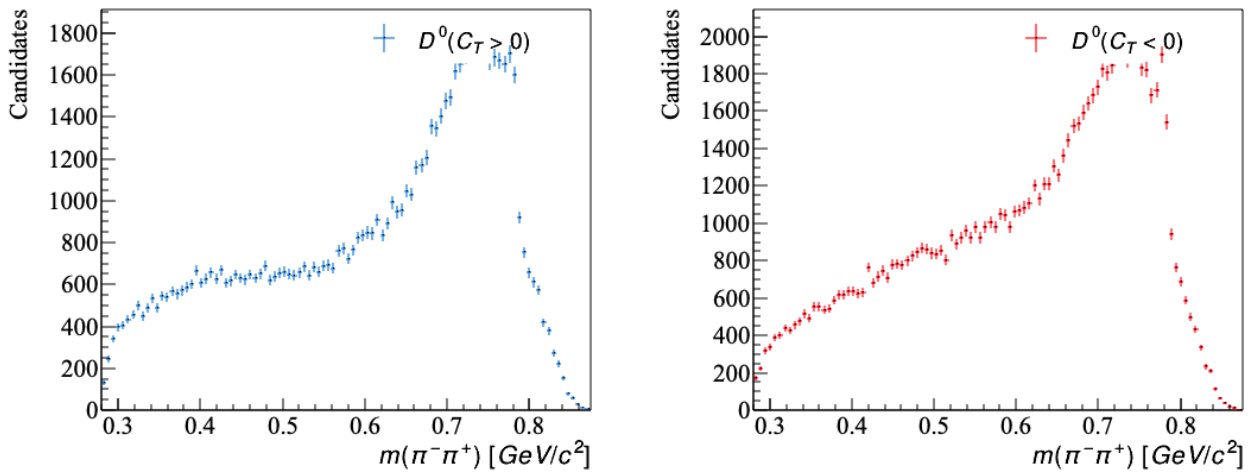


Figure 13: The binned distributions of invariant mass $m(\pi^-\pi^+)$ for different values of C_T .

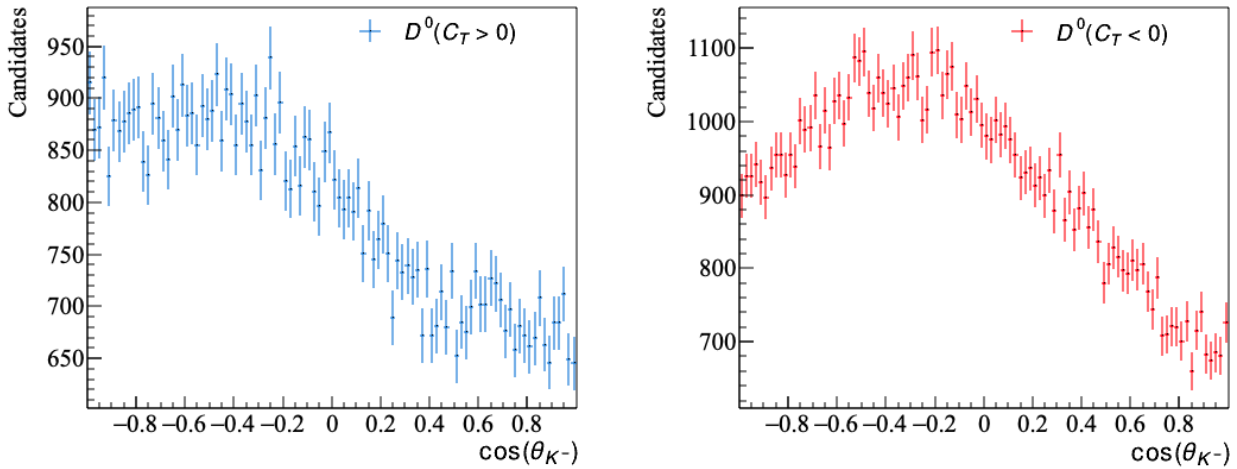


Figure 14: The binned distributions of helicity angle $\cos(\theta_{K^-})$ for different values of C_T .

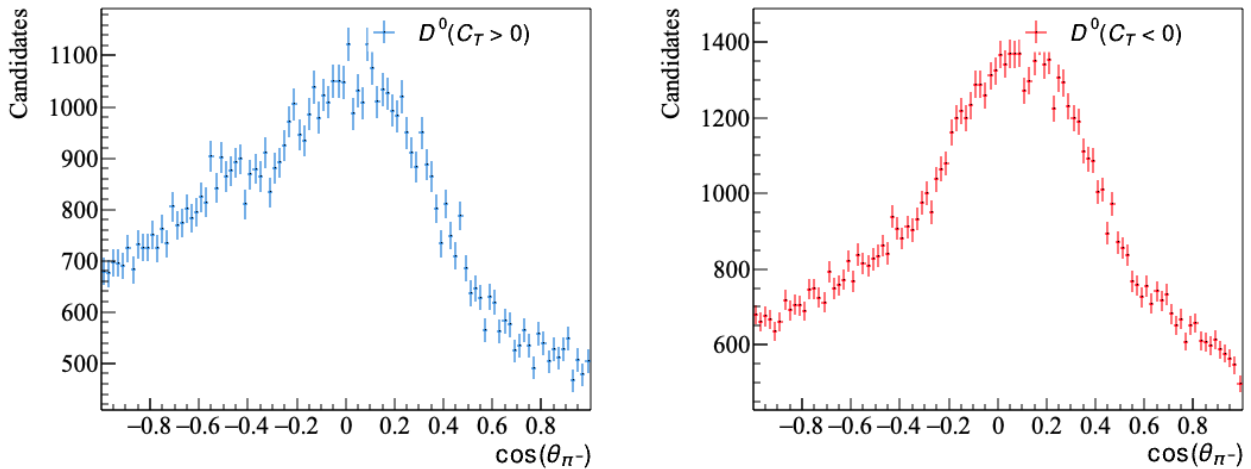


Figure 15: The binned distributions of helicity angle $\cos(\theta_{\pi^-})$ for different values of C_T .

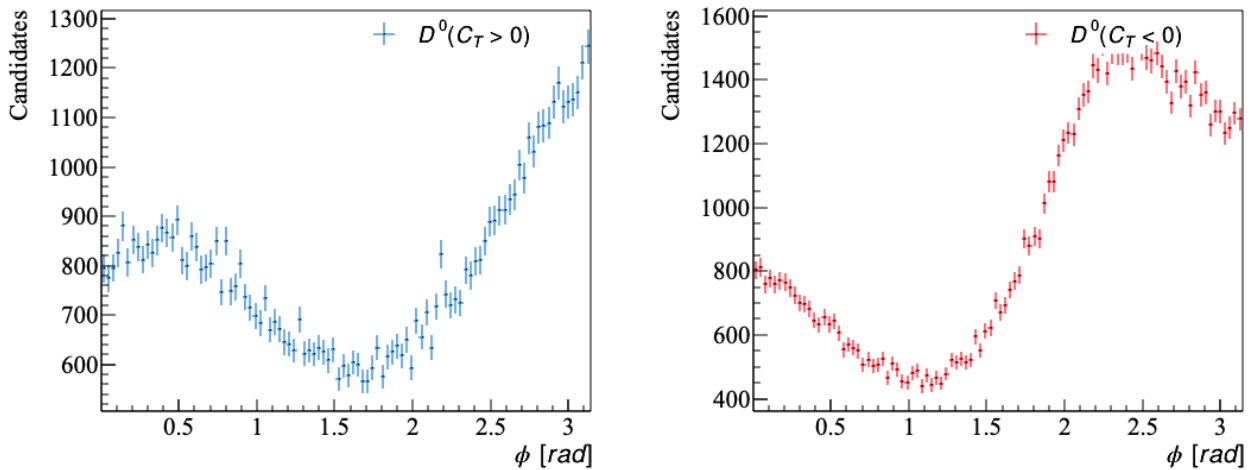


Figure 16: The binned distributions of the angle ϕ between the plane K^-K^+ and the plane $\pi^-\pi^+$ for different values of C_T .

2. $B^0 \rightarrow D^0 \bar{D}^0 K^+ \pi^-$

Use AmpGen to generate $B^0 \rightarrow D^0 \bar{D}^0 K^+ \pi^-$ events:

- add `B0toDDbar0K+pi-.opt` file to `~/AmpGen/build/bin/`
- inside the `B0toDDbar0K+pi-.opt` file, use the resonances from the MINT file (`4BodyModel.txt`), change the format of the resonance list to match the format of `.opt` files used in AmpGen.
- inside the `B0toDDbar0K+pi-.opt` file, change `kappa0` to `K(0) * (800) 0` - the particle name has been updated in PDG.
- inside the `B0toDDbar0K+pi-.opt` file, change the non resonance part
e.g. change `D0Dbar0` to `NonResS0{D0, Dbar0}`.
[This will improve the speed considerably when including the narrow D^* resonances. It only works if all decays are done in quasi-two-body steps (i.e. $B \rightarrow \psi K^*$ as a resonance works, but $B \rightarrow D\bar{D}K^*$ doesn't).]
- inside the `mass_width.csv` file, change line 385: `J=2, P=+ for particle D (s2) (2573)`.

Fit the results for different event files - from MINT and AmpGen...

a. old results from MINT - 1000 events: $A_T = 0.002 \pm 0.0316$

This still uses Eq.6 to fit but using a different approach - by summing over the Breit-Wigner functions for each peak. In this case, the events are not enough to make a clear fit for the left figure in Fig.18, the right figure in Fig.19, and the left figure in Fig.20. The fitting outcomes for resonance peaks are shown in Fig.17. For the successfully fitted peaks, it gives the expected results.

bin=40 A1=45 A2=40 A3=50						
resonance	mass(M)	err M	width	err w	Chi2	type
psi(3770)	3770	0.33	27.2	1		PDG
psi(3770)	3771.31	0.67	18.29	1.91	127.20	combined
psi(3770)	3771.37	1.26	20.61	3.80	44.53	C_T > 0
psi(3770)	3767.06	1.29	16.95	5.06	24.09	C_T < 0
psi(4040)	4039	1	80	10		PDG
psi(4040)	4117.43	3.80	192.86	12.04	127.20	combined
psi(4040)	4106.79	5.85	220.99	22.96	44.53	C_T > 0
psi(4040)	4155.43	4.53	84.13	11.20	24.09	C_T < 0
psi(4160)	4191	5	70	10		PDG
psi(4160)	760.09	276.88	1.06E6	1.32E4	127.20	combined
psi(4160)	-0.09	0.50	9.92E6	2.899E7	44.53	C_T > 0
psi(4160)	4027.25	5.10	61.49	11.41	24.09	C_T < 0
K*0(892)	895.55	0.2	47.3	0.5		PDG
K*0(892)	893.33	1.15	54.14	2.74	45.24	combined
K*0(892)	892.69	1.55	51.55	3.90	17.84	C_T > 0
K*0(892)	897.09	311.89	0.30	311.88	367.96	C_T < 0

Figure 17: The fitted values from the curves in Fig.18,19,20(MeV)

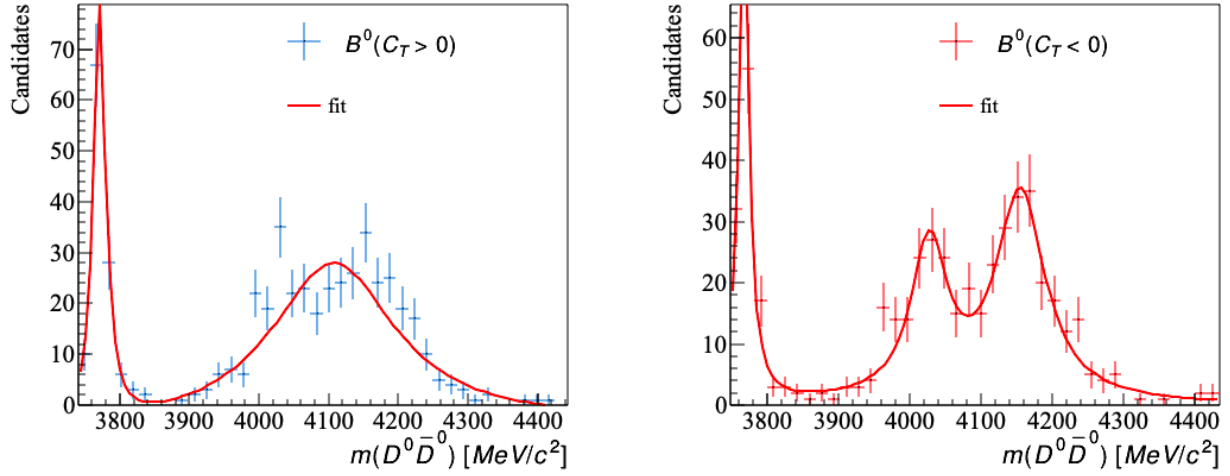


Figure 18: The binned distributions of invariant mass $m(D^0 \bar{D}^0)$ for different values of C_T .

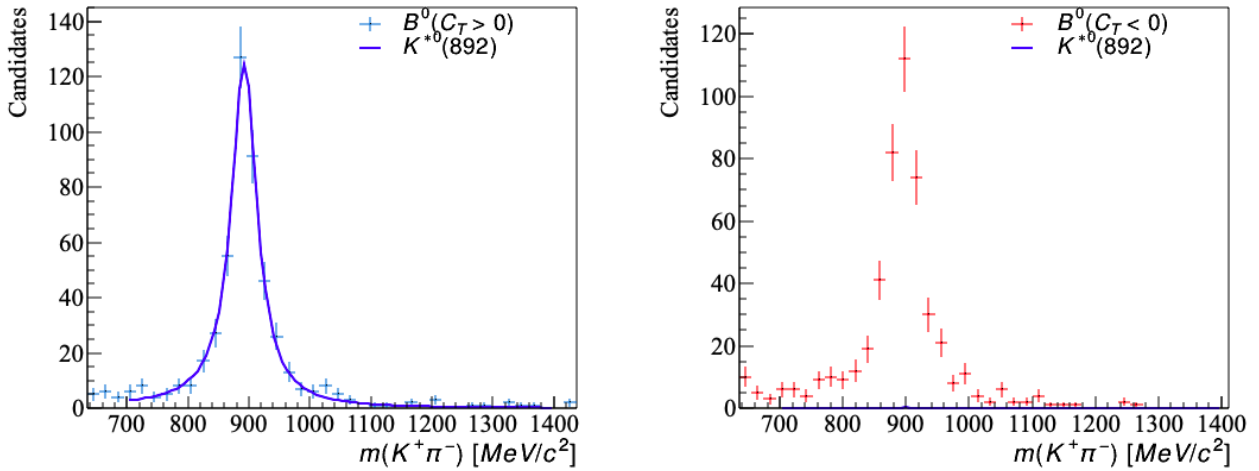


Figure 19: The binned distributions of invariant mass $m(K^+ \pi^-)$ for different values of C_T .

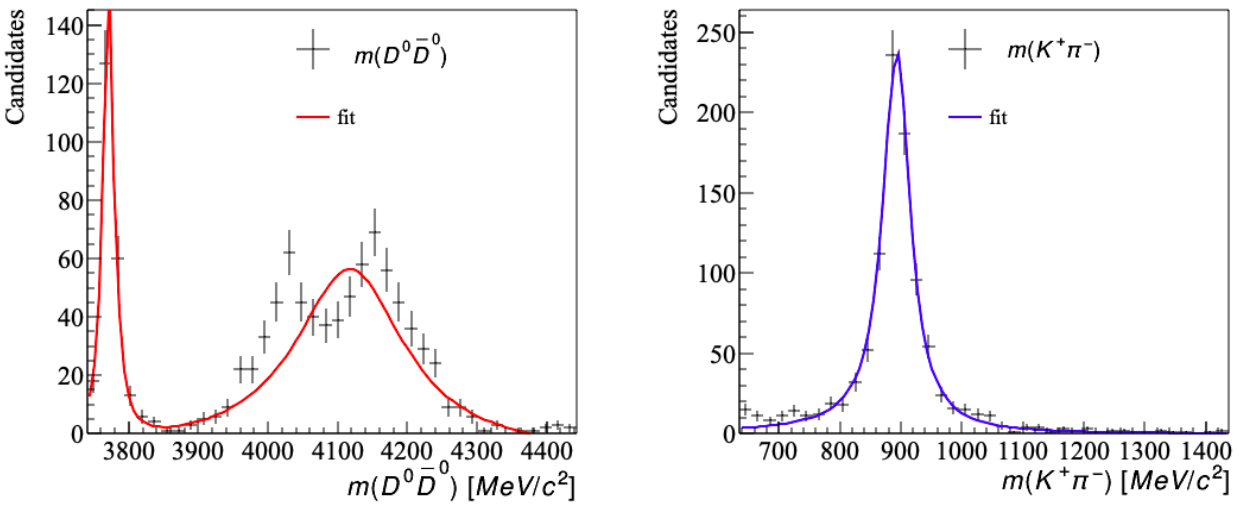


Figure 20: The binned distributions of invariant mass $m(D^0 \bar{D}^0)$ by combining the data from $C_T < 0$ and $C_T > 0$.

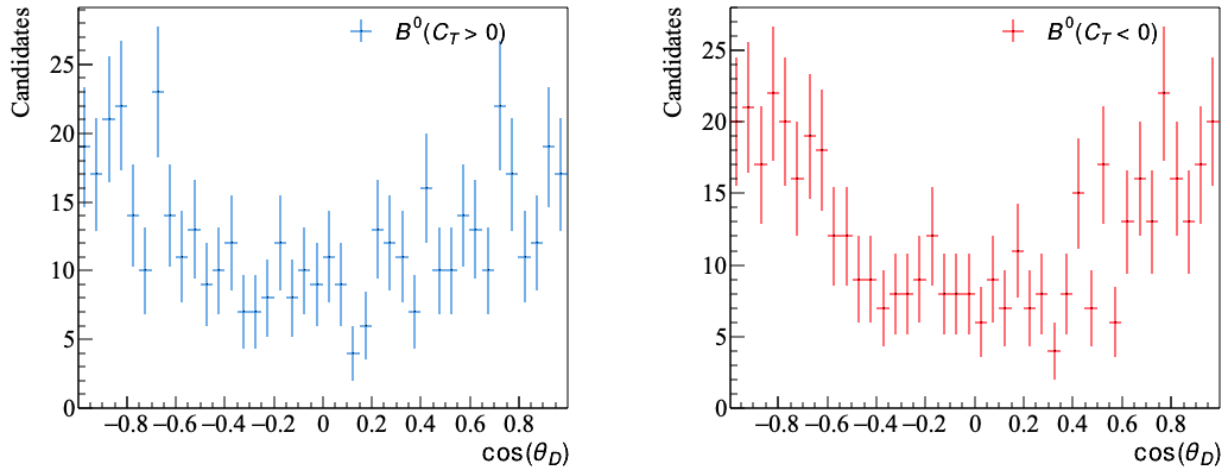


Figure 21: The binned distributions of helicity angle $\cos(\theta_{D^0})$ for different values of C_T .

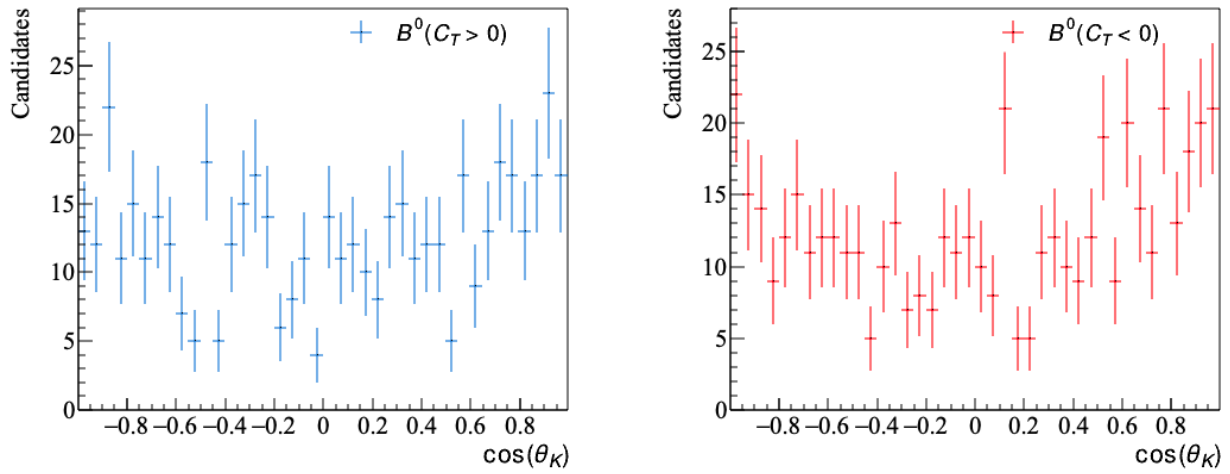


Figure 22: The binned distributions of helicity angle $\cos(\theta_{K^+})$ for different values of C_T .

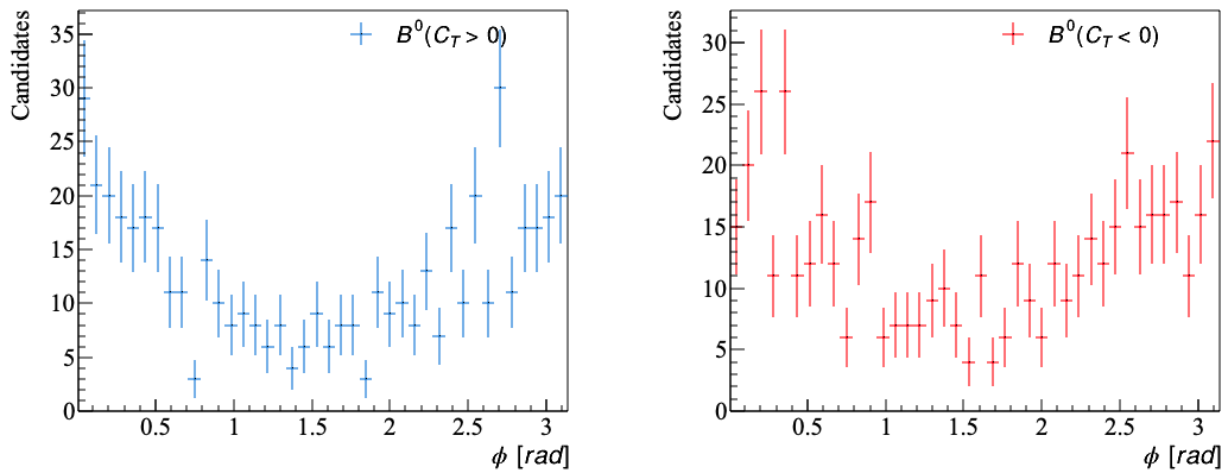


Figure 23: The binned distributions of the angle ϕ between the plane $D^0\bar{D}^0$ and the plane $K^+\pi^-$ for different values of C_T .

b. AmpGen - 10000 events: $A_T = 0.0156 \pm 0.0099987$

In order to have better fittings, more events were generated. This fit the data properly with errors being 10^2 smaller in the fitted parameters. An investigation in the confidence level of A_T , the errors in the parameters vs the number of events can be carried out.

For Fig.28, Fig.29, Fig.30, it was asked why the peaks are downwards rather than upwards in the LHCb seminar (8th Feb). It is also expected to be more flat for the helicity angles.

resonance	mass(M)	err_M	width	err_w	Chi2	type
psi(3770)	3.770	0.00033	0.0272	0.001		PDG
psi(3770)	3.7726	0.0005	0.0236	0.0010	578.2912	combined
psi(3770)	3.7718	0.0006	0.0215	0.0014	217.7001	$C_T > 0$
psi(3770)	3.7729	0.0007	0.0236	0.0014	243.6756	$C_T < 0$
psi(4040)	4.039	0.001	0.08	0.01		PDG
psi(4040)	4.0209	0.0020	0.1206	0.0049	578.2912	combined
psi(4040)	4.0203	0.0029	0.1305	0.0086	217.7001	$C_T > 0$
psi(4040)	4.0225	0.0031	0.1276	0.0083	243.6756	$C_T < 0$
psi(4160)	4.191	0.005	0.07	0.01		PDG
psi(4160)	4.1599	0.0014	0.0878	0.0028	578.2912	combined
psi(4160)	4.1612	0.0020	0.0944	0.0047	217.7001	$C_T > 0$
psi(4160)	4.1589	0.0022	0.0968	0.0045	243.6756	$C_T < 0$
K*0(892)	0.89555	0.0002	0.0473	0.0005		PDG
K*0(892)	0.8941	0.0003	0.0495	0.0008	123.0759	combined
K*0(892)	0.8943	0.0005	0.0498	0.0011	112.0466	$C_T > 0$
K*0(892)	0.8939	0.0005	0.0478	0.0010	94.4253	$C_T < 0$

Figure 24: The fitted values from the curves in Fig.25,26,27(MeV)

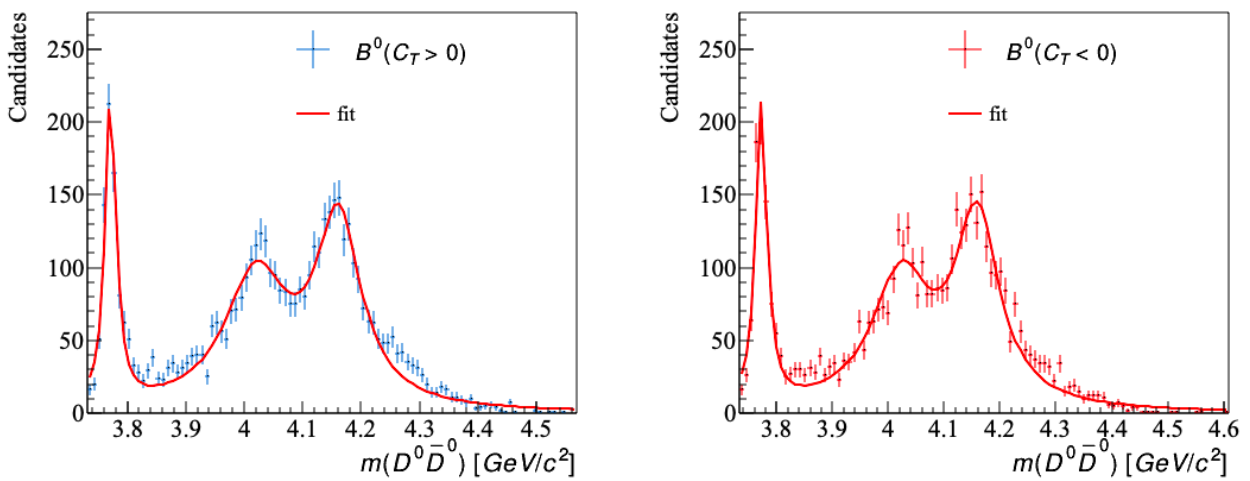


Figure 25: The binned distributions of invariant mass $m(D^0\bar{D}^0)$ for different values of C_T .

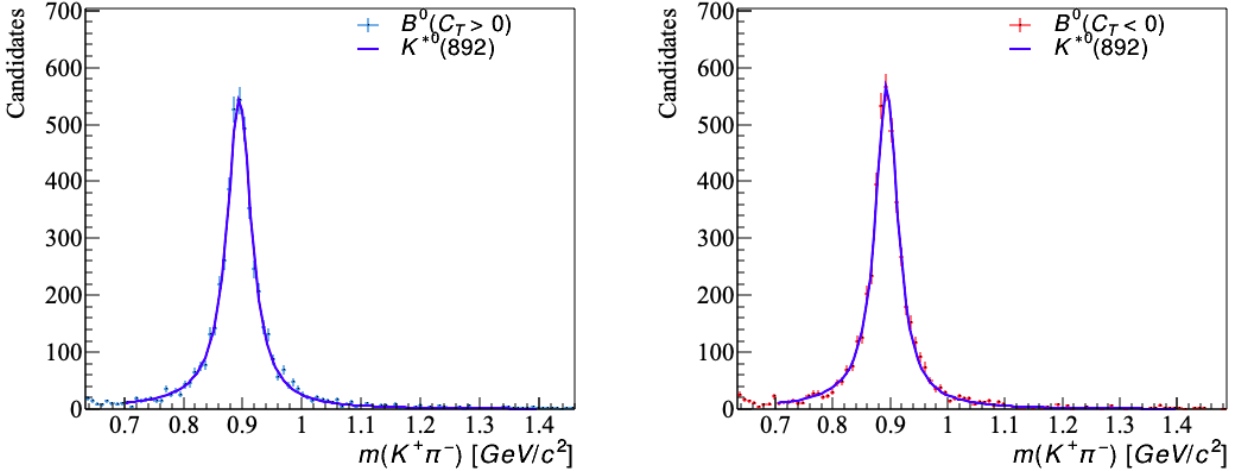


Figure 26: The binned distributions of invariant mass $m(K^+\pi^-)$ for different values of C_T .

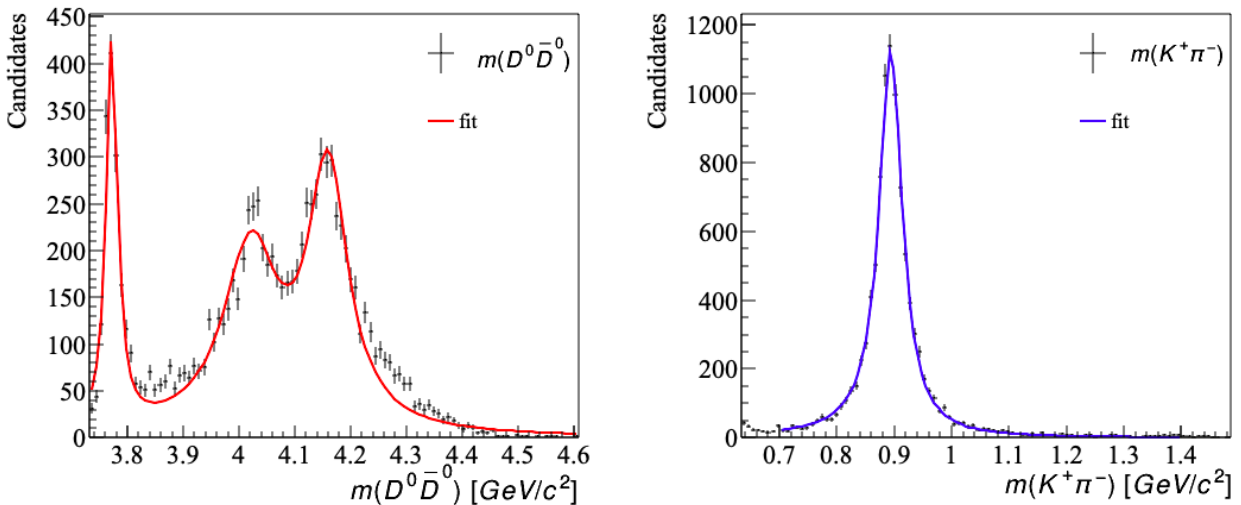


Figure 27: The binned distributions of invariant mass $m(D^0\bar{D}^0)$ for different values of C_T .

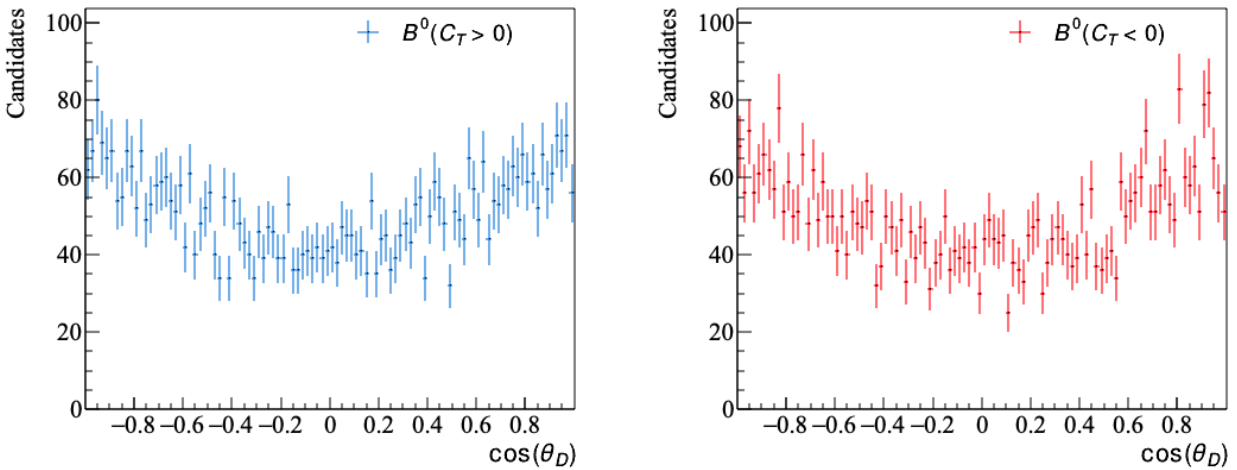


Figure 28: The binned distributions of helicity angle $\cos(\theta_{D^0})$ for different values of C_T .

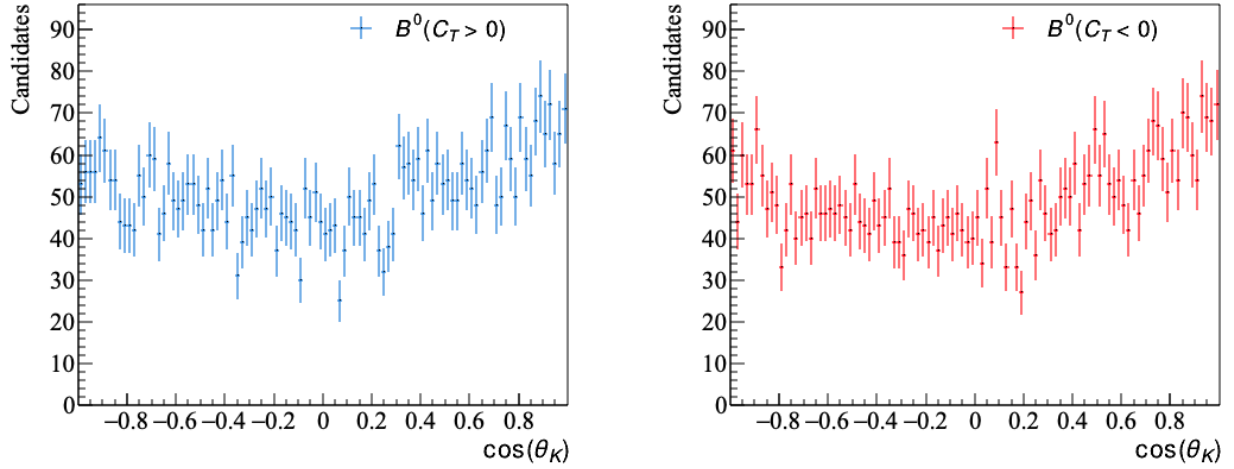


Figure 29: The binned distributions of helicity angle $\cos(\theta_{K^+})$ for different values of C_T .

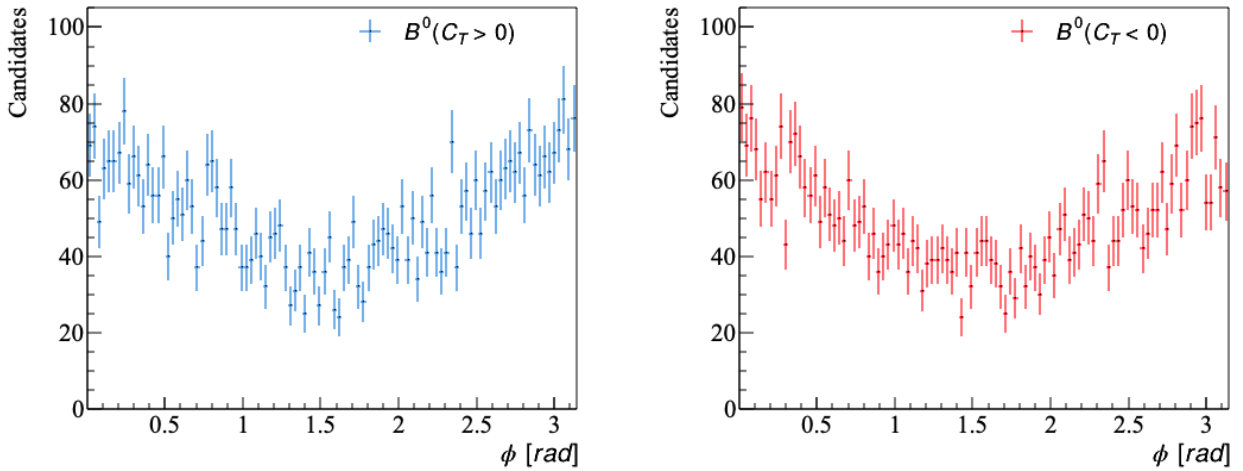


Figure 30: The binned distributions of the angle ϕ between the plane $D^0\bar{D}^0$ and the plane $K^+\pi^-$ for different values of C_T .

To do list:

- CP violation for D0 and for B0 decay.
- split the amplitude to account for different spins, first make the 1/3 of the original value and make the phase equal
- check the amount of CP violation vs number of events
- check P violation in several decay modes (all resonances, single resonance, etc)
- check the meaning of K~, pi# in the .root file generated (try flipping the sign of the momentum for _3_K~ and _4_pi#)
 - ⇒ have got the same results for CM variables

The charge conjugate decays can be generated using a different Seed in AmpGen (e.g. add a line in the .opt file: Seed 6) and inverting the sign of the 3-momenta for the generated MC data. This means initially we have got a particle goes to the (e.g.) +ve direction, and by flipping the sign, the particle goes to the negative direction, but this equivalent to its antiparticle goes to the +ve direction. By doing this for all the particles, we have generated the same decay but with charge-conjugate mesons. (Would there be a better explanation for this?)

The inverted 3-momentum gives the value of \bar{C}_T . To find the triple product asymmetry for the charge-conjugate decays, one need to count the number of events with $-\bar{C}_T > 0$ and $-\bar{C}_T < 0$.

a. Find the CP asymmetry in the $D^0 \rightarrow K^+ K^- \pi^+ \pi^-$ decay:

Re-run the `DtoKKpipi_v2.opt` file using Seed 5 and 7 with 171300 events, gives

$$\bar{A}_T = -0.072563 \pm 0.0024, A_T = -0.073987 \pm 0.0024 \text{ (previous results),}$$

and, hence $\mathcal{A}_{CP} = 0.5(A_T - \bar{A}_T) = -0.000712 \pm 0.0017$.

This is over a half smaller than the literature.⁴

b. Find the CP violation in $B^0 \rightarrow D^0 \bar{D}^0 K^+ \pi^-$ decay:

Re-run the `B0toDDbar0K+pi-.opt` file after adding `NonResS0`, with 10^4 events, using Seed 5 and 7, gives

$$A_T = 0.012 \pm 0.01, \bar{A}_T = 0.0102 \pm 0.01,$$

and, hence $\mathcal{A}_{CP} = 0.5(A_T - \bar{A}_T) = 0.0009 \pm 0.0071$.

For 10^5 events, with the B0 decay, using Seed 0 (no seed specified) and 8, gives

$$A_T = 0.0015 \pm 0.0034, \bar{A}_T = -0.00148 \pm 0.0031,$$

find $\mathcal{A}_{CP} = 0.0015 \pm 0.002$.

All the results are within the uncertainty and show no CP violation.

⁴The LHCb collaboration, “Search for CP Violation using T-odd Correlations in $D^0 \rightarrow K^+ K^- \pi^+ \pi^-$ Decays”.

This value of \mathcal{A}_{CP} was investigated further for a range of event numbers:

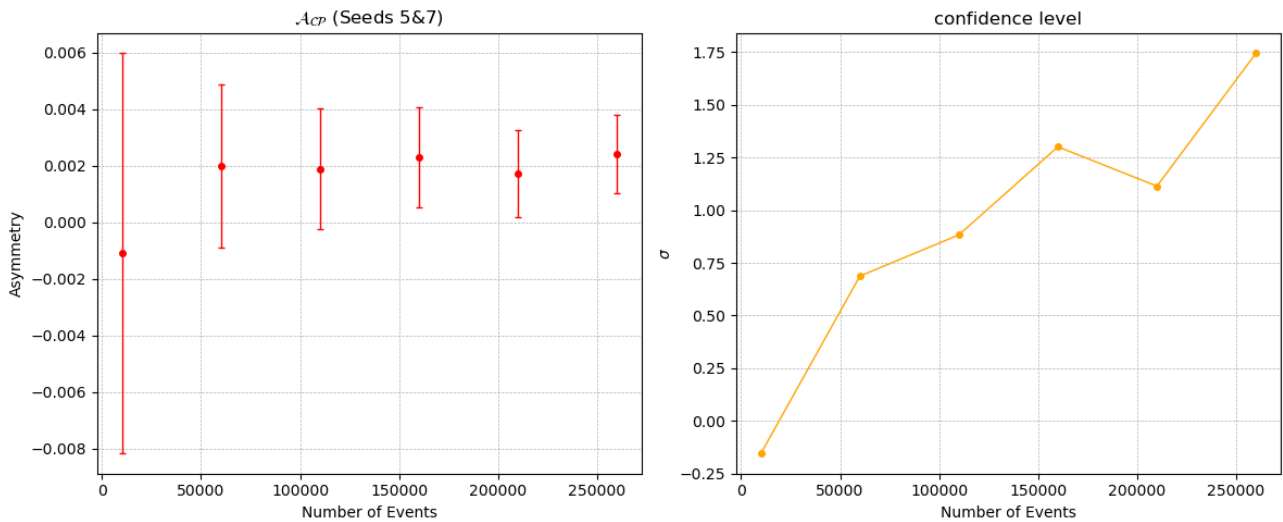


Figure 31: The asymmetries calculated for different number of events.

It can be seen that the \mathcal{A}_{CP} is slightly deviated from zero with errorbars becoming smaller and excluding zero, but the confidence level is less than 2σ , where $\sigma = \mathcal{A}_{CP}/\Delta(\mathcal{A}_{CP})$. Clearly, more events need to be generated to see the trend of asymmetry and error bars.

From Paras: [One is that we indeed still have to specify independent couplings of differing spin configurations separately. In practical terms, for the "vector-vector" decays i.e decays to two spin-1 particles (such as $B \rightarrow \psi K^*$) we need to specify S P and D waves, there should be examples of this in the $D \rightarrow KK\pi\pi$ opt file. We should discuss at some point how to split the amplitude and phase across the components (first instinct: make each amplitude 1/3 of the current value, and make all phases the same).]

The idea is we should take consideration of the different angular momentum states (the S, P, D waves) for the decay modes with two spin-1 particles in the intermediate states. For example, the decay $B^0 \rightarrow \psi(3770)K_0^*(892)$. The initial state B^0 has $J^P = 0^-$ (P-odd), while $\psi(3770)$ and $K_0^*(892)$ both has $J^P = 1^-$, where J is the intrinsic spin of the particle. Hence the total spin in the final states can be $S = 0, 1, 2$. Since the initial state has $J = 0$ one need $L + S = 0$ in the final state to conserve angular momentum (L is the orbital angular momentum quantum number), which results in $L = 0, 1, 2$ in the final state. This corresponds to value of $S = 0, 1, 2$, and is called S, P and D waves, respectively. The Parity eigenvalue for this decay mode can be calculated from (a deep discussion for this can be found in⁵):

$$P = (-1)^L \times \prod \text{(intrinsic parity)} = \begin{cases} (-1)^0(-1)(-1) = +1, & \text{if } L = 0 \text{ (S waves)} \\ (-1)^1(-1)(-1) = -1, & \text{if } L = 1 \text{ (P waves)} \\ (-1)^2(-1)(-1) = +1, & \text{if } L = 2 \text{ (D waves)} \end{cases} \quad (7)$$

Hence, the S and D waves are P-even and the P waves are P-odd, and P violation can be induced from the interference of these waves. The amount of P violation depends on the relative amplitude A_n and phase ϕ_n of the waves, where each decay mode with a particular wave has a coupling constant $A_n e^{i\phi_n}$. Thus, the inference amplitudes can be written as:

$$\begin{aligned} \mathcal{I} &= |A_1 e^{i\phi_1} + A_2 e^{i\phi_2}|^2 \\ &= (A_1 e^{i\phi_1} + A_2 e^{i\phi_2})(A_1 e^{-i\phi_1} + A_2 e^{-i\phi_2}) \\ &= A_1^2 + A_2^2 + A_1 A_2 (e^{i(\phi_2 - \phi_1)} + e^{i(\phi_1 - \phi_2)}) \\ &= A_1^2 + A_2^2 + 2A_1 A_2 \cos(\phi_2 - \phi_1) \end{aligned} \quad (8)$$

In the B0toDDbar0K+pi-.opt file, the two spin-1 particles are (all have $J^P = 1^-$):

$\psi(3770)$ and $K^*(892)0$
 $\psi(4040)$ and $K^*(892)0$
 $\psi(4160)$ and $K^*(892)0$
 $\psi(4415)$ and $K^*(892)0$

For a single resonance,

B0{psi(3770)0{D0,Dbar0},K*(892)0{K+,pi-}} 2 6.28 0.05 2 0. 10.

This was changed by taking 1/3 of the second number column - amplitude):

B0[S]{psi(3770)0{D0,Dbar0},K*(892)0{K+,pi-}} 2 2.093 0.05 2 0. 10.
B0[P]{psi(3770)0{D0,Dbar0},K*(892)0{K+,pi-}} 2 2.093 0.05 2 0. 10.
B0[D]{psi(3770)0{D0,Dbar0},K*(892)0{K+,pi-}} 2 2.093 0.05 2 0. 10.

- There are no errors generated and gives different results as before in the output .root file.

Next:

Adjust the p waves and check p-violation
test for more event numbers

⁵P. d'Argent et al. "Amplitude analyses of $D^0 \rightarrow \pi^+\pi^-\pi^+\pi^-$ and $D^0 \rightarrow K^+K^-\pi^+\pi^-$ decays". In: *J. HEP* 2017.5 (2017). ISSN: 1029-8479.

The events were generated with increasing event numbers and smaller intervals. It can be seen in Fig.32 that there is a fluctuation in the asymmetries at around $2 \cdot 10^5$ events and the asymmetries goes to zero at larger events numbers. This shows no CP and P violation. The errors in the asymmetries decreases asymptotically closing to zero as the event number increases.

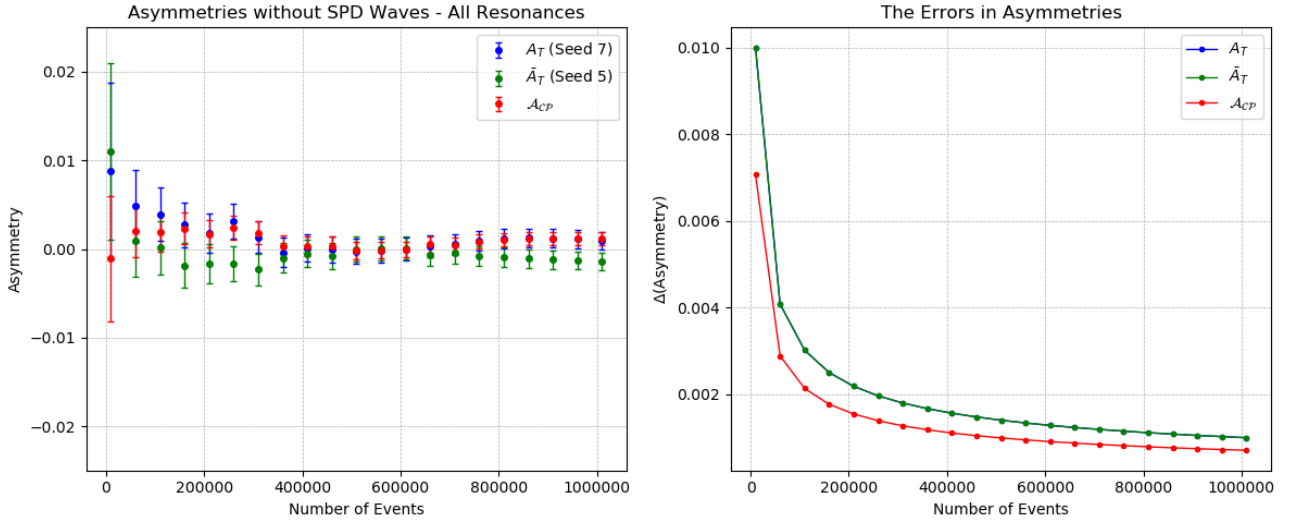


Figure 32: The asymmetries calculated for different number of events.

By adding the S, P, and D waves, the values of A_T and \bar{A}_T are no longer consistent with zero which means there are P violation induced in the regular and conjugate decays, as shown in Fig.33.,

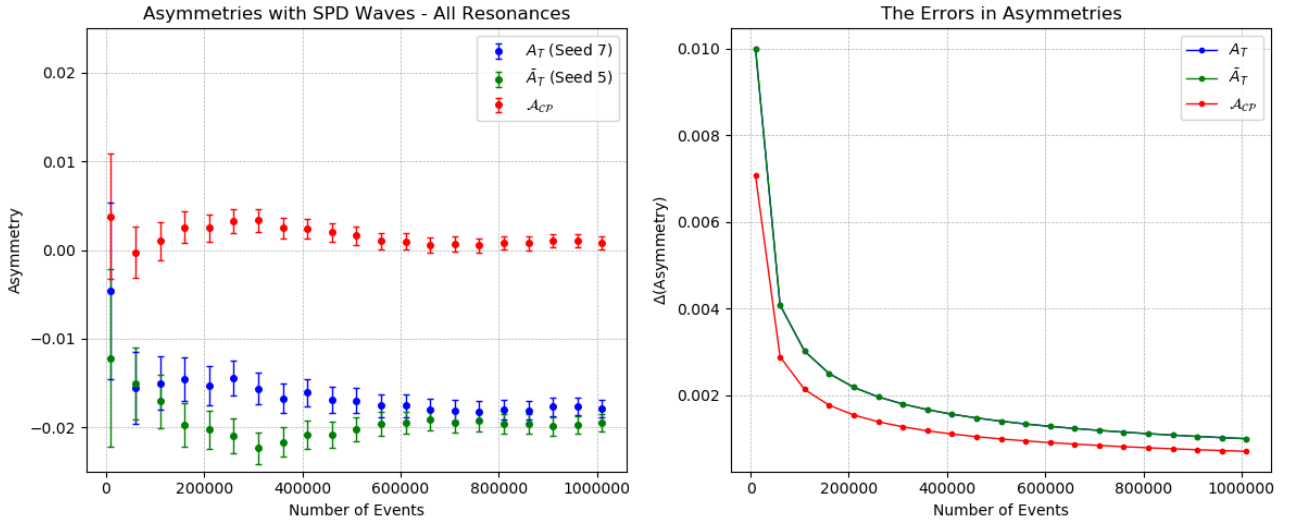


Figure 33: The asymmetries calculated for different number of events with equal SPD waves.

This part starts by changing the amplitude of P waves in the resonance files:

A. Change all P wave amplitudes

Input files: AmpGen/build/bin/spd_waves_gen

Output files: Simulations/B02DDbarKPi/p_waves

event file (.opt) Example:

```

1 EventType B0 D0 Dbar0 K+ pi-
2
3 B0{NonResS0{D0,Dbar0},K*(892)0{K+,pi-}} 0    2.09    1.  0  0  10
4
5 B0{NonResS0{D0,Dbar0},K(0)*(1430)0{K+,pi-}} 0    0.66    1.  0  0  10
6
7 B0{K(0)*(800)0{K+,pi-},NonResS0{D0,Dbar0}} 0    0.66    1.  0  0  10
8
9 B0{D(s2)(2573)+{D0,K+},Dbar0,pi-} 0      0.10   0.05 0      0.     10.
10
11 B0[S]{psi(3770)0{D0,Dbar0},K*(892)0{K+,pi-}} 2      2.093  0.05  2   0.  10.
12 B0[P]{psi(3770)0{D0,Dbar0},K*(892)0{K+,pi-}} 2      0.002093 0.05  2   0.  10.
13 B0[D]{psi(3770)0{D0,Dbar0},K*(892)0{K+,pi-}} 2      2.093  0.05  2   0.  10.
14
15 B0[P]{psi(4040)0{D0,Dbar0},K*(892)0{K+,pi-}} 0      0.000826 0.05  0   0.  10.
16 B0[S]{psi(4040)0{D0,Dbar0},K*(892)0{K+,pi-}} 0      0.826   0.05  0   0.  10.
17 B0[D]{psi(4040)0{D0,Dbar0},K*(892)0{K+,pi-}} 0      0.826   0.05  0   0.  10.
18
19 B0[D]{psi(4160)0{D0,Dbar0},K*(892)0{K+,pi-}} 0      1.31    0.05  0.  0.  10.
20 B0[S]{psi(4160)0{D0,Dbar0},K*(892)0{K+,pi-}} 0      1.31    0.05  0.  0.  10.
21 B0[P]{psi(4160)0{D0,Dbar0},K*(892)0{K+,pi-}} 0      0.00131 0.05  0.  0.  10.
22
23 B0[P]{psi(4415)0{D0,Dbar0},K*(892)0{K+,pi-}} 0      0.00051 0.05  0.  0.  10.
24 B0[S]{psi(4415)0{D0,Dbar0},K*(892)0{K+,pi-}} 0      0.51    0.05  0.  0.  10.
25 B0[D]{psi(4415)0{D0,Dbar0},K*(892)0{K+,pi-}} 0      0.51    0.05  0.  0.  10.
26
27 B0{psi(3770)0{D0,Dbar0},K(0)*(800)0{K+,pi-}} 0      1.99    0.05  0.  0.  10.
28 B0{psi(4040)0{D0,Dbar0},K(0)*(800)0{K+,pi-}} 0      0.78    0.05  0.  0.  10.
29 B0{psi(4160)0{D0,Dbar0},K(0)*(800)0{K+,pi-}} 0      1.24    0.05  0.  0.  10.
30 B0{psi(4415)0{D0,Dbar0},K(0)*(800)0{K+,pi-}} 0      0.48    0.05  0.  0.  10.
31
32 B0{psi(3770)0{D0,Dbar0},K(0)*(1430)0{K+,pi-}} 0      1.99    0.05  0.  0.  10.
33 B0{psi(4040)0{D0,Dbar0},K(0)*(1430)0{K+,pi-}} 0      0.78    0.05  0.  0.  10.
34 B0{psi(4160)0{D0,Dbar0},K(0)*(1430)0{K+,pi-}} 0      1.24    0.05  0.  0.  10.
35 B0{psi(4415)0{D0,Dbar0},K(0)*(1430)0{K+,pi-}} 0      0.48    0.05  0.  0.  10.
36
37 #B0{Z(c)(3900)+{D*(2010)+{D0,pi+},Dbar0},K-} 2   1   0   2   0   0

```

Figure 34: An example of event file for the plot in Fig.37

Changed the second number column in line 12, 15, 21, 23.

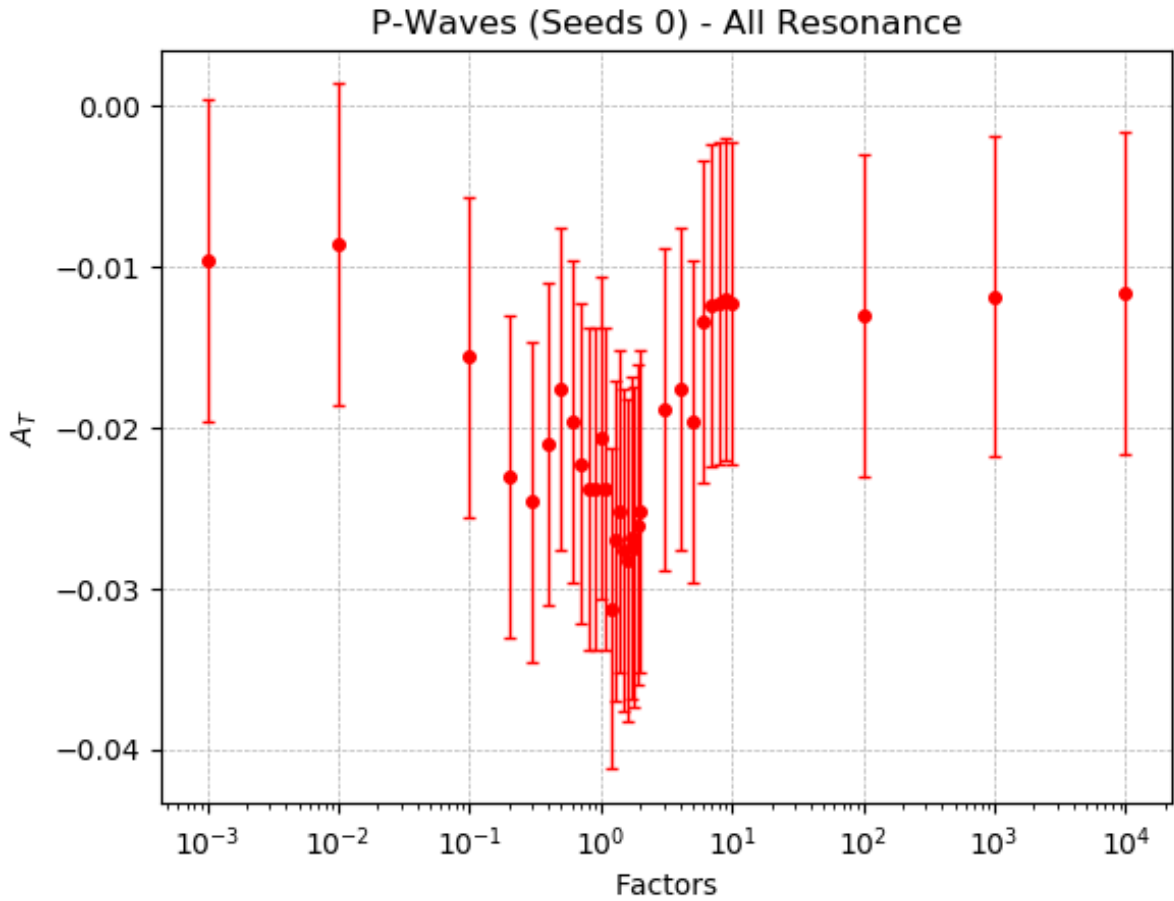


Figure 35: The change of A_T by multiplying all the P wave amplitudes with the factors in x-axis using 10^4 events.

All the events and P wave values are generated with the same seed - no seed specified (Seed 0).

B. Change all SP wave amplitudes and make them equal

Input files: AmpGen/build/bin/spd_waves_gen

Output files: Simulations/B02DDbarKPi/sp_waves

event file (.opt) Example:

```

1 EventType B0 D0 Dbar0 K+ pi-
2
3 B0{NonResS0{D0,Dbar0},K*(892)0{K+,pi-}} 0    2.09    1.  0   0   10
4
5 B0{NonResS0{D0,Dbar0},K(0)*(1430)0{K+,pi-}} 0    0.66    1.  0   0   10
6
7 B0{K(0)*(800)0{K+,pi-},NonResS0{D0,Dbar0}} 0    0.66    1.  0   0   10
8
9 B0{D(s2)(2573)+{D0,K+},Dbar0,pi-} 0      0.10    0.05 0      0.      10.
10
11 B0[S]{psi(3770)0{D0,Dbar0},K*(892)0{K+,pi-}} 2      0.002093  0.05    2  0.  10.
12 B0[P]{psi(3770)0{D0,Dbar0},K*(892)0{K+,pi-}} 2      0.002093  0.05    2  0.  10.
13 B0[D]{psi(3770)0{D0,Dbar0},K*(892)0{K+,pi-}} 2      2.093   0.05    2  0.  10.
14
15 B0[P]{psi(4040)0{D0,Dbar0},K*(892)0{K+,pi-}} 0      0.000826  0.05    0      0.  10.
16 B0[S]{psi(4040)0{D0,Dbar0},K*(892)0{K+,pi-}} 0      0.000826  0.05    0      0.  10.
17 B0[D]{psi(4040)0{D0,Dbar0},K*(892)0{K+,pi-}} 0      0.826    0.05    0      0.  10.
18
19 B0[D]{psi(4160)0{D0,Dbar0},K*(892)0{K+,pi-}} 0      1.31    0.05    0.  0.  10.
20 B0[S]{psi(4160)0{D0,Dbar0},K*(892)0{K+,pi-}} 0      0.00131  0.05    0.  0.  10.
21 B0[P]{psi(4160)0{D0,Dbar0},K*(892)0{K+,pi-}} 0      0.00131  0.05    0.  0.  10.
22
23 B0[P]{psi(4415)0{D0,Dbar0},K*(892)0{K+,pi-}} 0      0.00051  0.05    0.  0.  10.
24 B0[S]{psi(4415)0{D0,Dbar0},K*(892)0{K+,pi-}} 0      0.00051  0.05    0.  0.  10.
25 B0[D]{psi(4415)0{D0,Dbar0},K*(892)0{K+,pi-}} 0      0.51    0.05    0.  0.  10.
26
27 B0{psi(3770)0{D0,Dbar0},K(0)*(800)0{K+,pi-}} 0      1.99    0.05    0.  0.  10.
28 B0{psi(4040)0{D0,Dbar0},K(0)*(800)0{K+,pi-}} 0      0.78    0.05    0.  0.  10.
29 B0{psi(4160)0{D0,Dbar0},K(0)*(800)0{K+,pi-}} 0      1.24    0.05    0.  0.  10.
30 B0{psi(4415)0{D0,Dbar0},K(0)*(800)0{K+,pi-}} 0      0.48    0.05    0.  0.  10.
31
32 B0{psi(3770)0{D0,Dbar0},K(0)*(1430)0{K+,pi-}} 0      1.99    0.05    0.  0.  10.
33 B0{psi(4040)0{D0,Dbar0},K(0)*(1430)0{K+,pi-}} 0      0.78    0.05    0.  0.  10.
34 B0{psi(4160)0{D0,Dbar0},K(0)*(1430)0{K+,pi-}} 0      1.24    0.05    0.  0.  10.
35 B0{psi(4415)0{D0,Dbar0},K(0)*(1430)0{K+,pi-}} 0      0.48    0.05    0.  0.  10.
36
37 #B0{Z(c)(3900)+{D*(2010)+{D0,pi+},Dbar0},K-} 2  1  0  2  0  0

```

Figure 36: An example of event file for the plot in Fig.37

Changed the second number column in line 11, 12, 15, 16, 20, 21, 23, 24.

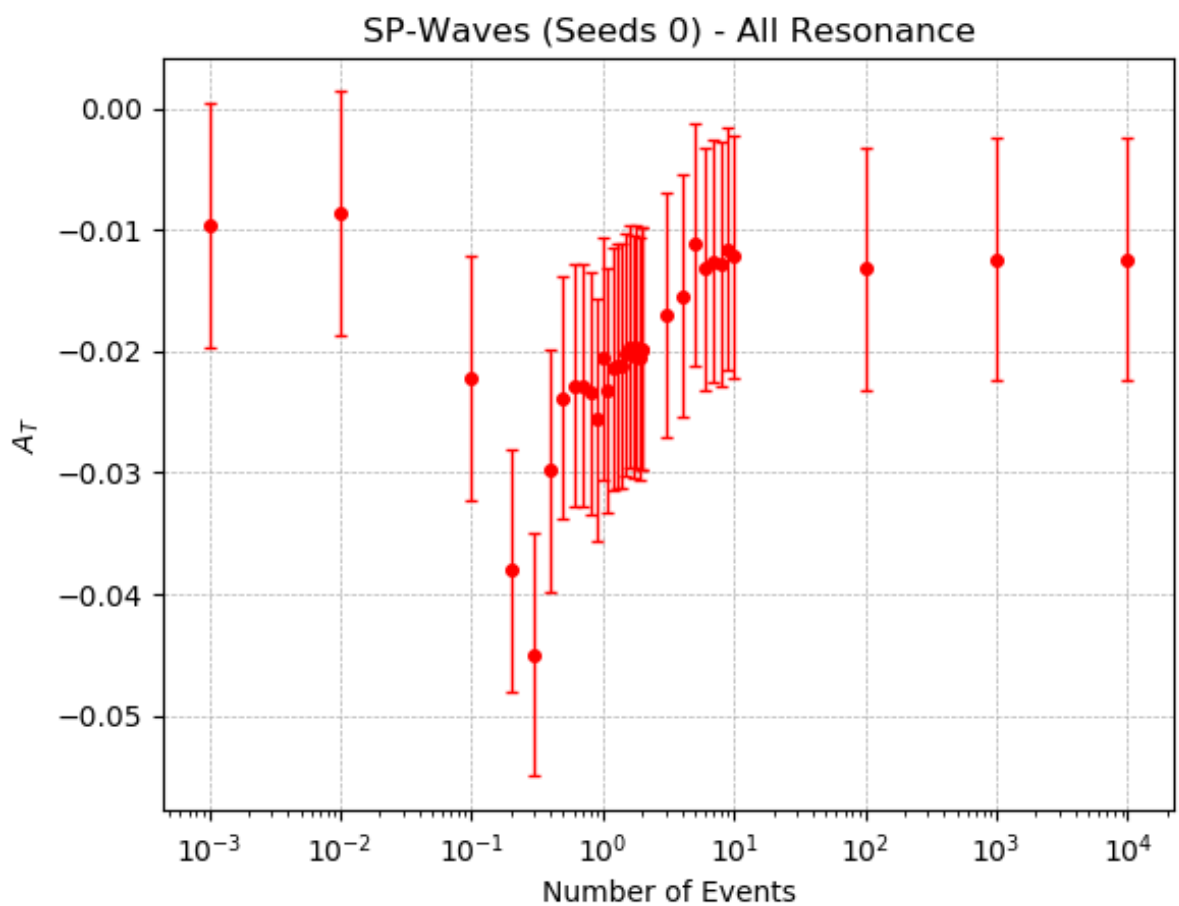


Figure 37: The change of A_T by multiplying all the S and P wave amplitudes with the factors in x-axis using 10^4 events.

C. P waves and SP waves for all resonances

Input files: AmpGen/build/bin/spd_waves_gen_sr2

Output files: Simulations/B02DDbarKPi/spd_waves_sr2

event file (.opt) Example:

```

~/AmpGen/build/bin/spd_waves_gen_sr2/B0toDDbar0K+pi-_p1E-3.opt
1 EventType B0 D0 Dbar0 K+ pi-
2
3 B0{NonResS0{D0,Dbar0},K*(892)0{K+,pi-}} 0    2.09    1.  0  0  10
4
5 B0{NonResS0{D0,Dbar0},K(0)*(1430)0{K+,pi-}} 0    0.66    1.  0  0  10
6
7 B0{K(0)*(800)0{K+,pi-},NonResS0{D0,Dbar0}} 0    0.66    1.  0  0  10
8
9 B0{D(s2)(2573)+{D0,K+},Dbar0,pi-} 0    0.10    0.05 0    0.    10.
10
11 B0[P]{psi(3770)0{D0,Dbar0},K*(892)0{K+,pi-}} 2    0.002093  0.05   2  0.  10.
12
13 B0[P]{psi(4040)0{D0,Dbar0},K*(892)0{K+,pi-}} 0    0.000826  0.05   0    0.  10.
14
15 B0[P]{psi(4160)0{D0,Dbar0},K*(892)0{K+,pi-}} 0    0.00131  0.05   0.  0.  10.
16
17 B0[P]{psi(4415)0{D0,Dbar0},K*(892)0{K+,pi-}} 0    0.00051  0.05   0.  0.  10.
18
19 B0{psi(3770)0{D0,Dbar0},K(0)*(800)0{K+,pi-}} 0    1.99    0.05   0.  0.  10.
20
21 B0{psi(4040)0{D0,Dbar0},K(0)*(800)0{K+,pi-}} 0    0.78    0.05   0.  0.  10.
22
23 B0{psi(4160)0{D0,Dbar0},K(0)*(800)0{K+,pi-}} 0    1.24    0.05   0.  0.  10.
24
25 B0{psi(4415)0{D0,Dbar0},K(0)*(800)0{K+,pi-}} 0    0.48    0.05   0.  0.  10.
26
27 B0{psi(3770)0{D0,Dbar0},K(0)*(1430)0{K+,pi-}} 0    1.99    0.05   0.  0.  10.
28
29 B0{psi(4040)0{D0,Dbar0},K(0)*(1430)0{K+,pi-}} 0    0.78    0.05   0.  0.  10.
30
31 B0{psi(4160)0{D0,Dbar0},K(0)*(1430)0{K+,pi-}} 0    1.24    0.05   0.  0.  10.
32
33 B0{psi(4415)0{D0,Dbar0},K(0)*(1430)0{K+,pi-}} 0    0.48    0.05   0.  0.  10.
34
35 #B0{Z(c)(3900)+{D*(2010)+{D0,pi+},Dbar0},K-} 2    1  0  2  0  0

```

Figure 38: An example of event file for the P-wave plot in Fig.40

Changed the second number column in line 11, 13, 15, 17.

Changed the second number column in line 11, 12, 14, 15, 17, 18, 20, 21.

```
~/AmpGen/build/bin/spd_waves_gen_sr2/B0toDDbar0K+pi-_sp1E-3.opt -
```

```

1 EventType B0 D0 Dbar0 K+ pi-
2
3 B0{NonResS0{D0,Dbar0},K*(892)0{K+,pi-}} 0 2.09 1. 0 0 10
4
5 B0{NonResS0{D0,Dbar0},K(0)*(1430)0{K+,pi-}} 0 0.66 1. 0 0 10
6
7 B0{K(0)*(800)0{K+,pi-},NonResS0{D0,Dbar0}} 0 0.66 1. 0 0 10
8
9 B0{D(s2)(2573)+{D0,K+},Dbar0,pi-} 0 0.10 0.05 0 0. 10.
10
11 B0[P]{psi(3770)0{D0,Dbar0},K*(892)0{K+,pi-}} 2 0.002093 0.05 2 0. 10.
12 B0[S]{psi(3770)0{D0,Dbar0},K*(892)0{K+,pi-}} 2 0.002093 0.05 2 0. 10.
13
14 B0[P]{psi(4040)0{D0,Dbar0},K*(892)0{K+,pi-}} 0 0.000826 0.05 0 0. 10.
15 B0[S]{psi(4040)0{D0,Dbar0},K*(892)0{K+,pi-}} 0 0.000826 0.05 0 0. 10.
16
17 B0[P]{psi(4160)0{D0,Dbar0},K*(892)0{K+,pi-}} 0 0.00131 0.05 0. 0. 10.
18 B0[S]{psi(4160)0{D0,Dbar0},K*(892)0{K+,pi-}} 0 0.00131 0.05 0. 0. 10.
19
20 B0[P]{psi(4415)0{D0,Dbar0},K*(892)0{K+,pi-}} 0 0.00051 0.05 0. 0. 10.
21 B0[S]{psi(4415)0{D0,Dbar0},K*(892)0{K+,pi-}} 0 0.00051 0.05 0. 0. 10.
22
23 B0{psi(3770)0{D0,Dbar0},K(0)*(800)0{K+,pi-}} 0 1.99 0.05 0. 0. 10.
24
25 B0{psi(4040)0{D0,Dbar0},K(0)*(800)0{K+,pi-}} 0 0.78 0.05 0. 0. 10.
26
27 B0{psi(4160)0{D0,Dbar0},K(0)*(800)0{K+,pi-}} 0 1.24 0.05 0. 0. 10.
28
29 B0{psi(4415)0{D0,Dbar0},K(0)*(800)0{K+,pi-}} 0 0.48 0.05 0. 0. 10.
30
31 B0{psi(3770)0{D0,Dbar0},K(0)*(1430)0{K+,pi-}} 0 1.99 0.05 0. 0. 10.
32
33 B0{psi(4040)0{D0,Dbar0},K(0)*(1430)0{K+,pi-}} 0 0.78 0.05 0. 0. 10.
34
35 B0{psi(4160)0{D0,Dbar0},K(0)*(1430)0{K+,pi-}} 0 1.24 0.05 0. 0. 10.
36
37 B0{psi(4415)0{D0,Dbar0},K(0)*(1430)0{K+,pi-}} 0 0.48 0.05 0. 0. 10.
38
39 #B0{Z(c)(3900)+{D*(2010)+{D0,pi+},Dbar0},K-} 2 1 0 2 0 0
40

```

Figure 39: An example of event file for the SP-wave plot in Fig.40

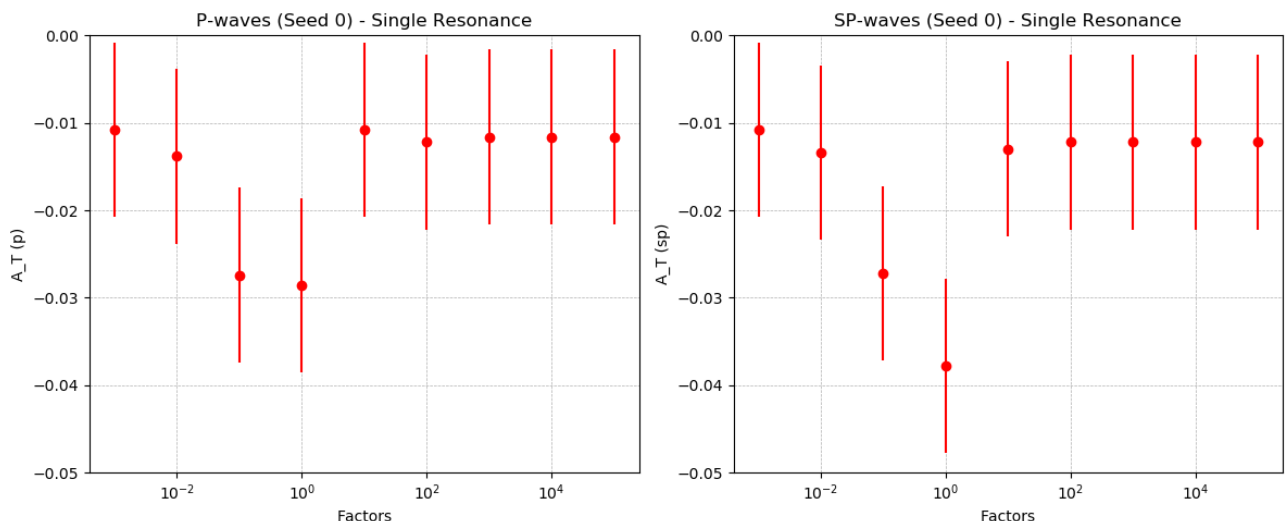


Figure 40: (left) The change of A_T by multiplying the P wave amplitudes with the factors in x-axis using 10^4 events. (right) The change of A_T by multiplying the S and P wave amplitudes equally with the factors in x-axis using 10^4 events.

Investigation on single resonance $\psi(3770)\text{K}^*(892)0$:

D. use only the P waves or SP waves for a single resonance

Input files: AmpGen/build/bin/spd_waves_gen_sr1

Output files: Simulations/B02DDbarKPi/spd_waves_sr1

event file (.opt) Example:

```
~/AmpGen/build/bin/spd_waves_gen_sr1/B0toDDbar0K+pi-_p1E-3.opt
1 EventType B0 D0 Dbar0 K+ pi-
2
3 B0[P]{psi(3770)0{D0,Dbar0},K*(892)0{K+,pi-}} 2 0.002093 0.05 2 0. 10.
```

Figure 41: An example of event file for the P-wave plot in Fig.43

Changed the second number column in line 3.

```
~/AmpGen/build/bin/spd_waves_gen_sr1/B0toDDbar0K+pi-_sp1E-3.opt
1 EventType B0 D0 Dbar0 K+ pi-
2
3
4
5 B0[S]{psi(3770)0{D0,Dbar0},K*(892)0{K+,pi-}} 2 0.002093 0.05 2 0. 10.
6 B0[P]{psi(3770)0{D0,Dbar0},K*(892)0{K+,pi-}} 2 0.002093 0.05 2 0. 10.
```

Figure 42: An example of event file for the SP-wave plot in Fig.43

Changed the second number column in line 5, 6. Reasons for flat?

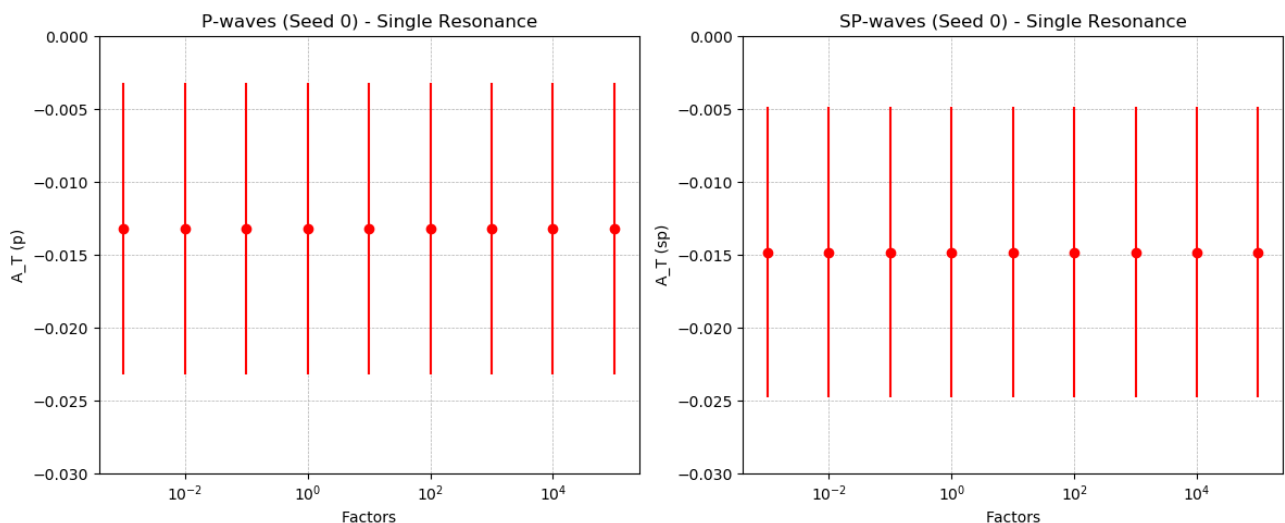


Figure 43: (left) The change of A_T by multiplying the P wave amplitudes with the factors in x-axis using 10^4 events. (right) The change of A_T by multiplying the S and P wave amplitudes equally with the factors in x-axis using 10^4 events.

Investigation on single resonance $\psi(4040)K^*(892)0$: E. P waves and SP waves single resonances with interferences

Input files: AmpGen/build/bin/spd_waves_gen_sr3
 AmpGen/build/bin/B0_event_spd_sr3_4040/sr1_seed200_10000 (for smaller intervals between -1 and 1)

Output files: Simulations/B02DDbarKPi/spd_waves_sr3
 Simulations/B02DDbarKPi/spd_waves_sr_4040

event file (.opt) Example:

```
~/AmpGen/build/bin/spd_waves_gen_sr3/B0toDDbar0K+pi-_p1E-3.opt +
1 EventType B0 D0 Dbar0 K+ pi-
2
3 B0[P]{psi(4040)0{D0,Dbar0},K*(892)0{K+,pi-}} 0 0.000826 0.05 0 0. 10.
4 B0[S]{psi(4040)0{D0,Dbar0},K*(892)0{K+,pi-}} 0 0.826 0.05 0 0. 10.
5
```

Figure 44: An example of event file for the P-wave plot in Fig.46

Changed the second number column in line 3.

```
~/AmpGen/build/bin/spd_waves_gen_sr3/B0toDDbar0K+pi-_sp1E-3.opt +
1 EventType B0 D0 Dbar0 K+ pi-
2
3 B0[P]{psi(4040)0{D0,Dbar0},K*(892)0{K+,pi-}} 0 0.000826 0.05 0 0. 10.
4 B0[S]{psi(4040)0{D0,Dbar0},K*(892)0{K+,pi-}} 0 0.000826 0.05 0 0. 10.
5 B0[D]{psi(4040)0{D0,Dbar0},K*(892)0{K+,pi-}} 0 0.826 0.05 0 0. 10.
```

Figure 45: An example of event file for the SP-wave plot in Fig.46

Changed the second number column in line 3, 4.

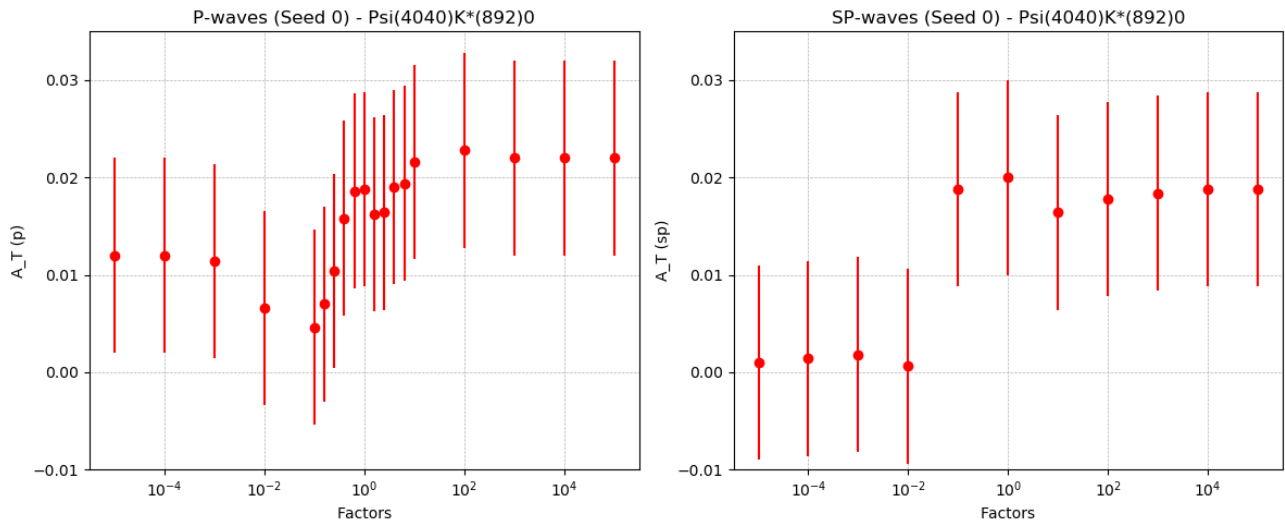


Figure 46: (left) The change of A_T by multiplying the P wave amplitudes with the factors in x-axis using 10^4 events. (right) The change of A_T by multiplying the S and P wave amplitudes equally with the factors in x-axis using 10^4 events.

21 Feb 2020, Friday

F. Split the events into ten files generated with a set of 10 seeds

(1) Same set of seed for each p wave amplitude:

Seed 0,10,20,30,40,50,60,70,80,90 — range (0,100,10)

Input files: AmpGen/build/bin/spd_waves_gen_sr3_seed

AmpGen/build/bin/B0_event_spd_sr3_4040/sr2_seed200_1000 (for smaller intervals between -1 and 1)

Output files: Simulations/B02DDbarKPi/spd_waves_combine_1E4_4040

Simulations/B02DDbarKPi/spd_waves_sr_4040

event file (.opt) Example:

```
~/AmpGen/build/bin/spd_waves_gen_sr3_seed/B0toDDbar0K+pi-_p1E-1_s20.opt
1 EventType B0 D0 Dbar0 K+ pi-
2
3 B0[P]{psi(4040)0{D0,Dbar0},K*(892)0{K+,pi-}} 0 0.0826 0.05 0 0. 10.
4 B0[S]{psi(4040)0{D0,Dbar0},K*(892)0{K+,pi-}} 0 0.826 0.05 0 0. 10.
5
6 Seed 20
```

Figure 47: An example of event file for the P-wave plot in Fig.48

Changed the second number column in line 3, 6.

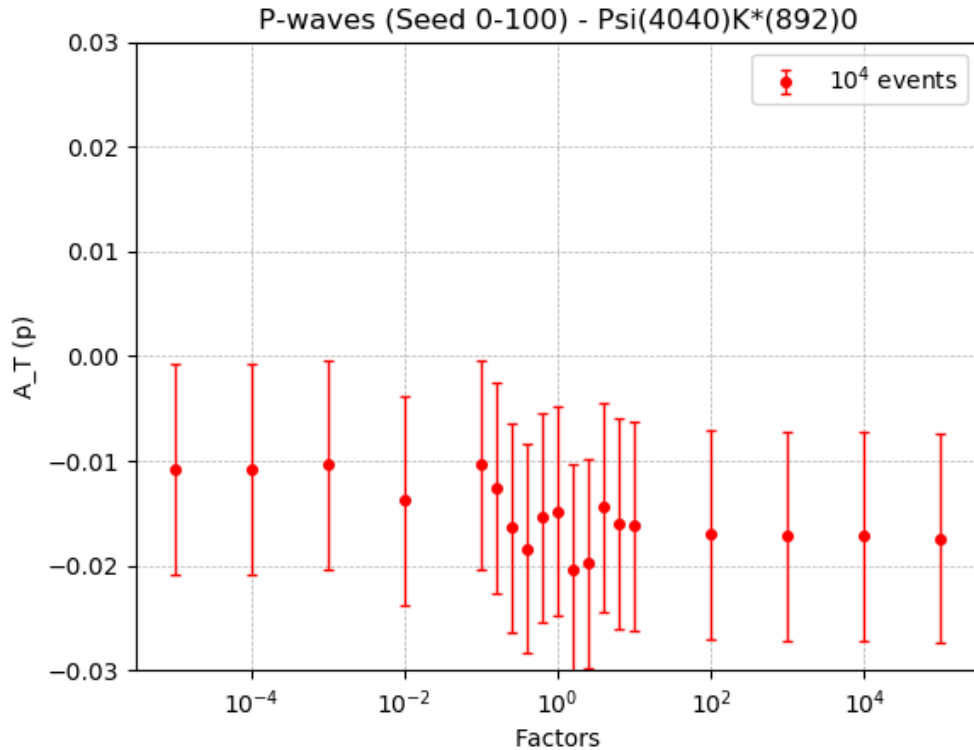


Figure 48: The change of A_T by multiplying the P wave amplitudes with the factors in x-axis using 10^4 events.

(2) Different sets of seed for each p wave amplitude:

e.g - Seed 0,20,40,60,80,100,120,140,160,180 — range (0,200,10) for $factor = 10^{-5}$

Seed 1,21,41,61,81,101,121,141,161,181 for $factor = 10^{-4}$

, etc...

Input files: AmpGen/build/bin/spd_waves_gen_sr3_seed2

AmpGen/build/bin/B0_event_spd_sr3_4040/sr3_seed200_1000 + sr3_seed200_10000 (for smaller intervals between -1 and 1)

Output files: Simulations/B02DDbarKPi/spd_waves_combined2_1E4_4040 + spd_waves_combined2_1E5_4040

Simulations/B02DDbarKPi/spd_waves_sr_4040

event file (.opt) Example:

```
~/AmpGen/build/bin/spd_waves_gen_sr3_seed2/output_opt_1E4/B0toDDbar0K+pi-_p1E-1_s64.opt
1 EventType B0 D0 Dbar0 K+ pi-
2
3 B0[P]{psi(4040)0{D0,Dbar0},K*(892)0{K+,pi-}} 0 0.0826 0.05 0 0. 10.
4 B0[S]{psi(4040)0{D0,Dbar0},K*(892)0{K+,pi-}} 0 0.826 0.05 0 0. 10.
5
6 Seed 64
```

Figure 49: An example of event file for the P-wave plot in Fig.??

Changed the second number column in line 3, 6.

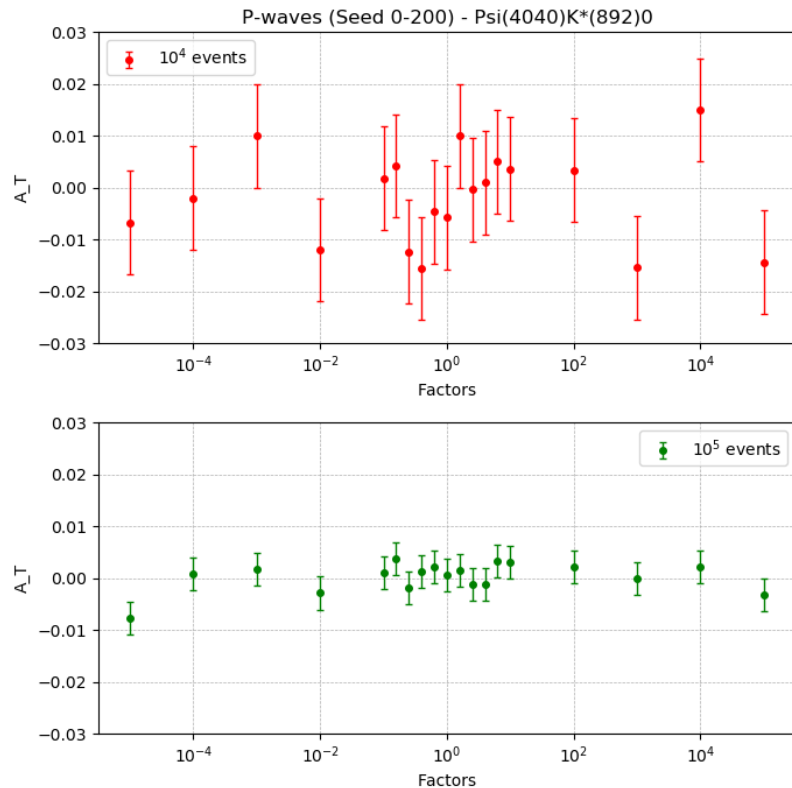


Figure 50: The change of A_T by multiplying the P wave amplitudes with the factors in x-axis using 10^4 and 10^5 events.

Put the results for $\psi(4040)\text{K}^*(892)0$ together with more events for the **E** and **F(1)** methods, this gives

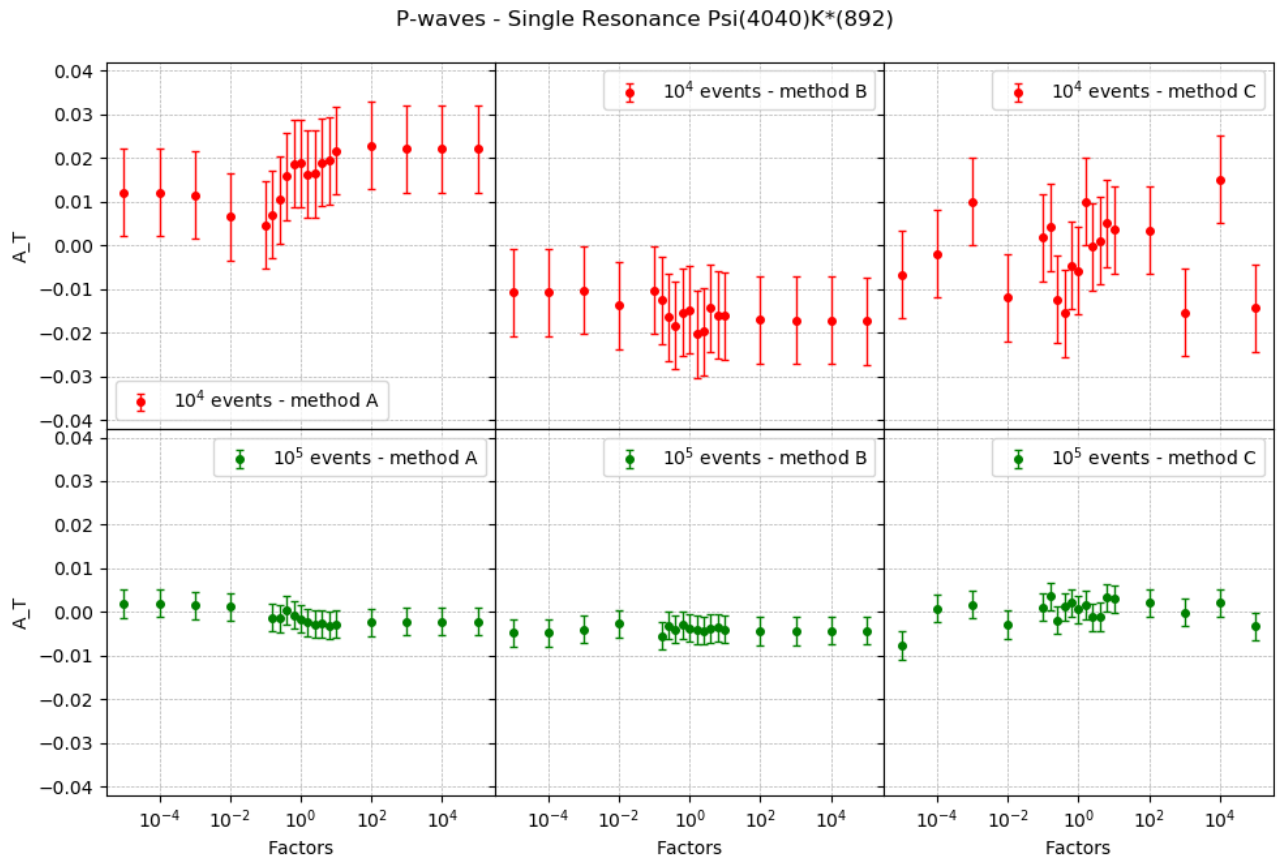


Figure 51: The change of A_T by multiplying the P wave amplitudes with the factors in x-axis using 10^4 and 10^5 events by generating events using three different methods.

More investigation on single resonance $\psi(3770)K^*(892)0$ using the methods stated in **E**, **F(1)** and **F(2)**.

Input files: AmpGen/build/bin/B0_event_spd_sr3_3770

Output files: Simulations/B02DDbarKPi/spd_waves_sr_3770

event file (.opt) Example:

(It was found we didn't specify the coordinate system in the event files. However, this doesn't effect the previous results since all the results were generated from real numbers - no phases)
We should also tell the units for the phase - I use radian.

```
~/AmpGen/build/bin/B0_event_spd_sr3_3770/B0toDbar0K+pi-.sr1.p.10000.opt
1 EventType B0 D0 Dbar0 K+ pi-
2
3 CouplingConstant::Coordinates polar
4
5 CouplingConstant::AngularUnits rad
6
7 B0[P]{psi(3770)0{D0,Dbar0},K*(892)0{K+,pi-}} 2 209300.000000000000000 0.0500000000000000 2 0.000000000000000 10.0000000000000000000
8 B0[S]{psi(3770)0{D0,Dbar0},K*(892)0{K+,pi-}} 2 2.093000000000000 0.050000000000000 2 0.000000000000000 10.0000000000000000000
```

Figure 52: An example of event file for the P-wave plot in Fig.53

Changed the second number column in line 7.

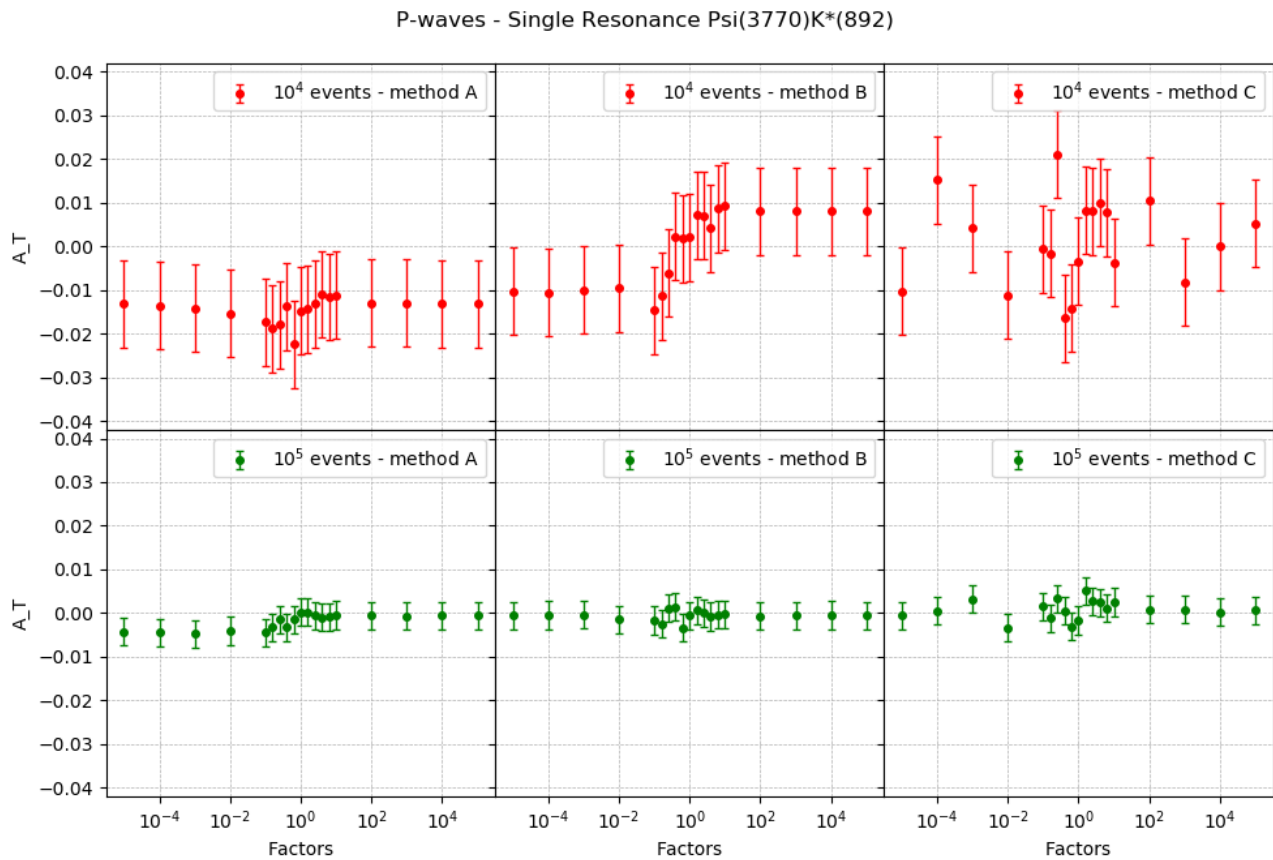


Figure 53: The change of A_T by multiplying the P wave amplitudes with the factors in x-axis using 10^4 and 10^5 events by generating events using three different methods.

Method A = **E**

Method B = **F(1)**

Method C = **F(2)**

More investigation on all resonance using the methods stated in F(2).

Input files: AmpGen/build/bin/B0_event_spd_nophase

Output files: Simulations/B02DDbarKPi/spd_waves_combine3_1E4 + spd_waves_combine3_1E5 + spd_waves_combine3_1E6

event file (.opt) Example: Changed the second number column in line 7, 8, 9, 10.

```

~/AmpGen/build/bin/B0_event_spd_nophase/B0toDbar0K+pi-_p.opt
1 EventType B0 D0 Dbar0 K+ pi-
2
3 CouplingConstant::Coordinates polar
4
5 CouplingConstant::AngularUnits rad
6
7 B0[P]{psi(3770){D0,Dbar0},K*(892){K+,pi-}} 2 13.295937219970446 0.05000000000000000 2.000000000000000 0.000000000000000 10.000000000000000
8 B0[P]{psi(4040){D0,Dbar0},K*(892){K+,pi-}} 0 5.211707665406396 0.05000000000000000 0.000000000000000 0.000000000000000 10.000000000000000
9 B0[P]{psi(4160){D0,Dbar0},K*(892){K+,pi-}} 0 8.265541212690533 0.05000000000000000 0.000000000000000 0.000000000000000 10.000000000000000
10 B0[P]{psi(4415){D0,Dbar0},K*(892){K+,pi-}} 0 3.217882456848986 0.05000000000000000 0.000000000000000 0.000000000000000 10.000000000000000
11
12 B0[S]{psi(3770){D0,Dbar0},K*(892){K+,pi-}} 2 2.093000000000000 0.05000000000000000 2.000000000000000 0.000000000000000 10.000000000000000
13 B0[D]{psi(3770){D0,Dbar0},K*(892){K+,pi-}} 2 2.093000000000000 0.05000000000000000 2.000000000000000 0.000000000000000 10.000000000000000
14 B0[S]{psi(4040){D0,Dbar0},K*(892){K+,pi-}} 0 0.826000000000000 0.05000000000000000 0.000000000000000 0.000000000000000 10.000000000000000
15 B0[D]{psi(4040){D0,Dbar0},K*(892){K+,pi-}} 0 0.826000000000000 0.05000000000000000 0.000000000000000 0.000000000000000 10.000000000000000
16 B0[S]{psi(4160){D0,Dbar0},K*(892){K+,pi-}} 0 1.310000000000000 0.05000000000000000 0.000000000000000 0.000000000000000 10.000000000000000
17 B0[D]{psi(4160){D0,Dbar0},K*(892){K+,pi-}} 0 1.310000000000000 0.05000000000000000 0.000000000000000 0.000000000000000 10.000000000000000
18 B0[S]{psi(4415){D0,Dbar0},K*(892){K+,pi-}} 0 0.510000000000000 0.05000000000000000 0.000000000000000 0.000000000000000 10.000000000000000
19 B0[D]{psi(4415){D0,Dbar0},K*(892){K+,pi-}} 0 0.510000000000000 0.05000000000000000 0.000000000000000 0.000000000000000 10.000000000000000
20
21 B0{NonResS0{D0,Dbar0},K*(892){K+,pi-}} 0 2.090000000000000 1.000000000000000 0.000000000000000 0.000000000000000 10.000000000000000
22 B0{NonResS0{D0,Dbar0},K(0)*(1430){K+,pi-}} 0 0.660000000000000 1.000000000000000 0.000000000000000 0.000000000000000 10.000000000000000
23 B0{K(0)*(800){K+,pi-},NonResS0{D0,Dbar0}} 0 0.660000000000000 1.000000000000000 0.000000000000000 0.000000000000000 10.000000000000000
24 B0{D(s2)(253)+(D0,K+),Dbar0,pi-} 0 0.100000000000000 0.050000000000000 0.000000000000000 0.000000000000000 10.000000000000000
25
26 B0{psi(3770){D0,Dbar0},K(0)*(800){K+,pi-}} 0 1.990000000000000 0.05000000000000000 0.000000000000000 0.000000000000000 10.000000000000000
27 B0{psi(4040){D0,Dbar0},K(0)*(800){K+,pi-}} 0 0.780000000000000 0.05000000000000000 0.000000000000000 0.000000000000000 10.000000000000000
28 B0{psi(4160){D0,Dbar0},K(0)*(800){K+,pi-}} 0 1.240000000000000 0.05000000000000000 0.000000000000000 0.000000000000000 10.000000000000000
29 B0{psi(4415){D0,Dbar0},K(0)*(800){K+,pi-}} 0 0.480000000000000 0.05000000000000000 0.000000000000000 0.000000000000000 10.000000000000000
30
31 B0{psi(3770){D0,Dbar0},K(0)*(1430){K+,pi-}} 0 0.990000000000000 0.05000000000000000 0.000000000000000 0.000000000000000 10.000000000000000
32 B0{psi(4040){D0,Dbar0},K(0)*(1430){K+,pi-}} 0 0.780000000000000 0.05000000000000000 0.000000000000000 0.000000000000000 10.000000000000000
33 B0{psi(4160){D0,Dbar0},K(0)*(1430){K+,pi-}} 0 1.240000000000000 0.05000000000000000 0.000000000000000 0.000000000000000 10.000000000000000
34 B0{psi(4415){D0,Dbar0},K(0)*(1430){K+,pi-}} 0 0.480000000000000 0.05000000000000000 0.000000000000000 0.000000000000000 10.000000000000000
35
36 #B0{Z(c)(3900)+(D*(2010)+(D0,pi+),Dbar0),K-} 2 1.000000000000000 0.000000000000000 2.000000000000000 0.000000000000000 0.000000000000000

```

Figure 54: An example of event file for the P-wave plot in Fig.55

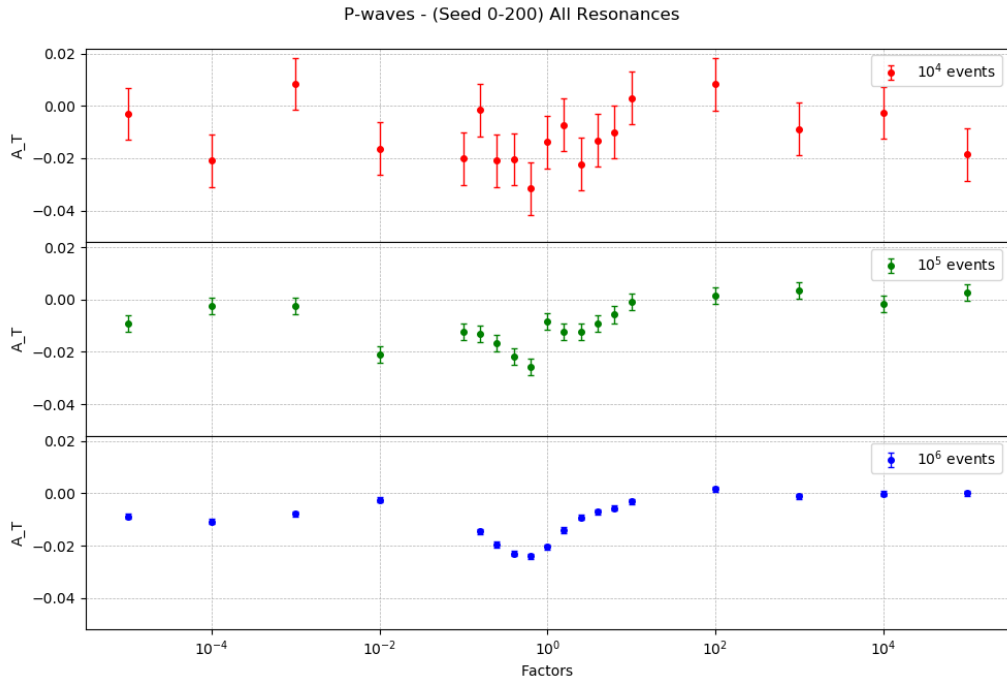


Figure 55: The change of A_T by multiplying the P wave amplitudes with the factors in x-axis using 10^4 , 10^5 and 10^6 events.

Start varying the phase of the resonance. The phase are chosen to be from -1.5π to 1.75π with intervals of 0.25π

For the single resonance - $\psi(3770)K^*(892)0$,

Input files: AmpGen/build/bin/B0_event_sr1_p_phase_1E5

Output files: Simulations/B02DDbarKPi/spd_waves_combine_phase_1E5

event file (.opt) Example:

```
~/AmpGen/build/bin/B0_event_sr1_p_phase_1E5/B0toDbar0K+pi-_p.opt
1 |Event Type B0 D0 Dbar0 K+ pi-
2
3 CouplingConstant::Coordinates polar
4
5 CouplingConstant::AngularUnits rad
6
7 B0[P]{psi(3770)0{D0,Dbar0},K*(892)0{K+,pi-}} 2 209300.0000000000000000 0.0500000000000000 2 5.497787143782139 10.00000000000000
8 B0[S]{psi(3770)0{D0,Dbar0},K*(892)0{K+,pi-}} 2 2.093000000000000 0.0500000000000000 2 0.00000000000000 10.00000000000000
```

Figure 56: An example of event file for the P-wave plot in Fig.57

Changed the second and the fifth number column in line 7.

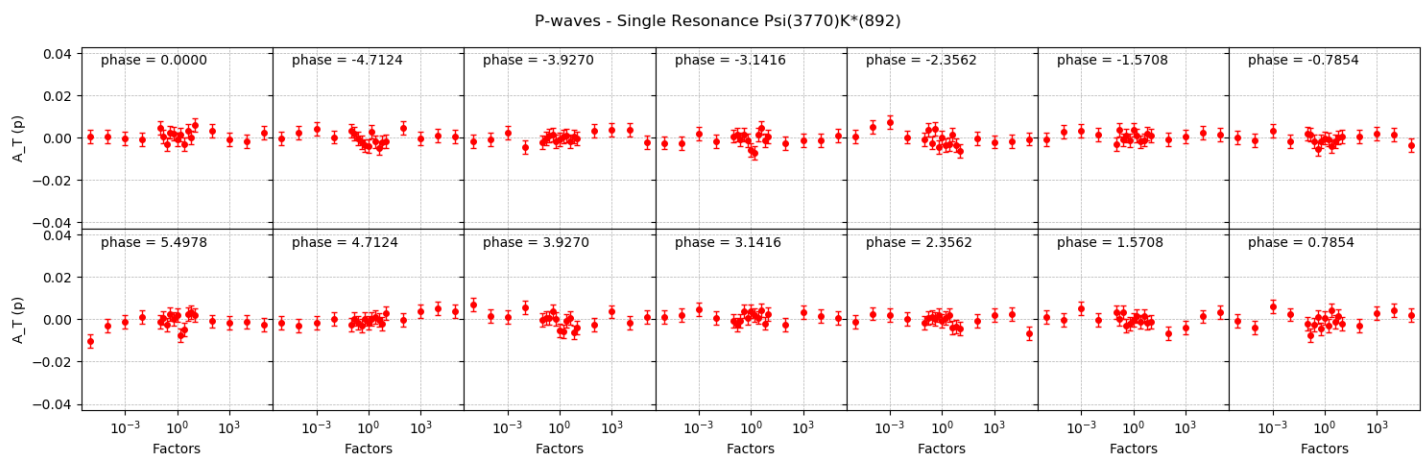


Figure 57: The change of A_T by multiplying the P wave amplitudes with the factors in x-axis using and changing the phase with 10^5 events.

- No obvious parity violation in this single resonance?

The whole process takes 22+7 hours. Would need some optimization in the codes for calculating A_T .

Have looked at the fitter in AmpGen by first generate 10^4 events using AmpGen and fit the results with SignalOnlyFitter:

SignalOnlyFitter

An example fitter is provided in `examples/SignalOnlyFitter.cpp`, which as the name suggests only has a single signal component in the fit. The free parameters of the fit are specified in the same way as the Generator, with the additional relevant slots being `DataSample` which specifies the signal sample to fit, which is presumed to already have the selection applied, and `Branches` which takes a list of branch names, and defaults to the format used by the Generator etc. More details can be found with

```
SignalOnlyFitter --help
```

For example, the fitter can be used to fit a toy MC sample generated by the generator by running:

```
Generator MyOpts.opt --nEvents 100000
SignalOnlyFitter MyOpts.opt --DataSample Generate_Output.root
```

Figure 58: Instruction of using the SignalOnlyFitter

The was done by unfixing (`fix=0`) the amplitudes and phases of the resonance in the resonance (.opt) file with all the resonances and the S, P and D waves for the two spin-1 resonance being included and fix only one resonance. Here fixing $\psi(3770)K^*(892)0[S]$ (set to be `fix=2`) for both amplitude and phase.

EventType	B0	D0	Dbar0	K+	pi-					
<code>B0{NonResS0{D0,Dbar0},K*(892)0{K+,pi-}}</code>	0			2.09	1.	0	0	10		
<code>B0{NonResS0{D0,Dbar0},K(0)*(1430)0{K+,pi-}}</code>	0			0.66	1.	0	0	10		
<code>B0{K(0)*(800)0{K+,pi-},NonResS0{D0,Dbar0}}</code>	0			0.66	1.	0	0	10		
<code>B0{D(s2)(2573)+{D0,K+},Dbar0,pi-}</code>	0			0.10	0.05	0	0.	10.		
<code>B0[S]{psi(3770)0{D0,Dbar0},K*(892)0{K+,pi-}}</code>	2			2.093	0.05	2	0.	10.		
<code>B0[P]{psi(3770)0{D0,Dbar0},K*(892)0{K+,pi-}}</code>	0			2.093	0.05	0	0.	10.		
<code>B0[D]{psi(3770)0{D0,Dbar0},K*(892)0{K+,pi-}}</code>	0			2.093	0.05	0	0.	10.		
<code>B0[P]{psi(4040)0{D0,Dbar0},K*(892)0{K+,pi-}}</code>	0			0.826	0.05	0	0.	10.		
<code>B0[S]{psi(4040)0{D0,Dbar0},K*(892)0{K+,pi-}}</code>	0			0.826	0.05	0	0.	10.		
<code>B0[D]{psi(4040)0{D0,Dbar0},K*(892)0{K+,pi-}}</code>	0			0.826	0.05	0	0.	10.		
<code>B0[D]{psi(4160)0{D0,Dbar0},K*(892)0{K+,pi-}}</code>	0			1.31	0.05	0	0.	10.		
<code>B0[S]{psi(4160)0{D0,Dbar0},K*(892)0{K+,pi-}}</code>	0			1.31	0.05	0	0.	10.		
<code>B0[P]{psi(4160)0{D0,Dbar0},K*(892)0{K+,pi-}}</code>	0			1.31	0.05	0	0.	10.		
<code>B0[P]{psi(4415)0{D0,Dbar0},K*(892)0{K+,pi-}}</code>	0			0.51	0.05	0	0.	10.		
<code>B0[S]{psi(4415)0{D0,Dbar0},K*(892)0{K+,pi-}}</code>	0			0.51	0.05	0	0.	10.		
<code>B0[D]{psi(4415)0{D0,Dbar0},K*(892)0{K+,pi-}}</code>	0			0.51	0.05	0	0.	10.		
<code>B0{psi(3770)0{D0,Dbar0},K(0)*(800)0{K+,pi-}}</code>	0			1.99	0.05	0	0.	10.		
<code>B0{psi(4040)0{D0,Dbar0},K(0)*(800)0{K+,pi-}}</code>	0			0.78	0.05	0	0.	10.		
<code>B0{psi(4160)0{D0,Dbar0},K(0)*(800)0{K+,pi-}}</code>	0			1.24	0.05	0	0.	10.		
<code>B0{psi(4415)0{D0,Dbar0},K(0)*(800)0{K+,pi-}}</code>	0			0.48	0.05	0	0.	10.		
<code>B0{psi(3770)0{D0,Dbar0},K(0)*(1430)0{K+,pi-}}</code>	0			1.99	0.05	0	0.	10.		
<code>B0{psi(4040)0{D0,Dbar0},K(0)*(1430)0{K+,pi-}}</code>	0			0.78	0.05	0	0.	10.		
<code>B0{psi(4160)0{D0,Dbar0},K(0)*(1430)0{K+,pi-}}</code>	0			1.24	0.05	0	0.	10.		
<code>B0{psi(4415)0{D0,Dbar0},K(0)*(1430)0{K+,pi-}}</code>	0			0.48	0.05	0	0.	10.		
<code>#B0{Z(c)(3900)+{D*(2010)+{D0,pi+},Dbar0},K-}</code>	0			1	0	0	0	0		

Figure 59: The amplitude model for the intermediate resonance used for the fit.

The fitting returns back the real and imaginary part of the amplitude in the resonances of the decay and percentage/probability for the each resonance to occur, based on the four momentum data. This also generates a plot.root file containing the phase space plots. It takes about 5 minutes to finish the fitting for 10^4 events.

A comparison was made between the generated MC data and the results from the amplitude fitting, as shown below:

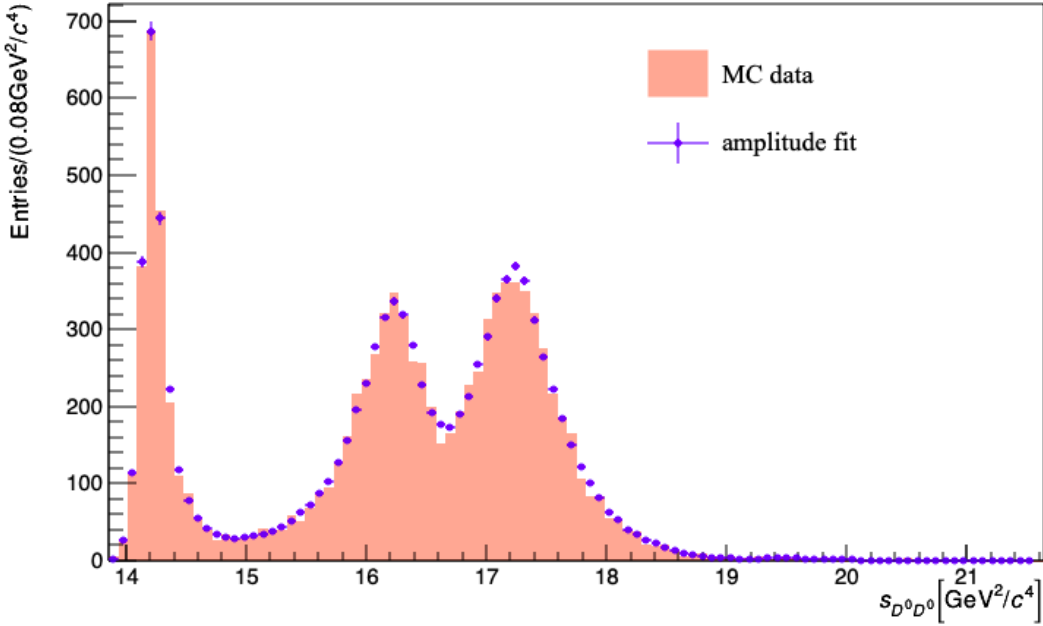


Figure 60: The verification of the fitter with the generated B^0 decays with 10000 events.

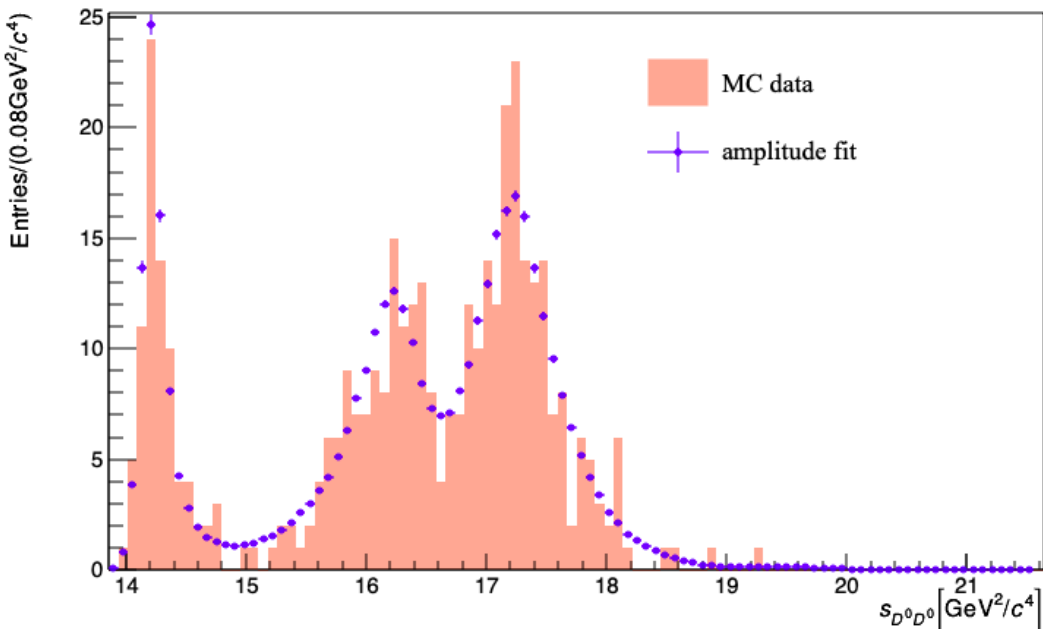


Figure 61: The verification of the fitter with the generated B^0 decays with 400 events (much fewer events).

The comparison of the ratio of the resonances contributed obtained from the fittings were made for different number of events using the Random Seed 7.

		400 events	1000 events	4000 events	10000 events	40000 events
B0[P]{psi(4160)0{D0,Dbar0},K*(892)0{K+,pi-}}	=	42.5 ± 5.22 %	42.02 ± 3.5 %	37.6 ± 1.68 %	36.62 ± 1.05 %	34.67 ± 0.51 %
B0[P]{psi(3770)0{D0,Dbar0},K*(892)0{K+,pi-}}	=	19.46 ± 2.98 %	19.68 ± 1.6 %	21.77 ± 0.82 %	22.19 ± 0.53 %	21.59 ± 0.26 %
B0[P]{psi(4040)0{D0,Dbar0},K*(892)0{K+,pi-}}	=	15.1 ± 3.49 %	15.69 ± 2.2 %	15.63 ± 1.11 %	16.74 ± 0.71 %	16.96 ± 0.35 %
B0[D]{psi(3770)0{D0,Dbar0},K*(892)0{K+,pi-}}	=	3.33 ± 1.3 %	4.26 ± 0.89 %	5.44 ± 0.49 %	5.42 ± 0.31 %	5.27 ± 0.15 %
B0[S]{psi(4160)0{D0,Dbar0},K*(892)0{K+,pi-}}	=	3.1 ± 1.58 %	3.73 ± 0.88 %	3.16 ± 0.5 %	2.93 ± 0.24 %	2.84 ± 0.11 %
B0[D]{psi(4160)0{D0,Dbar0},K*(892)0{K+,pi-}}	=	2.51 ± 1.46 %	2.51 ± 0.95 %	3.06 ± 0.38 %	2.92 ± 0.3 %	2.79 ± 0.14 %
B0{psi(4160)0{D0,Dbar0},K(0)*(800)0{K+,pi-}}	=	1.89 ± 1.18 %	2.25 ± 0.86 %	1.68 ± 0.38 %	1.46 ± 0.14 %	1.5 ± 0.09 %
B0{NonResS0{D0,Dbar0},K*(892)0{K+,pi-}}	=	1.3 ± 0.85 %	1.55 ± 0.61 %	1.61 ± 0.3 %	1.46 ± 0.18 %	1.48 ± 0.07 %
B0[S]{psi(4040)0{D0,Dbar0},K*(892)0{K+,pi-}}	=	1.25 ± 0.89 %	1.49 ± 0.62 %	1.33 ± 0.32 %	1.24 ± 0.16 %	1.37 ± 0.1 %
B0[P]{psi(4415)0{D0,Dbar0},K*(892)0{K+,pi-}}	=	0.82 ± 0.85 %	1.33 ± 0.45 %	1.33 ± 0.29 %	1.24 ± 0.2 %	1.19 ± 0.08 %
B0{psi(3770)0{D0,Dbar0},K(0)*(1430)0{K+,pi-}}	=	0.76 ± 0.56 %	1.14 ± 0.64 %	1.19 ± 0.21 %	1.14 ± 0.17 %	1.16 ± 0.08 %
B0{psi(4160)0{D0,Dbar0},K(0)*(1430)0{K+,pi-}}	=	0.71 ± 0.78 %	1.02 ± 0.53 %	1.13 ± 0.25 %	1 ± 0.17 %	0.99 ± 0.08 %
B0{K(0)*(800)0{K+,pi-},NonResS0{D0,Dbar0}}	=	0.63 ± 0.93 %	0.89 ± 0.49 %	1.11 ± 0.35 %	0.95 ± 0.16 %	0.96 ± 0.08 %
B0[S]{psi(3770)0{D0,Dbar0},K*(892)0{K+,pi-}}	=	0.54 ± 0.71 %	0.87 ± 0.53 %	0.79 ± 0.24 %	0.84 ± 0.18 %	0.67 ± 0.07 %
B0[D]{psi(4040)0{D0,Dbar0},K*(892)0{K+,pi-}}	=	0.49 ± 0.77 %	0.83 ± 0.64 %	0.77 ± 0.23 %	0.8 ± 0.16 %	0.65 ± 0.05 %
B0{psi(3770)0{D0,Dbar0},K(0)*(800)0{K+,pi-}}	=	0.49 ± 0.63 %	0.6 ± 0.47 %	0.73 ± 0.25 %	0.71 ± 0.12 %	0.64 ± 0.08 %
B0{NonResS0{D0,Dbar0},K(0)*(1430)0{K+,pi-}}	=	0.43 ± 0.61 %	0.55 ± 0.41 %	0.68 ± 0.18 %	0.7 ± 0.14 %	0.57 ± 0.07 %
B0{psi(4040)0{D0,Dbar0},K(0)*(800)0{K+,pi-}}	=	0.37 ± 0.62 %	0.53 ± 0.38 %	0.66 ± 0.26 %	0.63 ± 0.16 %	0.47 ± 0.06 %
B0[D]{psi(4415)0{D0,Dbar0},K*(892)0{K+,pi-}}	=	0.31 ± 0.52 %	0.41 ± 0.38 %	0.4 ± 0.17 %	0.44 ± 0.11 %	0.44 ± 0.05 %
B0{psi(4415)0{D0,Dbar0},K(0)*(1430)0{K+,pi-}}	=	0.24 ± 0.42 %	0.28 ± 0.34 %	0.21 ± 0.12 %	0.11 ± 0.05 %	0.06 ± 0.01 %
B0{psi(4040)0{D0,Dbar0},K(0)*(1430)0{K+,pi-}}	=	0.19 ± 0.39 %	0.16 ± 0.27 %	0.16 ± 0.09 %	0.08 ± 0.04 %	0.06 ± 0.02 %
B0{D(s2)(2573)+{D0,K+},Dbar0,pi-}	=	0.12 ± 0.26 %	0.13 ± 0.2 %	0.02 ± 0.03 %	0.03 ± 0.03 %	0.05 ± 0.01 %
B0[S]{psi(4415)0{D0,Dbar0},K*(892)0{K+,pi-}}	=	0.07 ± 0.23 %	0.13 ± 0.16 %	0.02 ± 0.04 %	0.03 ± 0.02 %	0.02 ± 0.01 %
B0{psi(4415)0{D0,Dbar0},K(0)*(800)0{K+,pi-}}	=	0.01 ± 0.07 %	0.02 ± 0.08 %	0.01 ± 0.02 %	0 ± 0.01 %	0.02 ± 0.01 %
Sum_B0	=	96.74 ± 8.35 %	102.21 ± 4.74 %	100.57 ± 2.29 %	99.79 ± 1.4 %	96.52 ± 0.66 %

Figure 62: The ratio of the contributed resonances for generated MC data with different number of events.

Next steps:

- induce CP violation by change the number of C_T by several percent
- binned analysis for the CM variables
- real data from LHCb

Start doing binned analysis following the method in the $D \rightarrow KK\pi\pi$ decay paper.⁶

This uses the five CM variables as the phase-space variables and divides the phase-space into 32 regions with each region containing similar number of events.

The method is to divide the list of the first CM variable into two bins with equal number of events in each bin and find the bin edges. The next step is to apply the bin edges to the next CM variable, make it two bins and divide events in each bin into equal quantity which makes 4 bins in total. Repeating this, results in $2^5 = 32$ bins for the 5th CM variable. More bin division could also be made for the CM variables, gives e.g. $3^5, 4^5$ phase regions with 3,4 divisions for the 5th CM variable.

The next step is to allocate the triple products C_T of the events into regions in terms of a combination of the CM variable ranges obtained from the bin edges. And then, the triple product asymmetries and CP asymmetries can be obtained from the C_T in each phase-space region. The way of arranging phase space regions can be different and gives different distributions for the asymmetries. The conjugate decays use the same binned scheme as obtained from the regular decays.

The P / CP asymmetries were found using three different methods: A. from the entire phase space, B. from different phase-space region, and C. from the fitting to the \mathcal{A}_{CP} across the phase space regions using a straight line $y = 0x + b$, where b is the asymmetry value. The fitting were also made with a CP symmetric curve (a straight line at $y = 0$) to find how well the data fits to no CP violation. For each fit, the value of the χ^2/ndf (ndf = number of degree of freedom) and the corresponding p-value were found:

$$\chi^2/\text{ndf} = \frac{1}{32} \sum_i \left(\frac{x_i - E_i}{\sigma_i} \right)^2, \quad (9)$$

where x_i and σ_i is value and the uncertainty data i , E_i is the expected value (or fitted value) of data i . The χ^2 has the probability distribution:⁷

$$P(\chi^2) \propto (\chi^2)^{\frac{\text{ndf}-2}{2}} e^{-\frac{\chi^2}{2}}, \quad (10)$$

where the mean of the χ^2 is equal to (ndf) and the standard deviation of the χ^2 is $\sqrt{2 \cdot \text{ndf}}$. The p-value is the probability of the value equal or greater than the χ^2 obtained from the fitting could arise by chance. If the χ^2 is low, this gives a larger p-value, which indicates the high confidence for the model to fit the data.

⁶The LHCb collaboration, “Search for CP Violation using T-odd Correlations in $D^0 \rightarrow K^+K^-\pi^+\pi^-$ Decays”.

⁷Chris Blake. *Lecture3: Hypothesis testing and model-fitting*. [Online; accessed 23-March-2020]. URL: <http://astronomy.swin.edu.au/~cblake/StatsLecture3.pdf>.

For 10^5 events with all the resonances included and S, P and D waves applied to the two spin-1 resonances (with equal relative P-wave amplitudes and zero phase offset), the results from the method A gives (this would be the same for all the bin arrangements):

A_T	\bar{A}_T	\mathcal{A}_{CP}
-0.021±0.03	-0.019±0.003	-0.001±0.002

Figure 63: The P and CP asymmetries found directly over all phase space regions.

For method B, using the `for` loop arrangement to allocate C_T into the phase-space regions, this gives the total number of C_T in each region:

[1422, 897, 1402, 905, 1387, 911, 1400, 905, 1401, 902, 1372, 911, 1400, 907, 1415, 899, 1458, 884, 1429, 893, 1395, 906, 1421, 892, 1444, 883, 1355, 920, 1380, 916, 1407, 902, 1222, 1940, 1204, 1969, 1187, 1973, 1199, 1965, 1203, 1977, 1187, 1991, 1198, 1971, 1205, 1952, 1237, 1907, 1222, 1932, 1192, 1966, 1211, 1937, 1224, 1923, 1178, 2012, 1185, 2002, 1201, 1959].

This summed over to give 87552 events, which is less than the original number of events of 10^5 . The reason might be that some events do not satisfy any arrangements of the phase-space variables in the 32 regions, and hence were miscounted.

This gives The bin arrangement:

region	phi	$m(D\bar{D})$	$m(K\pi)$	$\cos(\theta_D)$	$\cos(\theta_K)$
1	(0.00, 1.58)	(3.73, 4.05)	(0.63, 0.90)	(-1.00, 0.00)	(-1.00, 0.01)
2	(1.58, 3.14)	(4.05, 4.62)	(0.90, 1.51)	(0.00, 1.00)	(0.01, 1.00)
3	(0.00, 1.58)	(3.73, 4.05)	(0.63, 0.90)	(-1.00, 0.00)	(-1.00, 0.00)
4	(1.58, 3.14)	(4.05, 4.63)	(0.90, 1.50)	(0.00, 1.00)	(0.00, 1.00)
5	(0.00, 1.58)	(3.73, 4.05)	(0.63, 0.90)	(-1.00, -0.01)	(-1.00, 0.02)
6	(1.58, 3.14)	(4.05, 4.62)	(0.90, 1.50)	(-0.01, 1.00)	(0.02, 1.00)
7	(0.00, 1.58)	(3.73, 4.05)	(0.63, 0.90)	(-1.00, -0.01)	(-1.00, -0.00)
8	(1.58, 3.14)	(4.05, 4.63)	(0.90, 1.50)	(-0.01, 1.00)	(-0.00, 1.00)
9	(0.00, 1.58)	(3.73, 4.05)	(0.63, 0.90)	(-1.00, 0.00)	(-1.00, 0.00)
10	(1.58, 3.14)	(4.05, 4.62)	(0.90, 1.51)	(0.00, 1.00)	(0.00, 1.00)
11	(0.00, 1.58)	(3.73, 4.05)	(0.63, 0.90)	(-1.00, -0.01)	(-1.00, 0.01)
12	(1.58, 3.14)	(4.05, 4.63)	(0.90, 1.50)	(-0.01, 1.00)	(0.01, 1.00)
13	(0.00, 1.58)	(3.73, 4.05)	(0.63, 0.90)	(-1.00, 0.00)	(-1.00, 0.01)
14	(1.58, 3.14)	(4.05, 4.62)	(0.90, 1.50)	(0.00, 1.00)	(0.01, 1.00)
15	(0.00, 1.58)	(3.73, 4.05)	(0.63, 0.90)	(-1.00, -0.00)	(-1.00, 0.00)
16	(1.58, 3.14)	(4.05, 4.63)	(0.90, 1.50)	(-0.00, 1.00)	(0.00, 1.00)
17	(0.00, 1.58)	(3.73, 4.05)	(0.63, 0.90)	(-1.00, 0.00)	(-1.00, 0.02)
18	(1.58, 3.14)	(4.05, 4.62)	(0.90, 1.51)	(0.00, 1.00)	(0.02, 1.00)
19	(0.00, 1.58)	(3.73, 4.05)	(0.63, 0.90)	(-1.00, 0.00)	(-1.00, 0.01)
20	(1.58, 3.14)	(4.05, 4.63)	(0.90, 1.50)	(0.00, 1.00)	(0.01, 1.00)
21	(0.00, 1.58)	(3.73, 4.05)	(0.63, 0.90)	(-1.00, -0.01)	(-1.00, 0.02)
22	(1.58, 3.14)	(4.05, 4.62)	(0.90, 1.50)	(-0.01, 1.00)	(0.02, 1.00)
23	(0.00, 1.58)	(3.73, 4.05)	(0.63, 0.90)	(-1.00, -0.01)	(-1.00, 0.01)
24	(1.58, 3.14)	(4.05, 4.63)	(0.90, 1.50)	(-0.01, 1.00)	(0.01, 1.00)
25	(0.00, 1.58)	(3.73, 4.05)	(0.63, 0.90)	(-1.00, 0.00)	(-1.00, 0.02)
26	(1.58, 3.14)	(4.05, 4.62)	(0.90, 1.51)	(0.00, 1.00)	(0.02, 1.00)
27	(0.00, 1.58)	(3.73, 4.05)	(0.63, 0.90)	(-1.00, -0.01)	(-1.00, -0.00)
28	(1.58, 3.14)	(4.05, 4.63)	(0.90, 1.50)	(-0.01, 1.00)	(-0.00, 1.00)
29	(0.00, 1.58)	(3.73, 4.05)	(0.63, 0.90)	(-1.00, 0.00)	(-1.00, 0.00)
30	(1.58, 3.14)	(4.05, 4.62)	(0.90, 1.50)	(0.00, 1.00)	(0.00, 1.00)
31	(0.00, 1.58)	(3.73, 4.05)	(0.63, 0.90)	(-1.00, -0.00)	(-1.00, -0.00)
32	(1.58, 3.14)	(4.05, 4.63)	(0.90, 1.50)	(-0.00, 1.00)	(-0.00, 1.00)

Figure 64: The 32 regions of the five-dimensional phase space of the four-body, as in the order of: ϕ , $m(D^0\bar{D}^0)$, $m(K\pi)$, $\cos(\theta_D)$, $\cos(\theta_K)$.

The asymmetry distributions are:

region	A_T	A_Tbar	A_CP
1	(7.56 \pm 1.94)%	(12.98 \pm 1.91)%	(-2.71 \pm 1.36)%
2	(-36.76 \pm 1.75)%	(-35.65 \pm 1.74)%	(-0.56 \pm 1.23)%
3	(7.60 \pm 1.95)%	(12.50 \pm 1.92)%	(-2.45 \pm 1.37)%
4	(-37.02 \pm 1.73)%	(-36.01 \pm 1.73)%	(-0.51 \pm 1.22)%
5	(7.77 \pm 1.97)%	(12.29 \pm 1.93)%	(-2.26 \pm 1.38)%
6	(-36.82 \pm 1.73)%	(-36.01 \pm 1.72)%	(-0.41 \pm 1.22)%
7	(7.73 \pm 1.96)%	(11.86 \pm 1.92)%	(-2.06 \pm 1.37)%
8	(-36.93 \pm 1.73)%	(-35.98 \pm 1.73)%	(-0.48 \pm 1.22)%
9	(7.60 \pm 1.95)%	(12.67 \pm 1.92)%	(-2.53 \pm 1.37)%
10	(-37.34 \pm 1.73)%	(-35.76 \pm 1.73)%	(-0.79 \pm 1.22)%
11	(7.23 \pm 1.97)%	(12.03 \pm 1.94)%	(-2.40 \pm 1.38)%
12	(-37.22 \pm 1.72)%	(-36.15 \pm 1.72)%	(-0.53 \pm 1.22)%
13	(7.78 \pm 1.96)%	(12.65 \pm 1.92)%	(-2.44 \pm 1.37)%
14	(-36.97 \pm 1.73)%	(-35.68 \pm 1.73)%	(-0.65 \pm 1.22)%
15	(8.02 \pm 1.95)%	(12.14 \pm 1.91)%	(-2.06 \pm 1.36)%
16	(-36.93 \pm 1.74)%	(-35.73 \pm 1.74)%	(-0.60 \pm 1.23)%
17	(8.20 \pm 1.92)%	(13.32 \pm 1.89)%	(-2.56 \pm 1.35)%
18	(-36.65 \pm 1.76)%	(-35.61 \pm 1.75)%	(-0.52 \pm 1.24)%
19	(7.81 \pm 1.94)%	(12.74 \pm 1.91)%	(-2.47 \pm 1.36)%
20	(-36.78 \pm 1.75)%	(-35.47 \pm 1.74)%	(-0.66 \pm 1.23)%
21	(7.85 \pm 1.96)%	(12.38 \pm 1.93)%	(-2.27 \pm 1.37)%
22	(-36.91 \pm 1.73)%	(-35.90 \pm 1.72)%	(-0.50 \pm 1.22)%
23	(7.98 \pm 1.94)%	(12.11 \pm 1.91)%	(-2.06 \pm 1.36)%
24	(-36.94 \pm 1.75)%	(-35.53 \pm 1.74)%	(-0.70 \pm 1.23)%
25	(8.25 \pm 1.93)%	(13.05 \pm 1.90)%	(-2.40 \pm 1.35)%
26	(-37.06 \pm 1.75)%	(-35.44 \pm 1.75)%	(-0.81 \pm 1.24)%
27	(6.99 \pm 1.98)%	(11.85 \pm 1.94)%	(-2.43 \pm 1.39)%
28	(-37.24 \pm 1.71)%	(-36.42 \pm 1.71)%	(-0.41 \pm 1.21)%
29	(7.60 \pm 1.97)%	(12.55 \pm 1.93)%	(-2.47 \pm 1.38)%
30	(-37.22 \pm 1.72)%	(-36.04 \pm 1.71)%	(-0.59 \pm 1.21)%
31	(7.90 \pm 1.95)%	(12.12 \pm 1.92)%	(-2.11 \pm 1.37)%
32	(-36.95 \pm 1.74)%	(-35.85 \pm 1.73)%	(-0.55 \pm 1.23)%

Figure 65: The P and CP asymmetries found in 32 regions.(method B)

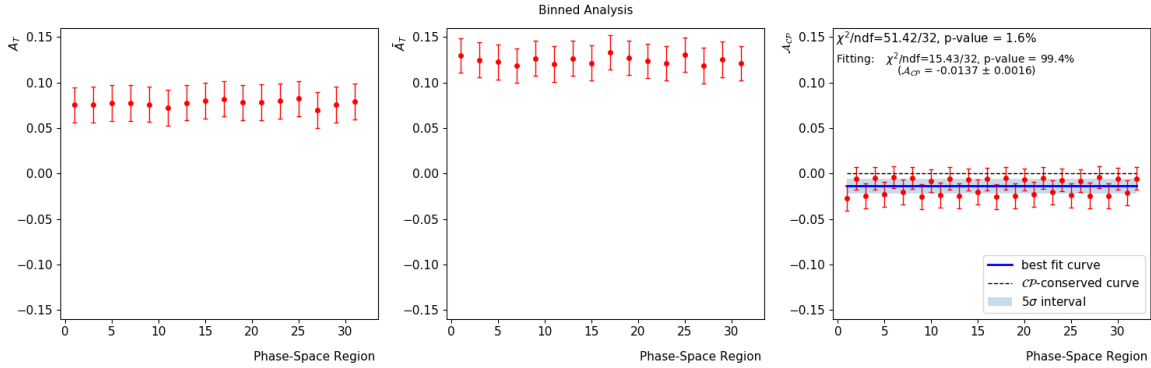


Figure 66: The distribution of the asymmetries using the binning scheme, the best fitted curve of A_{CP} (method C) and CP conserved curve.

This bin arrangement gives the distribution of A_{CP} in some regular pattern which shows a CP asymmetry. The reason might be there are too many points lost and the bin arrangements of ϕ changes very frequently \Rightarrow ?

The events are generated using all resonances with the S,P and D waves included for the two spin-1 resonances, and 10 random seeds. This changes the distributions of CM variables (ϕ and helicity angles) compared with the model without the S,P,D waves and with using one seed only by compared with Fig.28-30:

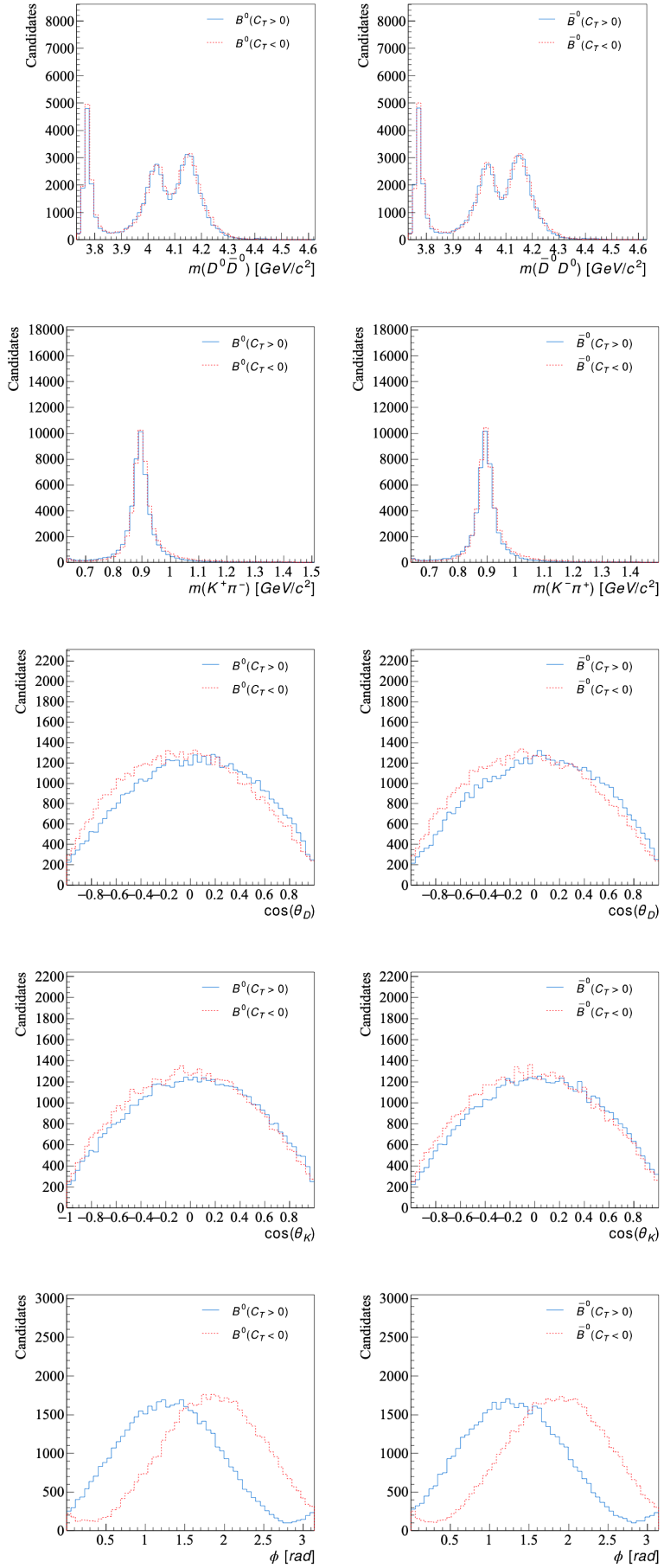


Figure 67: The CM variable distribution for the model with spd waves using 10 different random seeds.

The code is developed to allow different bin arrangements for the 32 phase space regions.

An alternative is:

region	phi	m(DDbar)	m(Kpi)	cos(theta_D)	cos(theta_K)
1	(0.00,1.58)	(3.73,4.05)	(0.63,0.90)	(-1.00,0.00)	(-1.00,0.01)
2	(0.00,1.58)	(3.73,4.05)	(0.63,0.90)	(-1.00,0.00)	(0.01,1.00)
3	(0.00,1.58)	(3.73,4.05)	(0.63,0.90)	(0.00,1.00)	(-1.00,0.00)
4	(0.00,1.58)	(3.73,4.05)	(0.63,0.90)	(0.00,1.00)	(0.00,1.00)
5	(0.00,1.58)	(3.73,4.05)	(0.90,1.51)	(-1.00,0.00)	(-1.00,0.02)
6	(0.00,1.58)	(3.73,4.05)	(0.90,1.51)	(-1.00,0.00)	(0.02,1.00)
7	(0.00,1.58)	(3.73,4.05)	(0.90,1.51)	(0.00,1.00)	(-1.00,-0.00)
8	(0.00,1.58)	(3.73,4.05)	(0.90,1.51)	(0.00,1.00)	(-0.00,1.00)
9	(0.00,1.58)	(4.05,4.62)	(0.63,0.90)	(-1.00,-0.01)	(-1.00,0.00)
10	(0.00,1.58)	(4.05,4.62)	(0.63,0.90)	(-1.00,-0.01)	(0.00,1.00)
11	(0.00,1.58)	(4.05,4.62)	(0.63,0.90)	(-0.01,1.00)	(-1.00,0.01)
12	(0.00,1.58)	(4.05,4.62)	(0.63,0.90)	(-0.01,1.00)	(0.01,1.00)
13	(0.00,1.58)	(4.05,4.62)	(0.90,1.50)	(-1.00,-0.01)	(-1.00,0.01)
14	(0.00,1.58)	(4.05,4.62)	(0.90,1.50)	(-1.00,-0.01)	(0.01,1.00)
15	(0.00,1.58)	(4.05,4.62)	(0.90,1.50)	(-0.01,1.00)	(-1.00,0.00)
16	(0.00,1.58)	(4.05,4.62)	(0.90,1.50)	(-0.01,1.00)	(0.00,1.00)
17	(1.58,3.14)	(3.73,4.05)	(0.63,0.90)	(-1.00,0.00)	(-1.00,0.02)
18	(1.58,3.14)	(3.73,4.05)	(0.63,0.90)	(-1.00,0.00)	(0.02,1.00)
19	(1.58,3.14)	(3.73,4.05)	(0.63,0.90)	(0.00,1.00)	(-1.00,0.01)
20	(1.58,3.14)	(3.73,4.05)	(0.63,0.90)	(0.00,1.00)	(0.01,1.00)
21	(1.58,3.14)	(3.73,4.05)	(0.90,1.50)	(-1.00,-0.01)	(-1.00,0.02)
22	(1.58,3.14)	(3.73,4.05)	(0.90,1.50)	(-1.00,-0.01)	(0.02,1.00)
23	(1.58,3.14)	(3.73,4.05)	(0.90,1.50)	(-0.01,1.00)	(-1.00,0.01)
24	(1.58,3.14)	(3.73,4.05)	(0.90,1.50)	(-0.01,1.00)	(0.01,1.00)
25	(1.58,3.14)	(4.05,4.63)	(0.63,0.90)	(-1.00,0.00)	(-1.00,0.02)
26	(1.58,3.14)	(4.05,4.63)	(0.63,0.90)	(-1.00,0.00)	(0.02,1.00)
27	(1.58,3.14)	(4.05,4.63)	(0.63,0.90)	(0.00,1.00)	(-1.00,-0.00)
28	(1.58,3.14)	(4.05,4.63)	(0.63,0.90)	(0.00,1.00)	(-0.00,1.00)
29	(1.58,3.14)	(4.05,4.63)	(0.90,1.50)	(-1.00,-0.00)	(-1.00,0.00)
30	(1.58,3.14)	(4.05,4.63)	(0.90,1.50)	(-1.00,-0.00)	(0.00,1.00)
31	(1.58,3.14)	(4.05,4.63)	(0.90,1.50)	(-0.00,1.00)	(-1.00,-0.00)
32	(1.58,3.14)	(4.05,4.63)	(0.90,1.50)	(-0.00,1.00)	(-0.00,1.00)

Figure 68: The 32 regions of the five-dimensional phase space of the four-body, as in the order of: ϕ , $m(D^0\bar{D}^0)$, $m(K\pi)$, $\cos(\theta_D)$, $\cos(\theta_K)$.

This gives the total number of C_T in each region:

[1422, 2125, 2051, 2205, 1820, 2209, 1932, 2243, 2255, 1973, 2568, 2358, 1914, 1549, 1757, 1850, 775, 1085, 1078, 1185, 1006, 1128, 1037, 1308, 1131, 1067, 1306, 1240, 978, 729, 754, 902, 1222, 888, 908, 778, 1452, 1036, 1330, 1367, 1156, 1440, 971, 1031, 1070, 1133, 980, 987, 2222, 1526, 1732, 1444, 2671, 1867, 2526, 239, 2, 2303, 2732, 1844, 1961, 1872, 2238, 1979, 1959].

This summed over to give 99957 events, which is closer to 10^5 - more events has fallen to satisfy the bin arrangements.

The asymmetries starts to make sense, where it shows a consistency to no CP violation with a p-value of 72.5% for a $\chi^2/\text{ndf}=0.84$. The value of \mathcal{A}_{CP} from the fitting is less than the value obtained from the entire phase space region (-0.001 ± 0.002)(method A). This might be due to the loss of events from bin arrangements. The results are shown below:

region	A_T	A_Tbar	A_CP
1	(7.56 +- 1.94)%	(12.98 +- 1.91)%	(-2.71 +- 1.36)%
2	(41.06 +- 1.66)%	(40.09 +- 1.67)%	(0.48 +- 1.18)%
3	(38.63 +- 1.70)%	(37.69 +- 1.71)%	(0.47 +- 1.20)%
4	(47.84 +- 1.61)%	(49.46 +- 1.57)%	(-0.81 +- 1.12)%
5	(11.25 +- 1.74)%	(9.28 +- 1.73)%	(0.98 +- 1.22)%
6	(36.15 +- 1.64)%	(36.17 +- 1.65)%	(-0.01 +- 1.16)%
7	(18.45 +- 1.72)%	(13.90 +- 1.74)%	(2.28 +- 1.22)%
8	(24.27 +- 1.61)%	(23.50 +- 1.62)%	(0.38 +- 1.14)%
9	(32.22 +- 1.62)%	(29.70 +- 1.67)%	(1.26 +- 1.16)%
10	(15.62 +- 1.69)%	(15.47 +- 1.72)%	(0.08 +- 1.20)%
11	(45.13 +- 1.50)%	(48.16 +- 1.46)%	(-1.52 +- 1.05)%
12	(39.16 +- 1.58)%	(39.44 +- 1.56)%	(-0.14 +- 1.11)%
13	(28.28 +- 1.76)%	(30.75 +- 1.77)%	(-1.23 +- 1.25)%
14	(15.51 +- 1.91)%	(16.04 +- 1.94)%	(-0.26 +- 1.36)%
15	(28.39 +- 1.83)%	(28.28 +- 1.82)%	(0.05 +- 1.29)%
16	(30.42 +- 1.79)%	(29.43 +- 1.78)%	(0.50 +- 1.26)%
17	(-48.28 +- 1.60)%	(-52.32 +- 1.56)%	(2.02 +- 1.12)%
18	(-16.89 +- 1.93)%	(-18.09 +- 1.91)%	(0.60 +- 1.36)%
19	(-23.27 +- 1.83)%	(-23.31 +- 1.86)%	(0.02 +- 1.30)%
20	(-9.85 +- 1.94)%	(-8.37 +- 1.93)%	(-0.74 +- 1.37)%
21	(-45.28 +- 1.47)%	(-45.44 +- 1.46)%	(0.08 +- 1.03)%
22	(-24.67 +- 1.77)%	(-23.61 +- 1.77)%	(-0.53 +- 1.25)%
23	(-41.79 +- 1.52)%	(-42.12 +- 1.52)%	(0.17 +- 1.07)%
24	(-29.30 +- 1.57)%	(-26.80 +- 1.60)%	(-1.25 +- 1.12)%
25	(-34.13 +- 1.60)%	(-33.04 +- 1.62)%	(-0.54 +- 1.14)%
26	(-43.83 +- 1.46)%	(-42.78 +- 1.47)%	(-0.52 +- 1.04)%
27	(-17.08 +- 1.76)%	(-14.76 +- 1.72)%	(-1.16 +- 1.23)%
28	(-22.52 +- 1.72)%	(-20.42 +- 1.74)%	(-1.05 +- 1.22)%
29	(-31.37 +- 1.78)%	(-36.66 +- 1.74)%	(2.65 +- 1.24)%
30	(-50.86 +- 1.58)%	(-50.62 +- 1.60)%	(-0.12 +- 1.13)%
31	(-44.82 +- 1.71)%	(-42.06 +- 1.74)%	(-1.38 +- 1.22)%
32	(-36.95 +- 1.74)%	(-35.85 +- 1.73)%	(-0.55 +- 1.23)%

Figure 69: The P and CP asymmetries found in 32 regions.(method B)

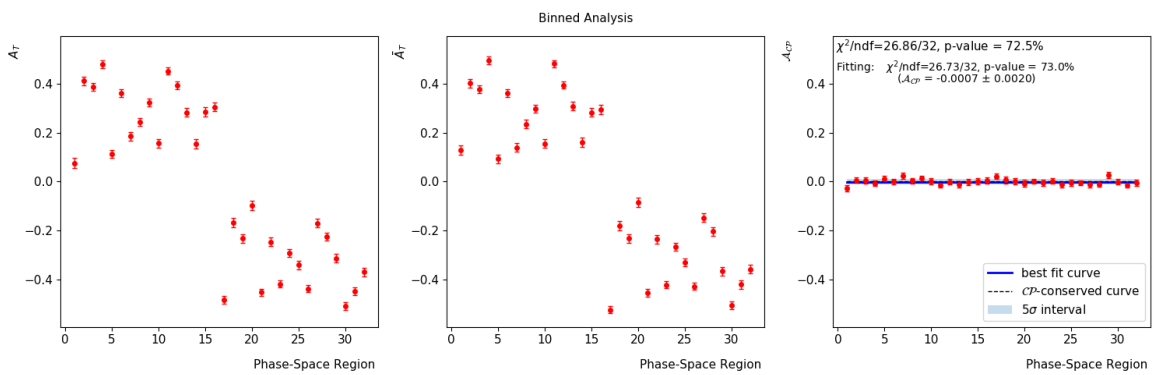


Figure 70: The distribution of the asymmetries using the binning scheme in Fig.69, the best fitted curve of \mathcal{A}_{CP} (method C) and CP conserved curve.

Another attempt of bin arrangements was tried by following the one in the literature⁸ as mentioned before:

region	phi	$m(D\bar{D})$	$m(K\pi)$	$\cos(\theta_D)$	$\cos(\theta_K)$
1	(0.00, 1.58)	(3.73, 4.05)	(0.63, 0.90)	(-1.00, 0.00)	(-1.00, 0.01)
2	(0.00, 1.58)	(3.73, 4.05)	(0.90, 1.51)	(-1.00, 0.00)	(-1.00, 0.00)
3	(0.00, 1.58)	(4.05, 4.62)	(0.63, 0.90)	(-1.00, -0.01)	(-1.00, 0.02)
4	(0.00, 1.58)	(4.05, 4.62)	(0.90, 1.50)	(-1.00, -0.01)	(-1.00, -0.00)
5	(1.58, 3.14)	(3.73, 4.05)	(0.63, 0.90)	(-1.00, 0.00)	(-1.00, 0.00)
6	(1.58, 3.14)	(3.73, 4.05)	(0.90, 1.50)	(-1.00, -0.01)	(-1.00, 0.01)
7	(1.58, 3.14)	(4.05, 4.63)	(0.63, 0.90)	(-1.00, 0.00)	(-1.00, 0.01)
8	(1.58, 3.14)	(4.05, 4.63)	(0.90, 1.50)	(-1.00, -0.00)	(-1.00, 0.00)
9	(0.00, 1.58)	(3.73, 4.05)	(0.63, 0.90)	(0.00, 1.00)	(-1.00, 0.02)
10	(0.00, 1.58)	(3.73, 4.05)	(0.90, 1.51)	(0.00, 1.00)	(-1.00, 0.01)
11	(0.00, 1.58)	(4.05, 4.62)	(0.63, 0.90)	(-0.01, 1.00)	(-1.00, 0.02)
12	(0.00, 1.58)	(4.05, 4.62)	(0.90, 1.50)	(-0.01, 1.00)	(-1.00, 0.01)
13	(1.58, 3.14)	(3.73, 4.05)	(0.63, 0.90)	(0.00, 1.00)	(-1.00, 0.02)
14	(1.58, 3.14)	(3.73, 4.05)	(0.90, 1.50)	(-0.01, 1.00)	(-1.00, -0.00)
15	(1.58, 3.14)	(4.05, 4.63)	(0.63, 0.90)	(0.00, 1.00)	(-1.00, 0.00)
16	(1.58, 3.14)	(4.05, 4.63)	(0.90, 1.50)	(-0.00, 1.00)	(-1.00, -0.00)
17	(0.00, 1.58)	(3.73, 4.05)	(0.63, 0.90)	(-1.00, 0.00)	(0.01, 1.00)
18	(0.00, 1.58)	(3.73, 4.05)	(0.90, 1.51)	(-1.00, 0.00)	(0.00, 1.00)
19	(0.00, 1.58)	(4.05, 4.62)	(0.63, 0.90)	(-1.00, -0.01)	(0.02, 1.00)
20	(0.00, 1.58)	(4.05, 4.62)	(0.90, 1.50)	(-1.00, -0.01)	(-0.00, 1.00)
21	(1.58, 3.14)	(3.73, 4.05)	(0.63, 0.90)	(-1.00, 0.00)	(0.00, 1.00)
22	(1.58, 3.14)	(3.73, 4.05)	(0.90, 1.50)	(-1.00, -0.01)	(0.01, 1.00)
23	(1.58, 3.14)	(4.05, 4.63)	(0.63, 0.90)	(-1.00, 0.00)	(0.01, 1.00)
24	(1.58, 3.14)	(4.05, 4.63)	(0.90, 1.50)	(-1.00, -0.00)	(0.00, 1.00)
25	(0.00, 1.58)	(3.73, 4.05)	(0.63, 0.90)	(0.00, 1.00)	(0.02, 1.00)
26	(0.00, 1.58)	(3.73, 4.05)	(0.90, 1.51)	(0.00, 1.00)	(0.01, 1.00)
27	(0.00, 1.58)	(4.05, 4.62)	(0.63, 0.90)	(-0.01, 1.00)	(0.02, 1.00)
28	(0.00, 1.58)	(4.05, 4.62)	(0.90, 1.50)	(-0.01, 1.00)	(0.01, 1.00)
29	(1.58, 3.14)	(3.73, 4.05)	(0.63, 0.90)	(0.00, 1.00)	(0.02, 1.00)
30	(1.58, 3.14)	(3.73, 4.05)	(0.90, 1.50)	(-0.01, 1.00)	(-1.00, -0.00)
31	(1.58, 3.14)	(4.05, 4.63)	(0.63, 0.90)	(0.00, 1.00)	(0.00, 1.00)
32	(1.58, 3.14)	(4.05, 4.63)	(0.90, 1.50)	(-0.00, 1.00)	(-0.00, 1.00)

Figure 71: The 32 regions of the five-dimensional phase space of the four-body, as in the order of: ϕ , $m(D^0\bar{D}^0)$, $m(K\pi)$, $\cos(\theta_D)$, $\cos(\theta_K)$.

This gives the total number of C_T in each region:

[1422, 1772, 2277, 1887, 746, 991, 1116, 981, 2098, 1988, 2608, 1768, 1086, 1017, 1307, 754, 2125, 2257, 1951, 1576, 1114, 1143, 1082, 727, 2158, 2187, 2318, 1839, 1178, 1017, 1239, 902, 1222, 1432, 1178, 1054, 2180, 2632, 2260, 1880, 919, 1366, 983, 982, 1743, 2499, 1846, 1979, 888, 1056, 1418, 1149, 1568, 1906, 2775, 2230, 766, 1328, 1018, 984, 1434, 2499, 1959].

This summed over to give 99723 events, which is also close to 10^5 .

The distributions of the calculated asymmetries looks more uniformly. The results are compatible with the CP conservation hypothesis at p-value of 81.9% for the $\chi^2/\text{ndf}=0.77$. The results are shown below:

⁸The LHCb collaboration, “Search for CP Violation using T-odd Correlations in $D^0 \rightarrow K^+K^-\pi^+\pi^-$ Decays”.

region	A_T	A_Tbar	A_CP
1	(7.56 \pm 1.94)%	(12.98 \pm 1.91)%	(-2.71 \pm 1.36)%
2	(10.61 \pm 1.76)%	(8.40 \pm 1.74)%	(1.11 \pm 1.24)%
3	(31.81 \pm 1.61)%	(29.56 \pm 1.66)%	(1.12 \pm 1.16)%
4	(28.32 \pm 1.77)%	(30.81 \pm 1.78)%	(-1.24 \pm 1.25)%
5	(-49.01 \pm 1.61)%	(-52.24 \pm 1.57)%	(1.61 \pm 1.13)%
6	(-45.29 \pm 1.48)%	(-45.58 \pm 1.47)%	(0.14 \pm 1.04)%
7	(-33.89 \pm 1.62)%	(-32.58 \pm 1.63)%	(-0.65 \pm 1.15)%
8	(-31.42 \pm 1.77)%	(-36.66 \pm 1.74)%	(2.62 \pm 1.24)%
9	(39.08 \pm 1.68)%	(37.74 \pm 1.69)%	(0.67 \pm 1.19)%
10	(18.55 \pm 1.70)%	(14.06 \pm 1.72)%	(2.24 \pm 1.21)%
11	(45.25 \pm 1.49)%	(47.85 \pm 1.44)%	(-1.30 \pm 1.04)%
12	(28.58 \pm 1.83)%	(28.42 \pm 1.81)%	(0.08 \pm 1.29)%
13	(-23.22 \pm 1.83)%	(-23.63 \pm 1.85)%	(0.20 \pm 1.30)%
14	(-42.15 \pm 1.53)%	(-42.10 \pm 1.53)%	(-0.02 \pm 1.08)%
15	(-17.09 \pm 1.75)%	(-14.74 \pm 1.72)%	(-1.18 \pm 1.23)%
16	(-44.82 \pm 1.71)%	(-42.06 \pm 1.74)%	(-1.38 \pm 1.22)%
17	(41.06 \pm 1.66)%	(40.09 \pm 1.67)%	(0.48 \pm 1.18)%
18	(36.25 \pm 1.62)%	(36.50 \pm 1.63)%	(-0.12 \pm 1.15)%
19	(15.82 \pm 1.70)%	(15.42 \pm 1.73)%	(0.20 \pm 1.21)%
20	(15.67 \pm 1.89)%	(16.17 \pm 1.92)%	(-0.25 \pm 1.35)%
21	(-16.93 \pm 1.90)%	(-18.69 \pm 1.90)%	(0.88 \pm 1.34)%
22	(-25.02 \pm 1.75)%	(-23.96 \pm 1.75)%	(-0.53 \pm 1.24)%
23	(-43.89 \pm 1.45)%	(-43.05 \pm 1.46)%	(-0.42 \pm 1.03)%
24	(-50.83 \pm 1.58)%	(-50.64 \pm 1.60)%	(-0.09 \pm 1.13)%
25	(47.61 \pm 1.63)%	(49.68 \pm 1.59)%	(-1.04 \pm 1.14)%
26	(24.44 \pm 1.64)%	(23.59 \pm 1.64)%	(0.42 \pm 1.16)%
27	(38.97 \pm 1.59)%	(39.59 \pm 1.57)%	(-0.31 \pm 1.12)%
28	(30.29 \pm 1.79)%	(29.30 \pm 1.79)%	(0.49 \pm 1.27)%
29	(-9.80 \pm 1.95)%	(-7.98 \pm 1.94)%	(-0.91 \pm 1.37)%
30	(-42.15 \pm 1.53)%	(-42.10 \pm 1.53)%	(-0.02 \pm 1.08)%
31	(-22.51 \pm 1.72)%	(-20.44 \pm 1.74)%	(-1.04 \pm 1.22)%
32	(-36.95 \pm 1.74)%	(-35.85 \pm 1.73)%	(-0.55 \pm 1.23)%

Figure 72: The P and CP asymmetries found in 32 regions.(method B)

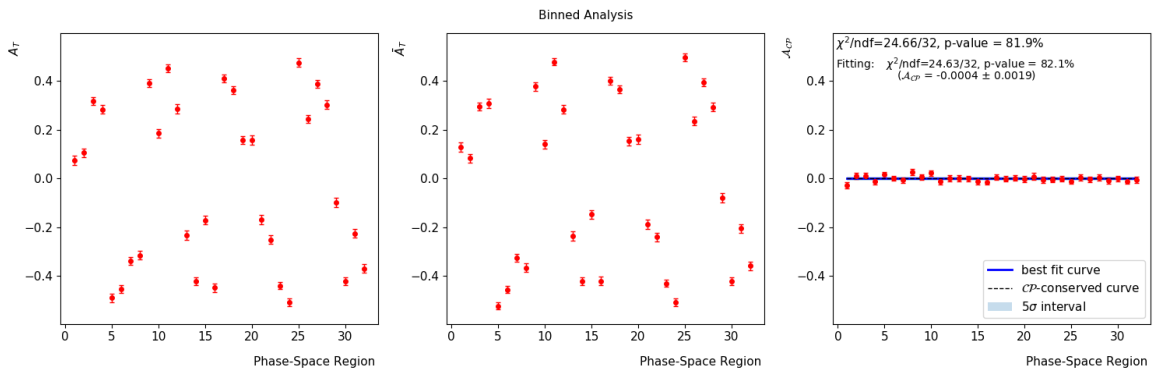


Figure 73: The distribution of the asymmetries using the binning scheme in Fig.72, the best fitted curve of A_{CP} (method C) and CP conserved curve.

First look of LHCb data (Run I): The data were cut for the classifier with `NN_weights > 0.9979`, which was obtained from the previous analysis steps. The overall selection efficiency is 4.08×10^{-4} , so we have got constant efficiency over the phase space and don't apply any corrections due to where the decay is in phase space.

The data contains the four momentum of the mother particle B^0 and the four daughter particles. They are labelled as:

```
B0_PE, B0_PX, B0_PY, B0_PZ,  
D0_PE, D0_PX, D0_PY, D0_PZ,  
D0bar_PE, D0bar_PX, D0bar_PY, D0bar_PZ,  
K_Kst0_PE, K_Kst0_PX, K_Kst0_PY, K_Kst0_PZ,  
Pi_Kst0_PE, Pi_Kst0_PX, Pi_Kst0_PY, Pi_Kst0_PZ.
```

The term with `_Kst0` means that particles K and π comes from the decay of K^* . There also contains e.g. `K_D0_PX`, `Pi_D0_PX`, `K_D0bar_PX`, indicates K and π comes from $D0$ or $D0bar$, which is used for flavour-tagging of the production of D^0 and \bar{D}^0 .

The data for regular decay and charge-conjugate decay were recognized from the values of `K_Kst0_ID`. For example, in the column of (e.g.) `D0_PX`, the event with ID=321 is the momentum of D^0 comes from the regular decay, while the event with ID=-321 is the momentum of D^0 comes from the conjugate decay. And similarly, in the column of `Dbar0_PX`, the event with ID=321 is the \bar{D}^0 comes from the regular decay and the value with ID=-321 is the \bar{D}^0 comes from the conjugate decay. For the momentum of K , it has the meaning K^+ and K^- for ID = 321 and -321 ,respectively. The total number of data obtained is 2678 with 1405 being regular and 1273 being charge-conjugate process. So the scalar product for the regular and conjugate process are given by:

$$C_T = \begin{cases} (D0_P \times D0bar_P) \cdot K_Kst0_P, & \text{for ID=321,} \\ (D0bar_P \times D0_P) \cdot K_Kst0_P, & \text{for ID=-321.} \end{cases} \quad (11)$$

The invariant masses of B^0 with different values of the triple product for the regular and conjugate processes are given by:

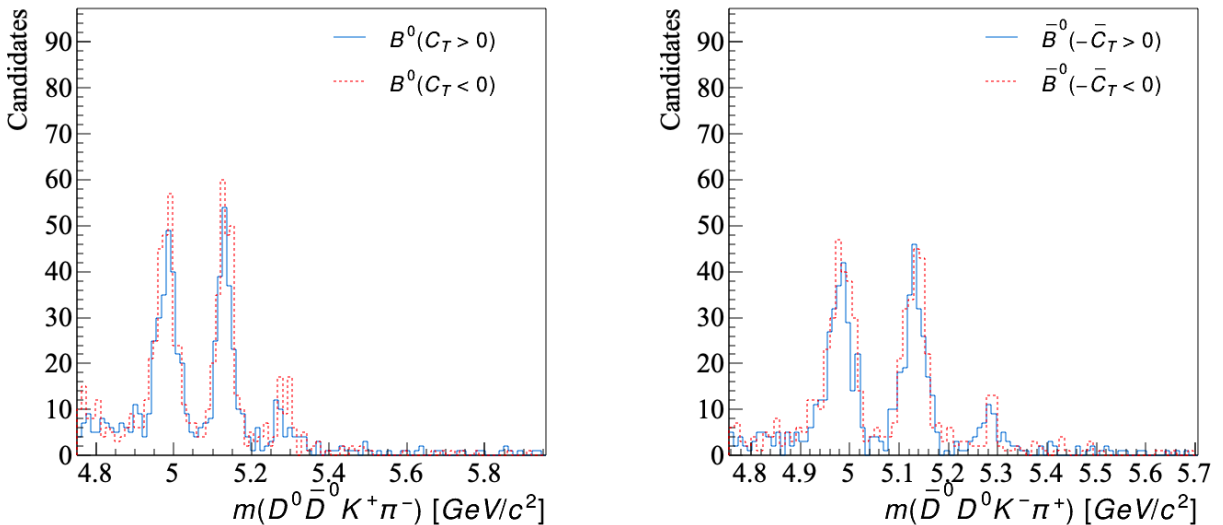


Figure 74: The invariant mass of $D^0 \bar{D}^0 K^+ \pi^-$ and its conjugate decays for different values of C_T .

The resonance is expected to happen at around $5.28\text{GeV}/c^2$. It shows that there are contributions from other sources: the background signal or the decays not coming from B^0 . The $sWeights = N_s / (N_s + N_b)$ are required to add to the data, which accounts for the probability for a particular event signal comes from the B^0 decay, here it assumes the $sWeights$ is the same as $inWeights$. More details for $sPlots$, $sWeights$, and $inWeights$ can be found in⁹¹⁰.

Note: [It is not clear if the background was studied over the whole phase space or not either (if not, then the background subtraction is only an approximation and we'll have to make note of that)].

After applying the $sWeights$, the additional noise is removed, leaves the contribution from B^0 only. This shows the correct resonance distribution for B^0 with 115 events:

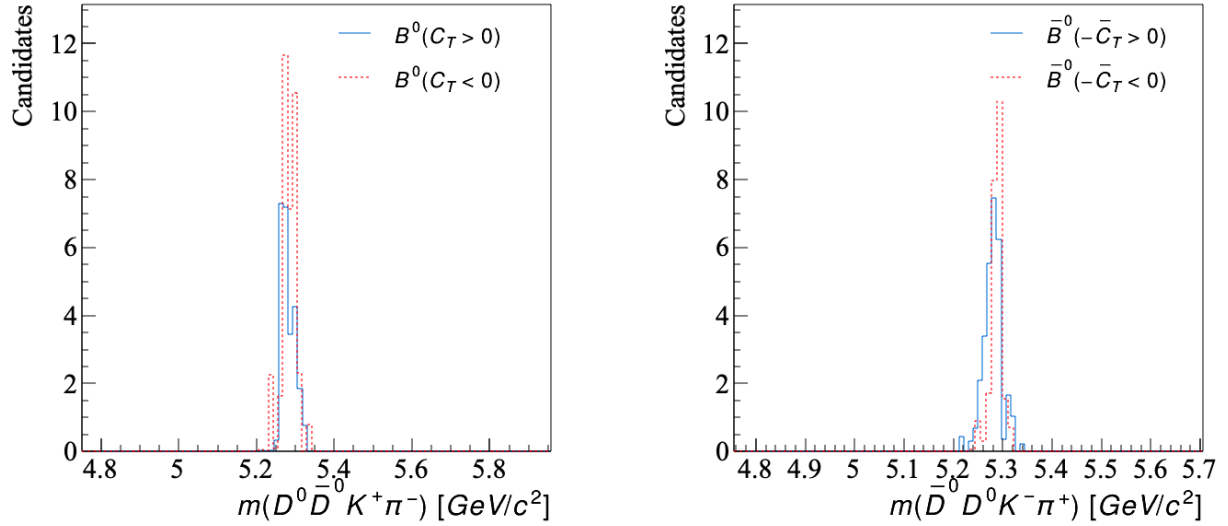


Figure 75: The invariant mass of $D^0\bar{D}^0K^+\pi^-$ and its conjugate decays for different values of C_T after applying the $sWeights$.

⁹M. Pivk and F.R. Le Diberder. “: A statistical tool to unfold data distributions”. In: *Nucl. Instrum. Meth. A* 555.1-2 (2005), 356–369. ISSN: 0168-9002.

¹⁰Alex Rogozhnikov. *sPlot: a technique to reconstruct components of a mixture*. [Online; accessed 23-March-2020]. 2015. URL: <http://arogozhnikov.github.io/2015/10/07/splot.html>.

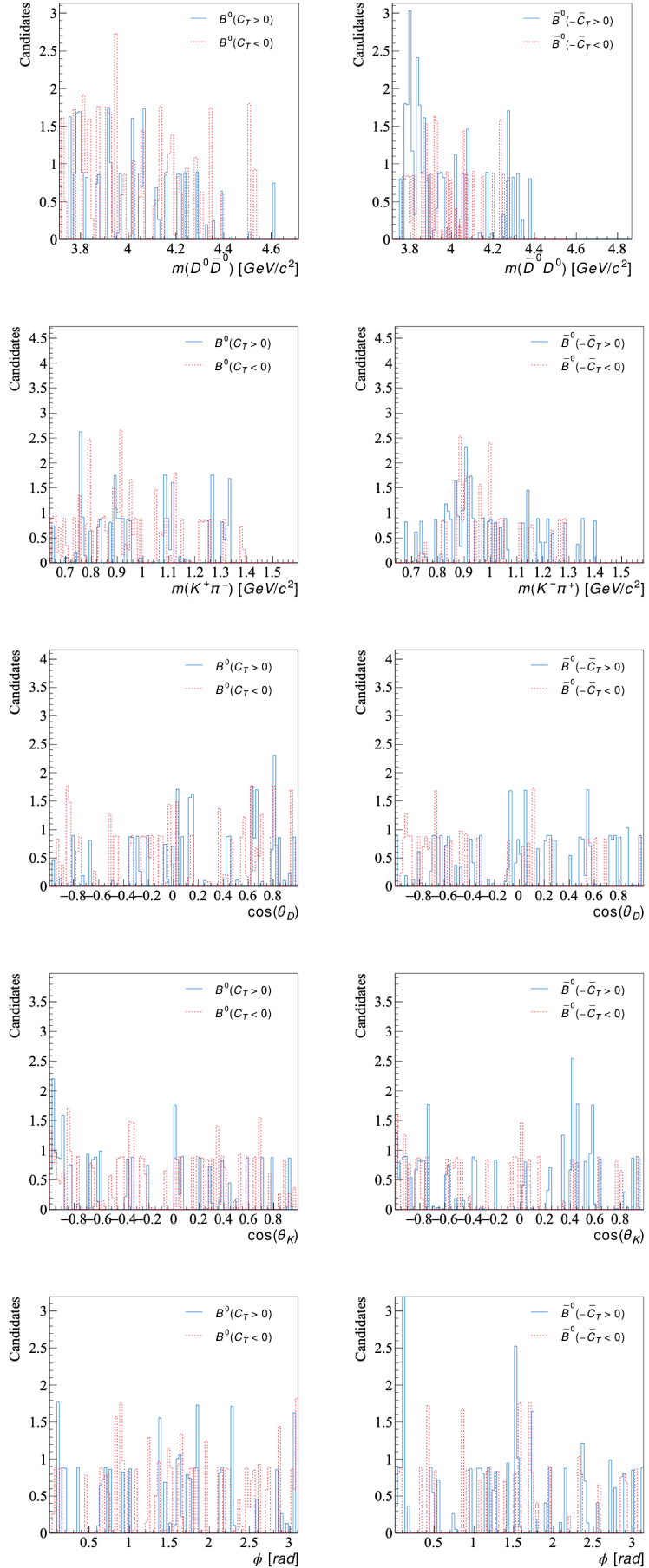


Figure 76: The distribution of the CM variable of the LHCb (Run I) data after adding the weights. This doesn't show an obvious correct distributions comparing to the previous simulated distribution in e.g. Fig.67. The reason might be the there are not enough number of events and the weights used in the B^0 decay doesn't apply to these variables.

This distribution of the weighted B^0 resonances are fitted using a Gaussian function:

$$f(x) = Ae^{-\frac{(x-x_0)^2}{2\sigma^2}}, \quad (12)$$

where A is the amplitude, x_0 is the mean and σ is the standard deviation of the distribution.

This fits the data well with little uncertainties in the parameters:

bin=100							
	A	err_A	mean	err_mean	sigma	err_sigma	type
B0	6.9500	0.3265	5.2761	0.0009	0.0171	0.0009	$B^0(C_T > 0)$
B0	10.6653	0.5292	5.2854	0.0009	0.0164	0.0009	$B^0(C_T < 0)$
B0	7.2257	0.2280	5.2806	0.0005	0.0141	0.0005	$\bar{B}^0(-C_T > 0)$
B0	10.7597	0.2029	5.2901	0.0002	0.0090	0.0002	$\bar{B}^0(-C_T < 0)$

Figure 77: The results of the parameters after fitting the B_0 resonance using the eq.12.

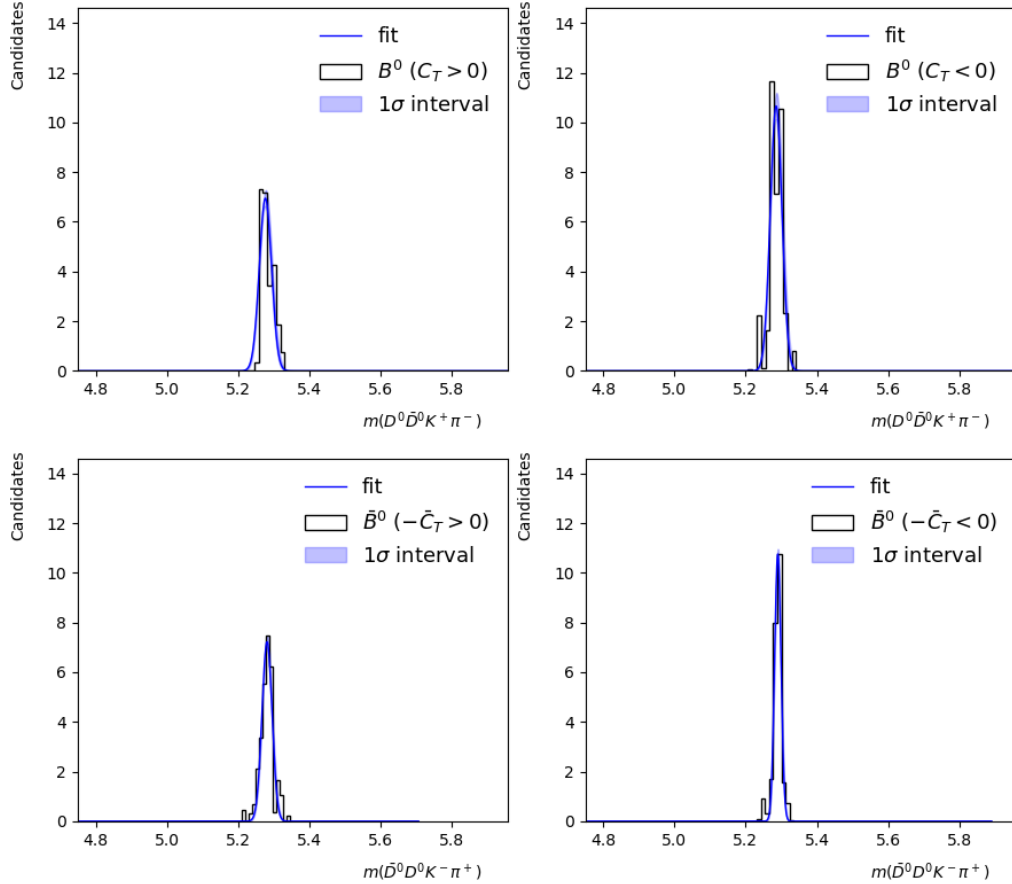


Figure 78: The fitted distribution of the B_0 resonance with showing the $1-\sigma$ tolerance.

To find the triple product and CP asymmetries for the LHCb data, the yields of the data for the four C_T cases were calculated. One way to calculate the yields is to find the integral of the Gaussian distribution (Eq.12) of the B^0 resonances in Fig.78 and divided by the bin width Δm . The calculation is given by:

$$\begin{aligned}\eta &= \frac{1}{\Delta m} \int_{-\infty}^{\infty} f(x) dx \\ &= \frac{1}{\Delta m} \int_{-\infty}^{\infty} A e^{-\frac{(x-x_0)^2}{2\sigma^2}} dx \\ &= \frac{A}{\Delta m} \int_{-\infty}^{\infty} e^{-ay^2} dy \quad y = x - x_0, a = \frac{1}{2\sigma^2} \\ &= \frac{A}{\Delta m} \sqrt{\frac{\pi}{a}} = \frac{A\sigma}{\Delta m} \sqrt{2\pi}.\end{aligned}\tag{13}$$

The uncertainties for the yields are contributed from two sources: the uncertainty in the yields it self (which can be treated as a Poisson distribution) and the uncertainty from the fittings. The first uncertainty is then given by

$$\sigma_{\eta\text{-self}} = \sqrt{\eta},\tag{14}$$

while the second uncertainty is found from partial derivatives:

$$\begin{aligned}\sigma_{\eta\text{-fit}} &= \sqrt{\left(\frac{\partial\eta}{\partial A}\Delta A\right)^2 + \left(\frac{\partial\eta}{\partial\sigma}\Delta\sigma\right)^2} \\ &= \sqrt{\left(\eta \frac{\Delta A}{A}\right)^2 + \left(\eta \frac{\Delta\sigma}{\sigma}\right)^2} \\ &= \eta \sqrt{\left(\frac{\Delta A}{A}\right)^2 + \left(\frac{\Delta\sigma}{\sigma}\right)^2}.\end{aligned}\tag{15}$$

Using the above equations to calculate η 's for the four Gaussian distribution gives the triple product and CP asymmetry for the regular and conjugate decay:

$$A_T = \frac{\eta(C_T > 0) - \eta(C_T < 0)}{\eta(C_T > 0) + \eta(C_T < 0)} \quad \text{and} \quad \bar{A}_T = \frac{\eta(-\bar{C}_T > 0) - \eta(-\bar{C}_T < 0)}{\eta(-\bar{C}_T > 0) + \eta(-\bar{C}_T < 0)},\tag{16}$$

$$\text{with } \mathcal{A}_{CP} = \frac{1}{2}(A_T - \bar{A}_T).\tag{17}$$

This gives the results:

```
===== Method 1 (from fittings) =====

yields
events          eta        err_self      err_fit
(C_T>0)       24.7322    4.9731      1.7745
(C_T<0)       35.6901    5.9741      2.7049
(-Cbar_T>0)   26.8409    5.1808      1.2939
(-Cbar_T<0)   21.3494    4.6205      0.6297

Asymmetries
A_T      errA_T      A_T_conj errA_T_conj  a_cp      err_a_cp
-0.1814  0.1767    0.1140    0.1700     -0.1477   0.1226
```

Figure 79: The yields and asymmetries calculated from the fitted Gaussian distributions of the B^0 resonances (from Fig.78).

The Triple product asymmetries in Fig.79 were larger than the predicted values from the simulation studies in the order of 10^{-2} for 10^5 events and doesn't show any P violation due to large errors. A larger size of events would reduce the error. The results for CP asymmetry is about 100 times larger than the simulation study but is still consistent with no CP violation.

An alternative method to find the yields is to sum over the bin heights of the distribution after applying the `sWeights` - this is equivalent to sum over the `sWeights` (gives the same results). This removes the uncertainties from the fitting and only accounts for the uncertainty from the yields itself.

For all the events i with $C_{T_i} > 0$ and `sWeights` w_i , the yields can be written as:

$$\eta(C_T > 0) = \sum_i w_i (C_{T_i} > 0), \quad (18)$$

and similar for the situations of $C_T < 0$, $-\bar{C}_T < 0$ and $-\bar{C}_T > 0$. The asymmetries were then found by using Eq.17.

The results are:

```
===== Method 2 (from weights) =====
events      eta(weights)    err_self(weights)
(C_T>0)     25.2125       5.0212
(C_T<0)     36.5357       6.0445
(-Cbar_T>0) 29.4434       5.4262
(-Cbar_T<0) 24.0639       4.9055

Asymmetries (using weights)
A_T        errA_T      A_T_conj errA_T_conj   a_cp      err_a_cp
-0.1834    0.1251     0.1005    0.1360      -0.1420    0.0924
```

Figure 80: The yields and asymmetries calculated from the sum of the `sWeights`.

Comparing this to the results in Fig.79, the asymmetries changes by 10^{-2} to 10^{-3} and the errors has been decreased by $3 \times 10^{-2} \sim 5 \times 10^{-2}$.

A third attempt is to cut the un-weighted data around the B^0 resonance (i.e. at $5.2\text{-}5.35\text{ }GeV/c^2$) and assume the signal comes from the B^0 decay only. One can use this data to find the asymmetries by applying the code for studying generated data. This gives the number of events of 136 (> 115). This gives the results of asymmetries:

```
===== Method 3 (from cuttings) =====
Asymmetries (cut data)
A_T        errA_T      A_T_conj errA_T_conj   a_cp      err_a_cp
-0.1471    0.0848     0.0909    0.0950      -0.1190    0.0637
```

Figure 81: The asymmetries calculated the data after cutting at 5.2 and $5.35\text{ }GeV/c^2$ in the un-weighted data.

Comparing to the results in Fig.79 and Fig.80, the asymmetries are getting closer to zero and the errors drop again to show the CP asymmetry with 1.8σ . From the simulation studies, we don't expect to see any CP violation with this amount of data. The results indicates an overestimation in the data of the B^0 decay.

Previously, an analysis in the LHCb Run I data was performed. Now add the Run II (2016) data, which is 2263 data points. This add Run I together to give $2263+2678 = 4941$ events. Data from Run II(2017&2018) is yet to be analysed, which will give 3 times more data. The method used is the same as for analysing Run I. The total weighted number of data is 203.

This shows the results of fitting parameters for the B^0 resonance (Gaussian distribution) and the values of the asymmetries from three different approaches:

```

bin=100
      A      err_A     mean   err_mean sigma  err_sigma type
B0 14.7170  0.4666  5.2770  0.0006  0.0159  0.0006  B0(C_T>0)
B0 17.9906  0.4740  5.2813  0.0005  0.0169  0.0005  B0(C_T<0)
B0 9.3004   0.1271  5.2778  0.0003  0.0191  0.0003  Bbar0(-C_T>0)
B0 13.2711  0.2594  5.2832  0.0003  0.0154  0.0003  Bbar0(-C_T<0)

===== Method 1 (from fittings) =====

yields
events          eta          err_self    err_fit
(C_T>0)        48.4851      6.9631     2.3480
(C_T<0)        62.0303      7.8759     2.4964
(-Cbar_T>0)    46.6837      6.8325     0.9749
(-Cbar_T<0)    44.4360      6.6660     1.3269

Asymmetries
A_T      errA_T    A_T_conj errA_T_conj   a_cp      err_a_cp
-0.1226   0.1254    0.0247    0.1227      -0.0736   0.0877

===== Method 2 (from weights) =====

events      eta(weights)    err_self(weights)
(C_T>0)      49.4107      7.0293
(C_T<0)      62.6628      7.9160
(-Cbar_T>0)  46.5319      6.8214
(-Cbar_T<0)  44.6955      6.6855

Asymmetries (using weights)
A_T      errA_T    A_T_conj errA_T_conj   a_cp      err_a_cp
-0.1182   0.0938    0.0201    0.1047      -0.0692   0.0703

===== Method 3 (from cuttings) =====

Asymmetries (cut data)
A_T      errA_T    A_T_conj errA_T_conj   a_cp      err_a_cp
-0.1228   0.0657    0.1053    0.0721      -0.1140   0.0488

```

Figure 82: The results of the fittings and the asymmetries from three different approaches for Run I and Run II (2016) data.

It can be seen that the results from the first two approaches are getting more closer to each other for a larger number of events and the uncertainties has been reduced. The values of \bar{A}_T has been significantly reduced from 0.1 to 0.02 after adding the Run II (2016) data, but the uncertainties remains large up to $> \pm 0.1$. The values for A_T , \bar{A}_T and A_{CP} have got the larger deviations from zero compared with simulation studies. The results from the third method shows P violation with 2.75σ - this is again not expected for this number of events according to previous simulation studies, which might be due to the contribution from the noises.

17 March 2020, Tuesday

Add a little more LHCb data - this gives $2678+2263+147+65 = 5153$ events before weighting, and 304 events after weighting - doesn't observe about 400 events (as expected). It was realised that the value of opt_cut used to cut the data with particular NN_weights would only work for the Run I data previously analysed. It might not work for the Run II (2016) data and the additional data.

The values of opt_cut are different for different data files. Now backup the old files and use the new files instead. They are:

Data_sig_tos_weights-Run1.pkl	opt_cut = 0.9968
Data_sig_tos_weights-Run2.pkl	opt_cut = 0.9693
Data_sig_tis_weights-Run1.pkl	opt_cut = 0.9988
Data_sig_tis_weights-Run2.pkl	opt_cut = 0.9708

Note: [TOS (Trigger on Signal) and TIS (Trigger independent of Signal) are different categories of data. We should find out the details before you write up your report but for now don't worry about it.]

By applying the new opt_cut, the number of events before weighting is $354+395+98+190 = 1037$, and after weighting is 399. The results from the three approaches are:

```

bin=100
      A      err_A     mean   err_mean sigma  err_sigma type
B0 8.5459  0.3211  5.2811  0.0008  0.0173  0.0008    B0(C_T>0)
B0 11.2582 0.3686  5.2797  0.0006  0.0157  0.0006    B0(C_T<0)
B0 9.4059  0.3081  5.2801  0.0006  0.0157  0.0006  Bbar0(-C_T>0)
B0 9.5836  0.4312  5.2826  0.0008  0.0145  0.0008  Bbar0(-C_T<0)

===== Method 1 (from fittings) =====

yields
events          eta          err_self      err_fit
(C_T>0)        94.6734      9.7300      5.4333
(C_T<0)        120.0595     10.9572      6.0044
(-Cbar_T>0)    91.0756      9.5434      4.5575
(-Cbar_T<0)    87.3979      9.3487      6.0065

Asymmetries
A_T      errA_T      A_T_conj errA_T_conj   a_cp      err_a_cp
-0.1182  0.1053     0.0206    0.1170      -0.0694    0.0787

===== Method 2 (from weights) =====

events      eta(weights)    err_self(weights)
(C_T>0)      92.6714      9.6266
(C_T<0)      123.0599     11.0932
(-Cbar_T>0)   91.7746      9.5799
(-Cbar_T<0)   91.6202      9.5718

Asymmetries (using weights)
A_T      errA_T      A_T_conj errA_T_conj   a_cp      err_a_cp
-0.1409  0.0674     0.0008    0.0738      -0.0709    0.0500

===== Method 3 (from cuttings) =====

Asymmetries (cut data)
A_T      errA_T      A_T_conj errA_T_conj   a_cp      err_a_cp
-0.0987  0.0501     0.0435    0.0538      -0.0711    0.0367

```

Figure 83: The results of the fittings and the asymmetries from three different approaches for Run I and Run II (2016) data (new data file).

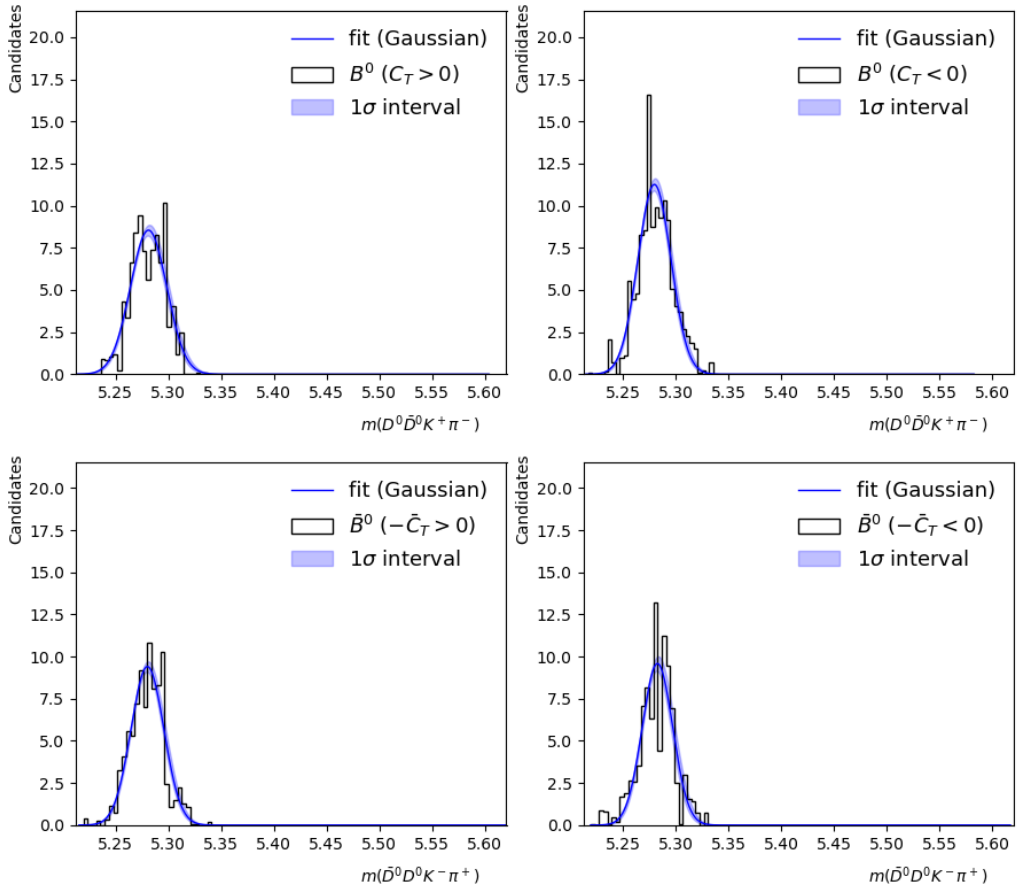


Figure 84: The fitted distribution of the B_0 resonance with showing the $1-\sigma$ tolerance for the Run I and Run II (2016) from new data files.

The distributions were also fitted by the relativistic Breit-Wigner distribution giving the results:

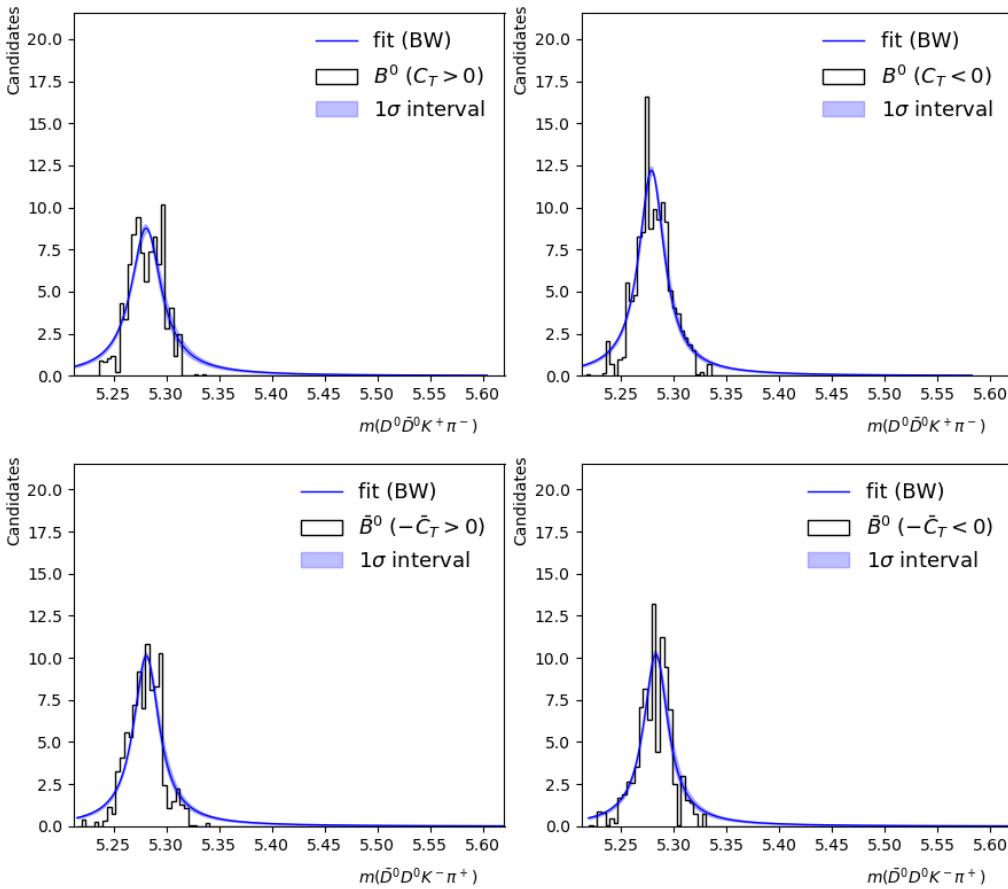


Figure 85: The fitted Breit-Wigner distribution of the B_0 resonance with showing the $1-\sigma$ tolerance for the Run I and Run II (2016) from new data files.

bin=100							
	A	err_A	E	err_E	width	err_width	type
B0	0.3946	0.0224	5.2808	0.0010	0.0353	0.0028	$B_0(C_T > 0)$
B0	0.4629	0.0200	5.2789	0.0006	0.0297	0.0018	$B_0(C_T < 0)$
B0	0.3847	0.0176	5.2810	0.0007	0.0298	0.0019	$\bar{B}^0(-C_T > 0)$
B0	0.3699	0.0207	5.2830	0.0008	0.0284	0.0023	$\bar{B}^0(-C_T < 0)$

Figure 86: The values of the fitted parameters from the Breit-Wigner distribution of the B_0 resonance for the Run I and Run II (2016) from new data files.

19 March 2020, Thursday

It's been noticed that the results are slightly different by removing the duplicated data (1% to 2% of them). I am not sure if it should be removed and why there is duplicated data?

After removing the duplicated data, the number of events before weighting is $347+390+98+190 = 1025$, and after weighting is 396.

The results are:

```

bin=100
      A     err_A     mean   err_mean sigma  err_sigma type
B0  8.5492  0.3215  5.2809  0.0007  0.0172  0.0007  B0(C_T>0)
B0 11.1967  0.3713  5.2797  0.0006  0.0157  0.0006  B0(C_T<0)
B0  9.4154  0.3091  5.2801  0.0006  0.0156  0.0006  Bbar0(-C_T>0)
B0  9.5489  0.4306  5.2828  0.0007  0.0143  0.0007  Bbar0(-C_T<0)

===== Method 1 (from fittings) =====

yields
events          eta        err_self      err_fit
(C_T>0)       93.8457    9.6874     5.3904
(C_T<0)       119.1591   10.9160    6.0361
(-Cbar_T>0)   90.9449    9.5365     4.5609
(-Cbar_T<0)   86.1737    9.2830     5.9355

Asymmetries
A_T      errA_T     A_T_conj errA_T_conj   a_cp      err_a_cp
-0.1188   0.1058    0.0269    0.1174      -0.0729    0.0790

===== Method 2 (from weights) =====

events      eta(weights)  err_self(weights)
(C_T>0)     91.9746     9.5903
(C_T<0)     121.9837   11.0446
(-Cbar_T>0) 91.4915     9.5651
(-Cbar_T<0)  90.7447     9.5260

Asymmetries (using weights)
A_T      errA_T     A_T_conj errA_T_conj   a_cp      err_a_cp
-0.1403   0.0677    0.0041    0.0741      -0.0722    0.0502

===== Method 3 (from cuttings) =====

Asymmetries (cut data)
A_T      errA_T     A_T_conj errA_T_conj   a_cp      err_a_cp
-0.0946   0.0503    0.0468    0.0540      -0.0707    0.0369

```

Figure 87: The results of the fittings and the asymmetries from three different approaches for Run I and Run II (2016) data (new data file) after removing the duplicated data.

An amplitude analysis was performed for the LHCb Run I and Run II (2016) data using the SignalOnlyFitter in AmpGen. A .root file for the data is required to use for the amplitude fit. The .root file should contain the four-momentum of the four daughter particles and the weight for the events (here we use the sWeights from the .pkl file). The values of genPDF is not necessary to perform the fit. The headers were created in the same format as the .root event file generated from AmpGen. The resonance (.opt) file used is same as before (which is described in page 36.)

The fit gives the results:

```

Wall time = 22.4661
CPU time = 60.6105
Making nodes
Making nodes
Time taken = 0.723615 number of nodes = 32
Splitting: 556 data 2000000 amongst 32 bins
Binned 1000000 sim. events
Chi2 per bin = 4.99725
Chi2 per dof = -159.912
-2LL = -139.785
Fit Status = 0
B0{NonResS0{D0,Dbar0},K(0)*(1430)0{K+,pi-}} = 32.54 ± 3.62 %
B0{psi(4415)0{D0,Dbar0},K(0)*(1430)0{K+,pi-}} = 15.11 ± 3.43 %
B0{K(0)*(800)0{K+,pi-},NonResS0{D0,Dbar0}} = 10.10 ± 2.61 %
B0{NonResS0{D0,Dbar0},K*(892)0{K+,pi-}} = 7.87 ± 1.94 %
B0[S]{psi(4415)0{D0,Dbar0},K*(892)0{K+,pi-}} = 3.62 ± 1.14 %
B0[D]{psi(4415)0{D0,Dbar0},K*(892)0{K+,pi-}} = 3.45 ± 1.31 %
B0[D]{psi(4040)0{D0,Dbar0},K*(892)0{K+,pi-}} = 1.49 ± 1.27 %
B0[S]{psi(4160)0{D0,Dbar0},K*(892)0{K+,pi-}} = 1.41 ± 1.29 %
B0[S]{psi(3770)0{D0,Dbar0},K*(892)0{K+,pi-}} = 1.14 ± 0.72 %
B0[P]{psi(3770)0{D0,Dbar0},K*(892)0{K+,pi-}} = 1.05 ± 0.62 %
B0[S]{psi(4040)0{D0,Dbar0},K*(892)0{K+,pi-}} = 1.01 ± 0.94 %
B0[P]{psi(4415)0{D0,Dbar0},K*(892)0{K+,pi-}} = 0.96 ± 0.57 %
B0{psi(4040)0{D0,Dbar0},K(0)*(800)0{K+,pi-}} = 0.53 ± 0.56 %
B0[P]{psi(4040)0{D0,Dbar0},K*(892)0{K+,pi-}} = 0.46 ± 0.46 %
B0{psi(4160)0{D0,Dbar0},K(0)*(800)0{K+,pi-}} = 0.37 ± 0.48 %
B0[D]{psi(4160)0{D0,Dbar0},K*(892)0{K+,pi-}} = 0.33 ± 0.55 %
B0{D(s2)(2573)+{D0,K+},Dbar0,pi-} = 0.30 ± 0.34 %
B0{psi(4415)0{D0,Dbar0},K(0)*(800)0{K+,pi-}} = 0.28 ± 0.37 %
B0{psi(4160)0{D0,Dbar0},K(0)*(1430)0{K+,pi-}} = 0.18 ± 0.37 %
B0[D]{psi(3770)0{D0,Dbar0},K*(892)0{K+,pi-}} = 0.16 ± 0.39 %
B0[P]{psi(4160)0{D0,Dbar0},K*(892)0{K+,pi-}} = 0.07 ± 0.22 %
B0{psi(3770)0{D0,Dbar0},K(0)*(800)0{K+,pi-}} = 0.03 ± 0.15 %
B0{psi(4040)0{D0,Dbar0},K(0)*(1430)0{K+,pi-}} = 0.00 ± 0.07 %
B0{psi(3770)0{D0,Dbar0},K(0)*(1430)0{K+,pi-}} = 0.00 ± 0.02 %
Sum_B0 = 82.58 ± 4.72 %

```

Figure 88: The results of the ratio of the resonances with the regular conjugate decays for the LHCb Run I and Run II (2016) data using AmpGen.

The amplitude fit projection gives the plots of the square of invariant masses:

The fitted projections seems to work except for the case for s(DDbar), where an unexpected peak pop-out. I tried to change the steps in the amplitude and phase (in radians), it doesn't make a big difference for the results.

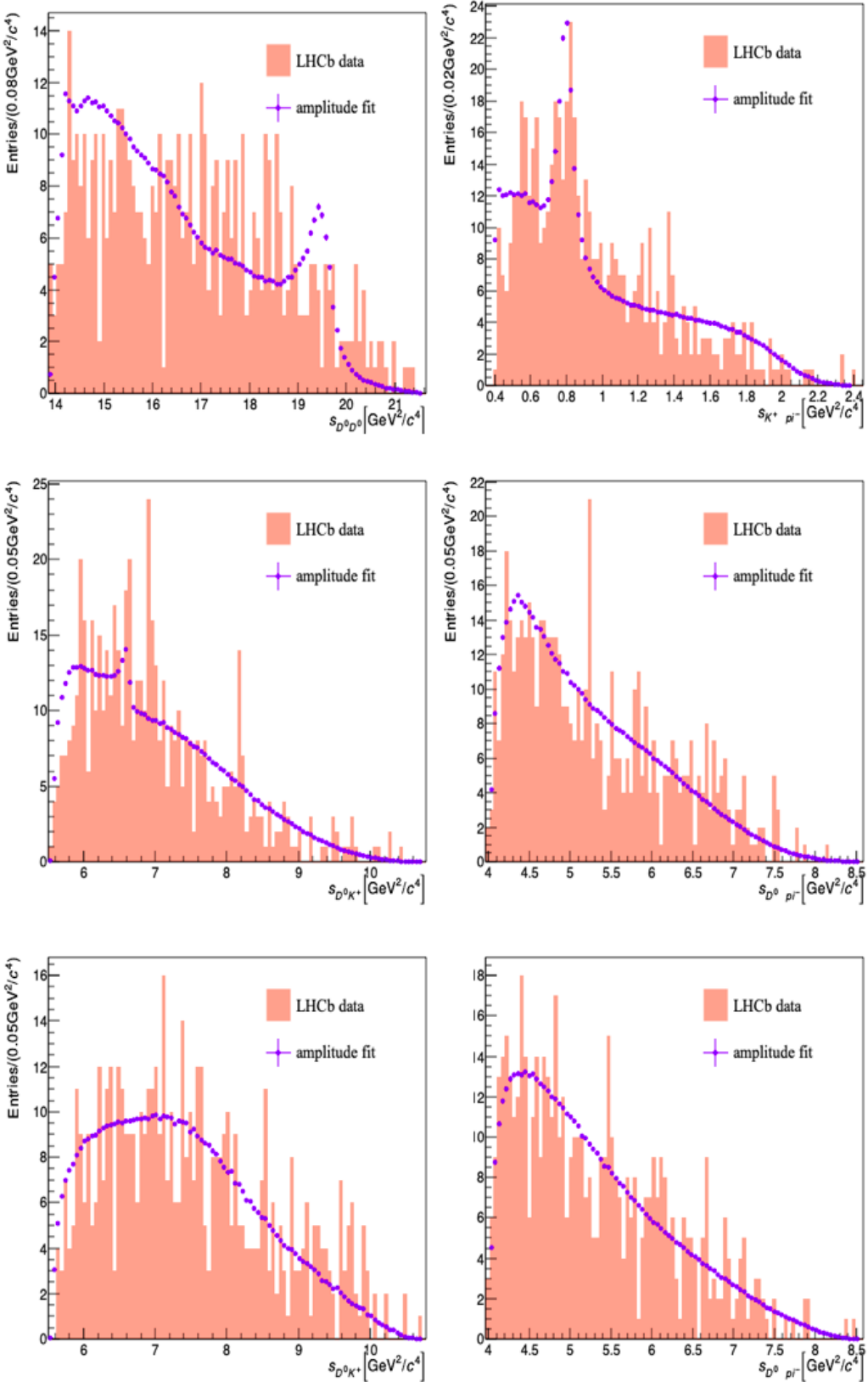


Figure 89: The fit projection outputs for the LHCb Run I and Run II (2016) data using AmpGen. It doesn't distinct D^0 and \bar{D}^0 in the label: the middle two plots represent D^0 , while the last two plots represent \bar{D}^0 .

The charge conjugate decays has also been analysed with the same method and resonance file. But I am not sure if I can use the same resonance file for fitting the charge conjugate decay, in which all the resonances would be treated as charge conjugate processes.

This gives the results:

```
Wall time = 27.0024
CPU time = 63.4846
Making nodes
Making nodes
Time taken = 0.637276 number of nodes = 32
Splitting: 481 data 2000000 amongst 32 bins
Binned 1000000 sim. events
Chi2 per bin = 3.25264
Chi2 per dof = -104.084
-2LL = -91.7032
Fit Status = 1
B0{NonResS0{D0,Dbar0},K(0)*(1430)0{K+,pi-}} = 41.38 ± 4.28 %
B0[D]{psi(4415)0{D0,Dbar0},K*(892)0{K+,pi-}} = 9.67 ± 2.74 %
B0{K(0)*(800)0{K+,pi-},NonResS0{D0,Dbar0}} = 7.40 ± 2.00 %
B0[S]{psi(4415)0{D0,Dbar0},K*(892)0{K+,pi-}} = 4.80 ± 1.46 %
B0[P]{psi(4415)0{D0,Dbar0},K*(892)0{K+,pi-}} = 3.55 ± 1.28 %
B0{psi(4415)0{D0,Dbar0},K(0)*(1430)0{K+,pi-}} = 3.01 ± 1.17 %
B0{NonResS0{D0,Dbar0},K*(892)0{K+,pi-}} = 2.80 ± 1.07 %
B0[D]{psi(3770)0{D0,Dbar0},K*(892)0{K+,pi-}} = 2.50 ± 1.06 %
B0[S]{psi(4040)0{D0,Dbar0},K*(892)0{K+,pi-}} = 2.03 ± 1.98 %
B0[P]{psi(3770)0{D0,Dbar0},K*(892)0{K+,pi-}} = 1.80 ± 1.03 %
B0[P]{psi(4040)0{D0,Dbar0},K*(892)0{K+,pi-}} = 1.24 ± 1.02 %
B0{psi(3770)0{D0,Dbar0},K(0)*(800)0{K+,pi-}} = 0.85 ± 0.60 %
B0[D]{psi(4040)0{D0,Dbar0},K*(892)0{K+,pi-}} = 0.49 ± 1.11 %
B0{psi(4040)0{D0,Dbar0},K(0)*(800)0{K+,pi-}} = 0.34 ± 0.44 %
B0{D(s2)(2573)+{D0,K+},Dbar0,pi-} = 0.29 ± 0.41 %
B0{psi(4415)0{D0,Dbar0},K(0)*(800)0{K+,pi-}} = 0.29 ± 0.43 %
B0{psi(3770)0{D0,Dbar0},K(0)*(1430)0{K+,pi-}} = 0.22 ± 0.32 %
B0{psi(4040)0{D0,Dbar0},K(0)*(1430)0{K+,pi-}} = 0.20 ± 0.35 %
B0[D]{psi(4160)0{D0,Dbar0},K*(892)0{K+,pi-}} = 0.16 ± 0.40 %
B0{psi(4160)0{D0,Dbar0},K(0)*(1430)0{K+,pi-}} = 0.08 ± 0.23 %
B0[P]{psi(4160)0{D0,Dbar0},K*(892)0{K+,pi-}} = 0.02 ± 0.14 %
B0{psi(4160)0{D0,Dbar0},K(0)*(800)0{K+,pi-}} = 0.00 ± 0.04 %
B0[S]{psi(4160)0{D0,Dbar0},K*(892)0{K+,pi-}} = 0.00 ± 0.03 %
B0[S]{psi(3770)0{D0,Dbar0},K*(892)0{K+,pi-}} = 0.00 ± 0.00 %
Sum_B0 = 83.24 ± 5.91 %
```

Figure 90: The results of the ratio of the resonances with the charge conjugate decays for the LHCb Run I and Run II (2016) data using AmpGen.

The amplitude fit projection gives the plots of the square of invariant masses:

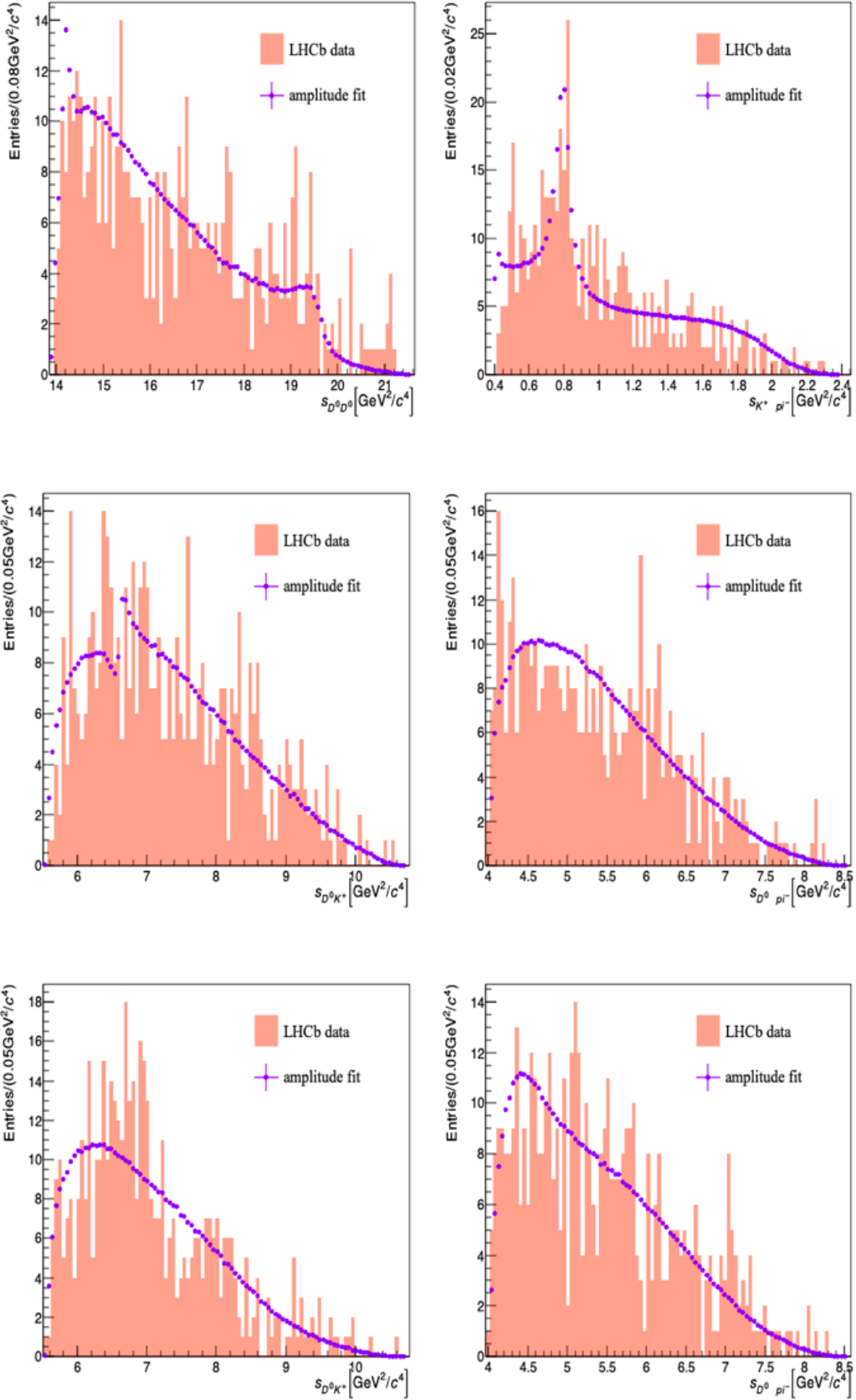


Figure 91: The fit projection outputs for the LHCb Run I and Run II (2016) data using AmpGen. Note the label should treated as conjugate particles (i.e. $K^+\pi^-$ should be $K^-\pi^+$). It doesn't distinct D^0 and \bar{D}^0 in the label: the middle two plots represent \bar{D}^0 , while the last two plots represent D^0 .

There are some changes and improvements made for the amplitude fittings:

- removed the duplicated events in the LHCb data file (refer to page 58)
- removed the random seed specified in the opt file
 - This would give slightly different fit results each time, and the resonance peaks in the fit projection will be less or more obvious.
- added error bars to the LHCb data
 - The error bars are invoked with `Sumw2()` (can also be given by default), which are given by the `sqrt(sum of squares of weight)` in each bin.
- corrected the fitting methods for the conjugate data
 - Since CP violation is small in our decay, the conjugate decay can be turned into regular decay by putting the particles in the same order as the regular decay ($B\bar{b}ar0 D\bar{b}ar0 D0 K\bar{P}I$ vs $B0 D0 D\bar{b}ar0 K\bar{P}I$) and flipping the three momenta, so then the conjugated data can be fitted using the same model as the regular data.
- fitted data for all the events by removing the resonance with a fit fraction less than 3σ
- plot more fit projections in the order of
 $s(D^0\bar{D}^0)$, $s(D^0K^+)$, $s(D^0\pi^-)$, $s(\bar{D}^0K^+)$, $s(\bar{D}^0\pi^-)$, $s(K^+\pi^-)$,
 $s(D^0\bar{D}^0K^+)$, $s(D^0\bar{D}^0\pi^-)$, $s(D^0K^+\pi^-)$, $s(\bar{D}^0K^+\pi^-)$
Note: in the figure label, D^0, \bar{D}^0 are not distinguished.

The fitting gives the values of the amplitudes and phases of the coupling constants of the resonances, and the fit fractions of the single and interfered resonances. The fit fraction of a single resonance j is defined as

$$f_j = \frac{\int |\mathcal{A}_j|^2 \mathcal{R}_4(\mathbf{x}) d^5\mathbf{x}}{\int |\sum_k \mathcal{A}_k|^2 \mathcal{R}_4(\mathbf{x}) d^5\mathbf{x}}, \quad \text{and} \quad \mathcal{A}_n = A_n e^{i\phi_n} \mathcal{M}_n, \quad (19)$$

where A_n and ϕ_n is the amplitude and phase of the coupling constants of the resonance n in the .opt file (first introduced in page 20), \mathcal{M}_i is the amplitude describing the dynamics of the decay (can be calculated from AmpGen), $\mathcal{R}_4(\mathbf{x})$ is the function representing the four-body phase space and the integration is taken over the five phase space variable (here we use the CM variables). Interference between the complex terms in the denominator would increase or decrease the value of denominator, and may lead to $\sum_{j=1}^N f_j \neq 100\%$. See foot note for more information on the fit fraction for 3-body¹¹ and 4-body¹² decays.

Since there are not many event, the regular and conjugate decay data can be combined to give maximize the number of data to be fitted. The fit projections and fit fractions is shown in Fig.92 and Fig.93, respectively. In the $s(K^+\pi^-)$ plot, the resonance peaks for $\psi(3770)$, $\psi(4040)$, $\psi(4160)$ and $\psi(4415)$ are managed to present, although the $\psi(4415)$ has a relative larger amplitude than expected. In the $s(K^+\pi^-)$ plot, it shows the $K_0^*(892)$ and $K^{(0)*}(800)$ (not obvious) resonances. In the $s(D^0K^+)$ plot, there is a $D_s^-(2573)$ resonance, I am not sure why this is possible given that the K^+ used are produced from K_0^* only. The sum of the fit fractions (`Sum_B0`) is consistent with 100% by considering the uncertainties.

¹¹D. Asner. *DALITZ PLOT ANALYSIS FORMALISM*. [Online; accessed 30-March-2020]. URL: <http://pdg.lbl.gov/2011/reviews/rpp2011-rev-dalitz-analysis-formalism.pdf>.

¹²R. Aaij et al. “Search for CP violation through an amplitude analysis of $D^0 \rightarrow K^+ K^{\pi^+\pi^-}$ decays”. In: *JHEP* 2019.2 (2019). ISSN: 1029-8479.

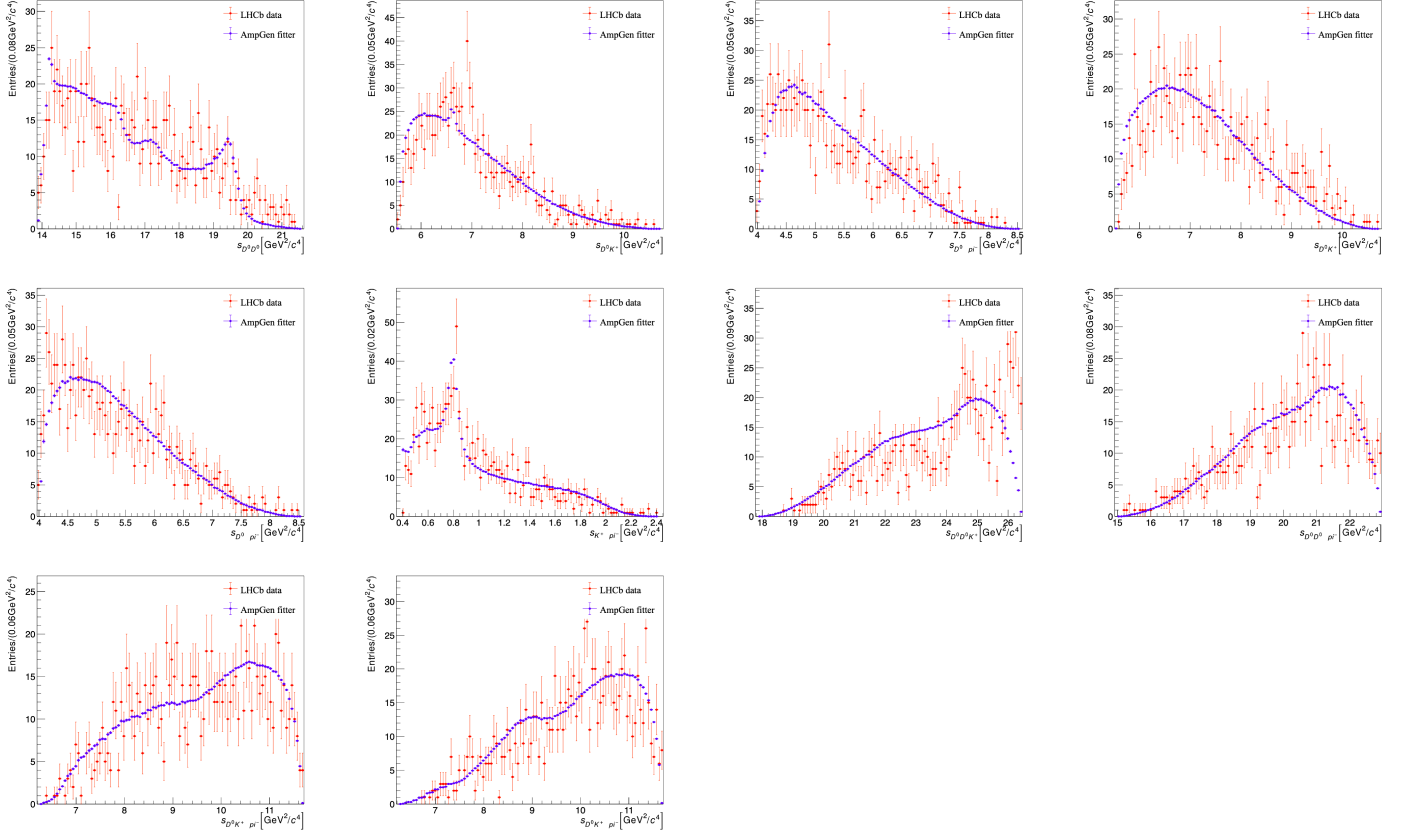


Figure 92: The phase-space distributions of the conjugate decay in terms of the square of invariant masses of particles.

$B0\{\psi(4415)0\{D0, \bar{D}\}, K(0)*(1430)0\{K^+, \pi^-\}\}$	=	38.60 ± 27.46	%
$B0\{\text{NonRes}S0\{D0, \bar{D}\}, K(0)*(1430)0\{K^+, \pi^-\}\}$	=	28.47 ± 26.50	%
$B0\{\psi(4415)0\{D0, \bar{D}\}, K(0)*(800)0\{K^+, \pi^-\}\}$	=	9.27 ± 17.11	%
$B0\{K(0)*(800)0\{K^+, \pi^-\}, \text{NonRes}S0\{D0, \bar{D}\}\}$	=	8.64 ± 13.40	%
$B0[P]\{\psi(4415)0\{D0, \bar{D}\}, K*(892)0\{K^+, \pi^-\}\}$	=	5.84 ± 7.29	%
$B0\{\text{NonRes}S0\{D0, \bar{D}\}, K*(892)0\{K^+, \pi^-\}\}$	=	5.28 ± 12.25	%
$B0[P]\{\psi(4160)0\{D0, \bar{D}\}, K*(892)0\{K^+, \pi^-\}\}$	=	3.35 ± 10.89	%
$B0\{\psi(4160)0\{D0, \bar{D}\}, K(0)*(800)0\{K^+, \pi^-\}\}$	=	2.99 ± 10.45	%
$B0\{\psi(4040)0\{D0, \bar{D}\}, K(0)*(800)0\{K^+, \pi^-\}\}$	=	2.77 ± 10.29	%
$B0[D]\{\psi(4160)0\{D0, \bar{D}\}, K*(892)0\{K^+, \pi^-\}\}$	=	2.61 ± 6.49	%
$B0[P]\{\psi(3770)0\{D0, \bar{D}\}, K*(892)0\{K^+, \pi^-\}\}$	=	2.50 ± 5.36	%
$B0\{\psi(4160)0\{D0, \bar{D}\}, K(0)*(1430)0\{K^+, \pi^-\}\}$	=	2.31 ± 10.33	%
$B0[S]\{\psi(4415)0\{D0, \bar{D}\}, K*(892)0\{K^+, \pi^-\}\}$	=	2.30 ± 4.68	%
$B0\{\psi(3770)0\{D0, \bar{D}\}, K(0)*(800)0\{K^+, \pi^-\}\}$	=	2.05 ± 4.71	%
$B0[D]\{\psi(4415)0\{D0, \bar{D}\}, K*(892)0\{K^+, \pi^-\}\}$	=	1.87 ± 4.62	%
$B0\{D(s2)(2573)+\{D0, K^+\}, \bar{D}, \pi^-\}$	=	1.74 ± 4.62	%
$B0[D]\{\psi(3770)0\{D0, \bar{D}\}, K*(892)0\{K^+, \pi^-\}\}$	=	1.47 ± 5.10	%
$B0[P]\{\psi(4040)0\{D0, \bar{D}\}, K*(892)0\{K^+, \pi^-\}\}$	=	1.42 ± 4.27	%
$B0[D]\{\psi(4040)0\{D0, \bar{D}\}, K*(892)0\{K^+, \pi^-\}\}$	=	0.98 ± 2.78	%
$B0[S]\{\psi(4160)0\{D0, \bar{D}\}, K*(892)0\{K^+, \pi^-\}\}$	=	0.90 ± 3.25	%
$B0\{\psi(3770)0\{D0, \bar{D}\}, K(0)*(1430)0\{K^+, \pi^-\}\}$	=	0.59 ± 1.76	%
$B0[S]\{\psi(4040)0\{D0, \bar{D}\}, K*(892)0\{K^+, \pi^-\}\}$	=	0.42 ± 1.76	%
$B0\{\psi(4040)0\{D0, \bar{D}\}, K(0)*(1430)0\{K^+, \pi^-\}\}$	=	0.10 ± 0.51	%
$B0[S]\{\psi(3770)0\{D0, \bar{D}\}, K*(892)0\{K^+, \pi^-\}\}$	=	0.00 ± 0.00	%
Sum_B0	=	126.57 ± 64.16	%

Figure 93: The results of fit fractions for all the decays for LHCb Run I and Run II (2016) data, which has got a number of events = 1025, reduced Chi2=18.145.

By removing the resonance with fit fraction less than 3σ :

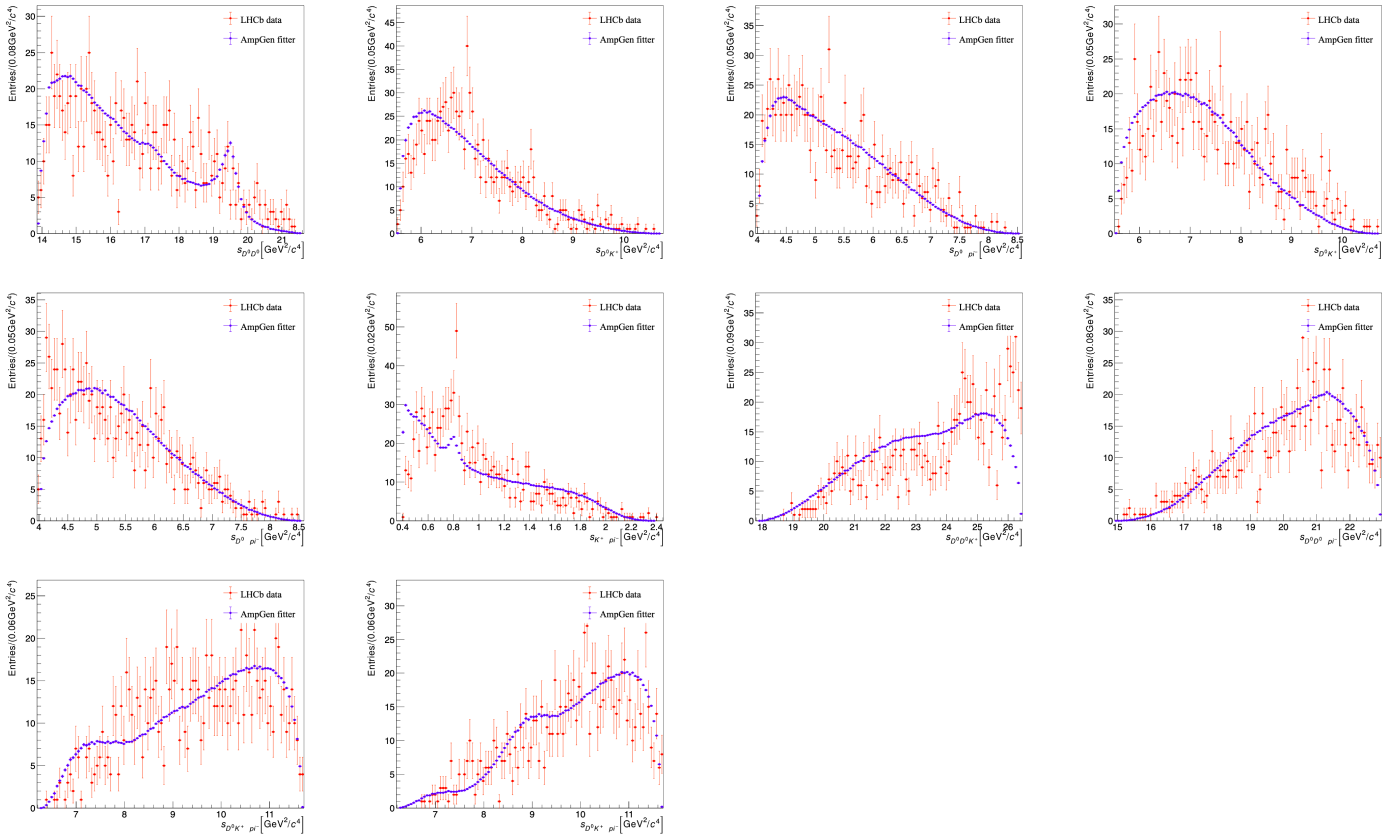


Figure 94: The phase-space distributions of the conjugate decay in terms of the square of invariant masses of particles (after removing some resonances).

$B0\{\text{NonResS0}\{D0, \bar{D}\}, K(0)*(1430)\}0\{K^+, \pi^-\}$	=	36.12 ± 2.83	%
$B0\{\psi(4415)\}0\{D0, \bar{D}\}, K(0)*(1430)\}0\{K^+, \pi^-\}$	=	15.43 ± 2.75	%
$B0\{K(0)*(800)\}0\{K^+, \pi^-\}, \text{NonResS0}\{D0, \bar{D}\}$	=	13.80 ± 1.97	%
$B0[S]\{\psi(4160)\}0\{D0, \bar{D}\}, K*(892)\}0\{K^+, \pi^-\}$	=	3.36 ± 0.77	%
$B0[D]\{\psi(4040)\}0\{D0, \bar{D}\}, K*(892)\}0\{K^+, \pi^-\}$	=	0.73 ± 0.58	%
$B0\{\psi(3770)\}0\{D0, \bar{D}\}, K(0)*(800)\}0\{K^+, \pi^-\}$	=	0.71 ± 0.49	%
$B0[S]\{\psi(3770)\}0\{D0, \bar{D}\}, K*(892)\}0\{K^+, \pi^-\}$	=	0.46 ± 0.33	%
Sum_B0	=	70.63 ± 2.98	%

Figure 95: The results of fit fractions for all the decays for LHCb Run I and Run II (2016) data (after removing some resonances), which has got a number of events = 1025, reduced Chi2=8.22.

The fit has also been performed for the regular and conjugate decay events separately (see Fig.96, 97 and Fig.98, 99, respectively). It can be seen that the conjugate decay fit better than the regular decay with the $\psi(4415)$ peak and the uncertainties of the fit fractions being smaller. However, due to the random seed used are different, the results could be different. A comparison could be made for the regular and conjugate decays using the same seed number. One can also find the asymmetry from the fit fractions.

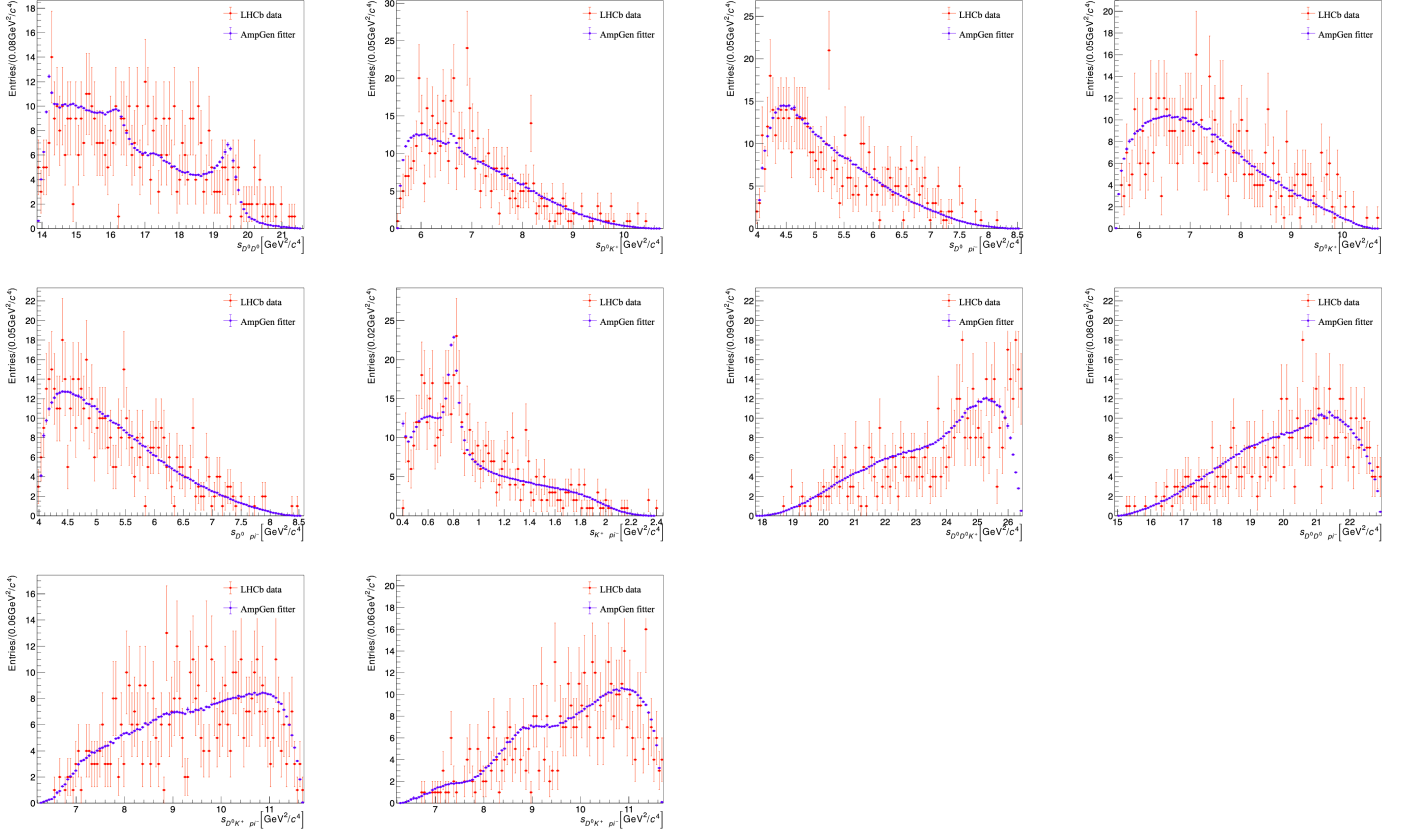


Figure 96: The phase-space distributions of the regular decay in terms of the square of invariant masses of particles.

$B0\{\psi(4415)0\{D0, \bar{D}\}, K(0)*(1430)0\{K^+, \pi^-\}\}$	=	41.48 ± 23.96	%
$B0\{\text{NonRes}S0\{D0, \bar{D}\}, K(0)*(1430)0\{K^+, \pi^-\}\}$	=	26.99 ± 37.18	%
$B0\{\psi(4415)0\{D0, \bar{D}\}, K(0)*(800)0\{K^+, \pi^-\}\}$	=	10.51 ± 37.59	%
$B0\{K(0)*(800)0\{K^+, \pi^-\}, \text{NonRes}S0\{D0, \bar{D}\}\}$	=	9.02 ± 32.98	%
$B0\{\text{NonRes}S0\{D0, \bar{D}\}, K*(892)0\{K^+, \pi^-\}\}$	=	6.26 ± 5.97	%
$B0[D]\{\psi(4160)0\{D0, \bar{D}\}, K*(892)0\{K^+, \pi^-\}\}$	=	4.23 ± 9.67	%
$B0[S]\{\psi(4160)0\{D0, \bar{D}\}, K*(892)0\{K^+, \pi^-\}\}$	=	2.85 ± 10.89	%
$B0[P]\{\psi(4415)0\{D0, \bar{D}\}, K*(892)0\{K^+, \pi^-\}\}$	=	2.83 ± 8.55	%
$B0[D]\{\psi(4415)0\{D0, \bar{D}\}, K*(892)0\{K^+, \pi^-\}\}$	=	2.54 ± 10.48	%
$B0[S]\{\psi(4415)0\{D0, \bar{D}\}, K*(892)0\{K^+, \pi^-\}\}$	=	2.25 ± 7.62	%
$B0[P]\{\psi(3770)0\{D0, \bar{D}\}, K*(892)0\{K^+, \pi^-\}\}$	=	2.24 ± 8.01	%
$B0\{\psi(3770)0\{D0, \bar{D}\}, K(0)*(800)0\{K^+, \pi^-\}\}$	=	1.94 ± 7.93	%
$B0[P]\{\psi(4040)0\{D0, \bar{D}\}, K*(892)0\{K^+, \pi^-\}\}$	=	1.67 ± 8.57	%
$B0\{\psi(4160)0\{D0, \bar{D}\}, K(0)*(1430)0\{K^+, \pi^-\}\}$	=	1.36 ± 9.15	%
$B0\{\psi(4040)0\{D0, \bar{D}\}, K(0)*(1430)0\{K^+, \pi^-\}\}$	=	0.84 ± 3.64	%
$B0\{\psi(3770)0\{D0, \bar{D}\}, K(0)*(1430)0\{K^+, \pi^-\}\}$	=	0.57 ± 5.14	%
$B0[D]\{\psi(4040)0\{D0, \bar{D}\}, K*(892)0\{K^+, \pi^-\}\}$	=	0.57 ± 4.99	%
$B0[D]\{\psi(3770)0\{D0, \bar{D}\}, K*(892)0\{K^+, \pi^-\}\}$	=	0.47 ± 3.69	%
$B0[S]\{\psi(4040)0\{D0, \bar{D}\}, K*(892)0\{K^+, \pi^-\}\}$	=	0.43 ± 3.33	%
$B0\{\psi(4160)0\{D0, \bar{D}\}, K(0)*(800)0\{K^+, \pi^-\}\}$	=	0.42 ± 4.13	%
$B0[P]\{\psi(4160)0\{D0, \bar{D}\}, K*(892)0\{K^+, \pi^-\}\}$	=	0.33 ± 2.63	%
$B0\{\psi(4040)0\{D0, \bar{D}\}, K(0)*(800)0\{K^+, \pi^-\}\}$	=	0.28 ± 1.81	%
$B0[D(s2)(2573)+\{D0, K^+\}, \bar{D}, \pi^-]$	=	0.10 ± 0.70	%
$B0[S]\{\psi(3770)0\{D0, \bar{D}\}, K*(892)0\{K^+, \pi^-\}\}$	=	0.00 ± 0.00	%
Sum_B0	=	120.30 ± 62.36	%

Figure 97: The results of fit fractions for the regular decays for LHCb Run I and Run II (2016) data, which has got a number of events = 511, reduced Chi2=-9..

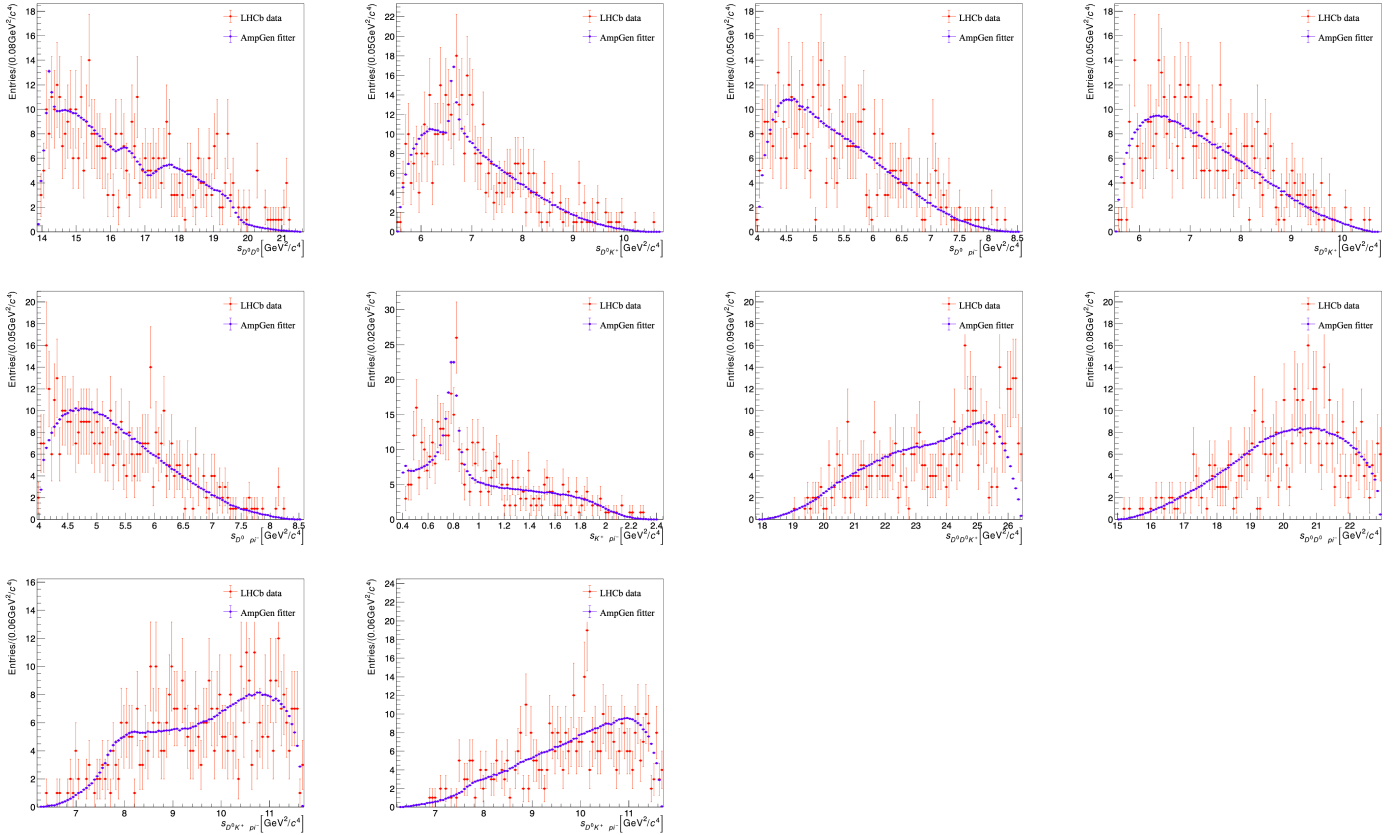


Figure 98: The phase-space distributions of the conjugate decay in terms of the square of invariant masses of particles.

$B0\{\text{NonResS0}\{D0, Dbar0\}, K(0)*(1430)\bar{0}\{K+, \bar{\pi}\}\}$	=	37.16 \pm 4.36	%
$B0[D]\{\psi(4415)\bar{0}\{D0, Dbar0\}, K*(892)\bar{0}\{K+, \bar{\pi}\}\}$	=	14.69 \pm 4.75	%
$B0\{K(0)*(800)\bar{0}\{K+, \bar{\pi}\}, \text{NonResS0}\{D0, Dbar0\}\}$	=	8.85 \pm 2.70	%
$B0[P]\{\psi(4415)\bar{0}\{D0, Dbar0\}, K*(892)\bar{0}\{K+, \bar{\pi}\}\}$	=	7.57 \pm 2.14	%
$B0[S]\{\psi(4415)\bar{0}\{D0, Dbar0\}, K*(892)\bar{0}\{K+, \bar{\pi}\}\}$	=	4.36 \pm 1.93	%
$B0\{\text{NonResS0}\{D0, Dbar0\}, K*(892)\bar{0}\{K+, \bar{\pi}\}\}$	=	4.02 \pm 2.80	%
$B0[D]\{\psi(3770)\bar{0}\{D0, Dbar0\}, K*(892)\bar{0}\{K+, \bar{\pi}\}\}$	=	3.72 \pm 1.58	%
$B0[P]\{\psi(4160)\bar{0}\{D0, Dbar0\}, K*(892)\bar{0}\{K+, \bar{\pi}\}\}$	=	3.37 \pm 2.15	%
$B0[D]\{\psi(4160)\bar{0}\{D0, Dbar0\}, K*(892)\bar{0}\{K+, \bar{\pi}\}\}$	=	3.07 \pm 2.55	%
$B0\{\psi(4160)\bar{0}\{D0, Dbar0\}, K(0)*(800)\bar{0}\{K+, \bar{\pi}\}\}$	=	2.18 \pm 2.25	%
$B0\{D(s2)(2573)+\{D0, K+\}, Dbar0, \bar{\rho}\}$	=	1.88 \pm 0.92	%
$B0[S]\{\psi(3770)\bar{0}\{D0, Dbar0\}, K*(892)\bar{0}\{K+, \bar{\pi}\}\}$	=	1.80 \pm 1.06	%
$B0\{\psi(4040)\bar{0}\{D0, Dbar0\}, K(0)*(800)\bar{0}\{K+, \bar{\pi}\}\}$	=	1.58 \pm 1.80	%
$B0\{\psi(4415)\bar{0}\{D0, Dbar0\}, K(0)*(1430)\bar{0}\{K+, \bar{\pi}\}\}$	=	1.48 \pm 1.73	%
$B0[S]\{\psi(4040)\bar{0}\{D0, Dbar0\}, K*(892)\bar{0}\{K+, \bar{\pi}\}\}$	=	1.15 \pm 1.37	%
$B0\{\psi(3770)\bar{0}\{D0, Dbar0\}, K(0)*(1430)\bar{0}\{K+, \bar{\pi}\}\}$	=	0.88 \pm 1.21	%
$B0\{\psi(4040)\bar{0}\{D0, Dbar0\}, K(0)*(1430)\bar{0}\{K+, \bar{\pi}\}\}$	=	0.65 \pm 1.18	%
$B0[D]\{\psi(4040)\bar{0}\{D0, Dbar0\}, K*(892)\bar{0}\{K+, \bar{\pi}\}\}$	=	0.65 \pm 1.06	%
$B0\{\psi(3770)\bar{0}\{D0, Dbar0\}, K(0)*(800)\bar{0}\{K+, \bar{\pi}\}\}$	=	0.50 \pm 0.61	%
$B0\{\psi(4415)\bar{0}\{D0, Dbar0\}, K(0)*(800)\bar{0}\{K+, \bar{\pi}\}\}$	=	0.44 \pm 0.89	%
$B0[P]\{\psi(4040)\bar{0}\{D0, Dbar0\}, K*(892)\bar{0}\{K+, \bar{\pi}\}\}$	=	0.42 \pm 0.73	%
$B0\{\psi(4160)\bar{0}\{D0, Dbar0\}, K(0)*(1430)\bar{0}\{K+, \bar{\pi}\}\}$	=	0.23 \pm 0.86	%
$B0[S]\{\psi(4160)\bar{0}\{D0, Dbar0\}, K*(892)\bar{0}\{K+, \bar{\pi}\}\}$	=	0.22 \pm 0.55	%
$B0[P]\{\psi(3770)\bar{0}\{D0, Dbar0\}, K*(892)\bar{0}\{K+, \bar{\pi}\}\}$	=	0.01 \pm 0.07	%
Sum_B0	=	100.99 \pm 9.69	%

Figure 99: The results of fit fractions for the conjugate decays for LHCb Run I and Run II (2016) data, which has got a number of events = 474, reduced Chi2=-4.97.

References

- Aaij, R. et al. “Search for CP violation through an amplitude analysis of $D^0 \rightarrow K^+ K^{\pi^+\pi^-}$ decays”. In: *JHEP* 2019.2 (2019). ISSN: 1029-8479.
- Argent, P. d’ et al. “Amplitude analyses of $D^0 \rightarrow \pi^+\pi^-\pi^+\pi^-$ and $D^0 \rightarrow K^+K^-\pi^+\pi^-$ decays”. In: *J. HEP* 2017.5 (2017). ISSN: 1029-8479.
- Asner, D. *DALITZ PLOT ANALYSIS FORMALISM*. [Online; accessed 30-March-2020]. URL: <http://pdg.lbl.gov/2011/reviews/rpp2011-rev-dalitz-analysis-formalism.pdf>.
- Blake, Chris. *Lecture3: Hypothesis testing and model-fitting*. [Online; accessed 23-March-2020]. URL: <http://astronomy.swin.edu.au/~cblake/StatsLecture3.pdf>.
- Pivk, M. and F.R. Le Diberder. “: A statistical tool to unfold data distributions”. In: *Nucl. Instrum. Meth. A* 555.1-2 (2005), 356–369. ISSN: 0168-9002.
- Rogozhnikov, Alex. *sPlot: a technique to reconstruct components of a mixture*. [Online; accessed 23-March-2020]. 2015. URL: <http://arogozhnikov.github.io/2015/10/07/splot.html>.
- The LHCb collaboration. “Search for CP Violation using T-odd Correlations in $D^0 \rightarrow K^+K^-\pi^+\pi^-$ Decays”. In: *J. HEP* 2014.10 (2014). ISSN: 1029-8479.
- Wikipedia contributors. *Lorentz transformation — Wikipedia, The Free Encyclopedia*. [Online; accessed 23-March-2020]. 2014. URL: https://en.wikipedia.org/w/index.php?title=Lorentz_transformation&oldid=600359480.
- . *Relativistic Breit–Wigner distribution — Wikipedia, The Free Encyclopedia*. [Online; accessed 23-March-2020]. 2019. URL: https://en.wikipedia.org/w/index.php?title=Relativistic_Breit%20%80%93Wigner_distribution&oldid=912044809.